Liger at W. M. Keck Observatory: Overall Design and Science Drivers

Shelley A. Wright[a,b], Tucker Jones[c], James Larkin[d], Renate Kupke[e], Marc Kassis[f], Aaron Brown[a], David Andersen[g], Lee Armus[h], Bryson Cale[a], Maren Cosens[i], Devin Chu[d], Tuan Do[d], Chris Fassanacht[c], Deanne Fisher[j], Michael Fitzgerald[d], Andrea Ghez[d], Jenny Greene[k], Takeru Hayashi[d], Aurélien Hees[l], Jessie Hirtenstein[c], Chris Johnson[d], Jacqueline Keane[m], Patrick Kelly[n], Evan Kirby[o], Theodora Karalidi[p], Quinn Konopacky[a], Evan Kress[e], Jessica Lu[q], Jim Lyke[f], Kenneth Magnone[e], Jérôme Maire[a], Rosalie McGurk[f], Anne Medling[r], Maxwell Millar-Blanchaer[s], Quinn Minor[t], Reston Nash[h], Anna Nierenberg[t], Naveen Reddy[v], Michael Rich[d], Jean-Baptiste Ruffio[a], Nils-Erik Rundquist[a], Sanchit Sabhlok[b], David Sand[w], Ryan Sanders[x], Karin Sandstrom[a], Alice Shapley[d], Ji-Man Sohn[d], Arun Surya[y], Tommaso Treu[d], Eric Wang[d], Kanaka Warad[g], Robert Weber[h], James Wiley[b], Peter Wizinowich[f], Michael H. Wong[z], and Sherry Yeh[f]

[a]Department of Astronomy & Astrophysics, University of California San Diego, USA
[b]Department of Physics, University of California San Diego, USA
[c]Department of Physics, University of California Davis, USA
[d]Department of Physics & Astronomy, University of California Los Angeles, USA
[e]Department of Astronomy & Astrophysics, University of California Santa Cruz, USA
[f]W.M. Keck Observatory, Waimea, HI, USA
[g]Thirty Meter Telescope International Observatory, Pasadena, CA, USA
[h]Department of Astronomy, California Institute of Technology, Pasadena, CA, USA
[i]Carnegie Observatories, Pasadena, CA, USA
[j]Swinburne University of Technology, Melbourne, Australia
[k]Department of Astrophysical Studies, Princeton University, New Jersey, USA
[l]Observatoire de Paris, Laboratoire National de m´etrologie et d'Essais, France
[m]Institute for Astronomy, University of Hawaii, Oahu, HI, USA
[n]School of Physics and Astronomy, University of Minnesota, Minneapolis, USA
[o]Department of Physics & Astronomy, University of Notre Dame, Notre Dame, IN, USA
[p]Department of Physics, Planetary Sciences Group, University of Central Florida, USA
[q]Department of Astronomy & Astrophysics, University of California Berkeley, USA
[r]Department of Physics & Astronomy, University of Toledo, OH, USA
[s]Department of Physics, University of California Santa Barbara, USA
[t]Borough of Manhattan Community College, City University of New York, USA
[u]Department of Physics, University of California Merced, USA
[v]Department of Physics, University of California Riverside, USA
[w]Steward Observatory, University of Arizona, USA
[x]Physics & Astronomy, University of Kentucky, Lexington, KY
[y]Indian Institute of Astrophysics, Bangalore, India
[z]Center for Integrative Planetary Science, University of California Berkeley, USA

Send correspondence to s2wright@ucsd.edu

Ground-based and Airborne Instrumentation for Astronomy X, edited by Julia J. Bryant, Kentaro Motohara, Joël R. D. Vernet, Proc. of SPIE Vol. 13096, 130960G
© 2024 SPIE · 0277-786X · doi: 10.1117/12.3020803

ABSTRACT

Liger is a next-generation near-infrared (0.81 - 2.45 μm) integral field spectrograph (IFS) and imaging camera for the W. M. Keck Observatory (WMKO) adaptive optics (AO) system. The instrument concept originated by coupling designs from WMKO AO instruments and the future Thirty Meter Telescope IRIS spectrograph. Liger is designed for the Keck I telescope to operate behind the upcoming Keck All-sky Precision Adaptive optics (KAPA) system. The imaging camera sequentially feeds an IFS that makes use of slicer assembly for the coarsest sampling (75 mas and 150 mas per spaxel) and lenslet array (14 mas and 31 mas per spaxel) for diffraction-limited sampling. The imaging camera makes use of off-axis parabolas and a Hawaii-2RG detector to achieve a 14 mas/pixel plate scale and 20.5"×20.5" field of view. The IFS offers a range of spectral resolving power of R=4,000 − 10,000 and yields large fields of view for an AO-fed IFS. Liger will enable new science by providing enhanced capabilities, including higher spectral resolving power, access to shorter wavelengths, and larger fields of view than any current or planned ground- or space-based IFS system. Liger will be able to unlock previously inaccessible science across a wide range of the cosmos, such as dark matter substructure, supermassive black holes, the Galactic Center, exoplanet atmospheres, and the time-variable Solar System. We present the overall design of the Liger subsystems and review unique science drivers.

Keywords: Near-infrared, Integral Field Spectrograph, Imager, Cryogenic, Adaptive Optics, Spectroscopy, Astrometry, Photometry

1. INTRODUCTION

Integral field spectrographs (IFS) play a critical role in both ground-based and space-based observational astronomy today. Prior to the development of IFS technology in the 1990's, astronomical optical and infrared spectroscopy was dominated by slit-based methods.[1] IFS can simultaneously capture spectral and spatial data across a two-dimensional field of view, opening up a range of new and unique science programs. However, it took several decades of instrumentation development for IFS to become prevalent. In addition to the usual instrumentation challenges of throughput, efficiency, and stability, IFS inherently face several unique design challenges. These include the optical design complexity required to sample the focal plane into individual spectral components, achieving a wide field of view while maintaining high spatial resolution with limited detector and optics sizes, and maintaining mechanical and thermal stability to ensure calibration and alignment over long observation periods, as well as handling complex data processing. Research and development over the last two decades, including advancements in higher quality optics (e.g., larger mirrors and lenses with lower wavefront errors, higher throughput fibers, polishing of small format mirrors), and more sensitive and larger format detectors, have significantly advanced IFS technology. Today, optical and infrared IFS facility-class instruments are becoming standard at all major ground-based and space-based observatories.

The development of infrared integral field spectroscopy (IFS) took another decade as larger format infrared detectors were being created in the late 1990s. The breakthrough came with the first 256x256 detector available on the open market, which enabled the creation of the first cryogenic infrared IFS at Palomar Observatory on the 200-inch telescope.[2] As larger format infrared detectors continued to advance, the development of infrared-based IFS for 8-10m class telescopes became possible. During a similar period, Adaptive Optics (AO) systems began to be commissioned at ground-based 8-10m facility-class observatories.[3]

Infrared IFS, coupled with AO, have made excellent strides in development, but there are even greater challenges with sampling the finer plate scales necessary to sample an AO beam. The optical performance of the optics must have superb wavefront errors (WFE) to avoid degrading the AO quality point spread functions (PSF), and wide field format cameras with fast focal ratios are necessary for proper spatial sampling. Additionally, infrared IFS are limited by the number of pixels per infrared detector, which affects the optimization of spectral coverage and field of view (FoV) on the sky. These challenges are compounded by the need to operate the instruments at infrared wavelengths in large (>1 m^3) cryogenic (<70K) chambers to house these wide-field short focal ratio cameras and spectrograph components. Leading AO science cases also require superb stability for calibrations to achieve both high-precision astrometry and photometry. All of these design considerations makes these instruments costly in design and fabrication. For these reasons, to date, there have only been six IFS instruments coupled with 8-10m telescopes using AO systems. Only three are facility-class AO-IFSs

(NIFS/Gemini, SINFONI/VLT, OSIRIS/WMKO) with a broad range of science capabilities, one is a newer facility-class system paired with a new AO system, and two are specialized IFSs designed for extreme-AO and high-contrast capabilities.

NIFS[4] on Gemini Observatory was commissioned in 2003 and is a slicer-based IFS system originally optimized for seeing-limited observations, but later commissioned to be used by the Gemini-North AO system. SINFONI[5] on Very Large Telescope(VLT) was commissioned as an upgrade of SPIFFI[6] in 2004 to serve as a slicer-based IFS system that was both seeing-limited and later AO-fed from the initial VLT AO system, and in 2023 it was upgraded further to ERIS/VLT.[7] OSIRIS/WMKO[8] is a lenslet-based IFS commissioned in 2005, and was the first IFS designed specifically for sampling the diffraction-limit of an 8-10-meter class AO system. MUSE/VLT[9] is a wide-field slicer-based IFS commissioned in 2014 that is primarily for seeing-limited optical (0.46 – 0.93 μm) observations, but offers an AO mode at red optical wavelengths (0.7 – 0.9 μm) with GALACSI.[10] The specialized extreme AO IFS systems, GPI/Gemini[11] and SPHERE/VLT,[12] were commissioned in 2013 for high-contrast exoplanet research. Both GPI and SPHERE use a lenslet-based IFS, like WMKO/OSIRIS, to preserve the WFE to reach diffraction-limited performance. All of these IFS are first-generation systems that have made significant impact on a broad range of science programs.

Following the lessons learned of these ground-based IFSs, designs for the James Webb Space Telescope (JWST) commenced in the early 2000's with NIRSpec[13] (and MIRI[14] at longer wavelengths). Compared to ground-based AO-fed IFS, the JWST NIRSpec IFS is limited to lower spectral resolving power (R<3000) and coarser spatial sampling (100mas per spaxel). Both the IFS of NIRSpec and MIRI are lenslet-based integral field units (IFU) that sample the FoV with a microlenslet array, similar to WMKO/OSIRIS, for the same reasons to preserve the high-fidelity point spread function (PSF). Notably, all AO-fed IFSs, as well as the JWST IFSs, use either a slicer (array of mirrors) or lenslet-based IFU.

To-date, IFSs that demand high optical performance fidelity and low wavefront error (WFE) make use of lenslet-based IFUs. These design considerations between a slicer and lenslet IFU have been well-documented and discussed within the community for the last decade. Briefly, besides any fundamental WFE quality differences between the optics (lenslets vs. slicer mirrors), the primary advantage of lenslet-based IFU is that focal plane is first sampled and then dispersed through a spectrograph. While a slicer-based IFU has to be resampled and reformated through multiple slitlets before dispersed by the spectrograph and therfore has a reduced WFE quality compared to a lenslet-based IFU. Nevertheless, slicer-based IFUs have distinct advantages in that the spectra are more easily packed onto a 2D detector, allowing for larger FoVs and cleaner spectral extraction. Therefore, there is a complex trade-off between spatial sampling (resolved sources vs. diffraction-limited performance), FoV and spectral sampling achieved by the IFS, astrometric precision and accuracy, and direct sensitivity.

Next-generation IFS instruments are in design development using the latest research and development in detectors and optics for W. M. Keck Observatory (Liger[15]), Gemini Observatory (GIRMOS[16]), and ERIS/VLT as a recent upgrade to the SINFONI.[7] GIRMOS is a dual slicer-based IFS that is being designed in Canada for Gemini-North's AO system (GNAO). At longer wavelengths (>2-5 μm), SCALES is a Keck Observatory AO IFS that will utilize both a lenslet-array for spatial sampling and a slicer for reformatting the spectra on the detector.[17] The slicer formatting in this is allowed given the angular resolution differences at longer wavelengths ($> 2\mu$m) with a prime science directive of characterizing directly-imaged exoplanets.

Liger is a next generation instrument that optimizes a single IFS system with both a slicer and lenslet-based IFU to achieve both the diffraction-limited performance of the Keck-I 10-meter telescope, while offering powerful sensitivity for resolved sources. Liger completed its Final Design Phase in 2023 and is now in the fabrication phase. Liger is designed to take advantage of the Keck All-sky Precision Adaptive-optics (KAPA[18]) system, which will increase AO sky coverage with higher Strehl ratios, and enable operations at shorter wavelengths ($<1\mu$m). KAPA is on track for operations in 2025. Liger combines a near-infrared imaging camera and an IFS that operate simultaneously. The Liger spectrograph shares an identical design with the first light TMT instrument, IRIS.[19] While the imaging camera, spectrograph re-imaging optics, and cryostat are unique to Liger, the IFS channels duplicate the IRIS slicer and lenslet IFU systems. All major mechanisms within the spectrograph, including a large surrogate mirror assembly and housing, mask slide, grating turret, and rotary mechanisms for the reimaging optics and periscope mirrors, have been prototyped. This paper details the design and fabrication efforts of the Liger instrument, as well as its unique science drivers.

2. LIGER SYSTEM OVERVIEW & CAPABILITIES

Liger covers the wavelength range 0.81 - 2.45 μm and combines a diffraction-limited IFS and imaging camera.[15,20,21] Both the imager and spectrograph can be used simultaneously, and the light first passes through the imaging optics before entering the spectrograph in what we term a "sequential design." Figure 1 illustrates the Liger optical path. Two small pickoff mirrors close to the imaging detector direct two FOVs into the lenslet and slicer systems. This sequential design has many advantages, including greatly reducing the number of complex mechanisms and optical elements, and providing significant optical performance improvements for a dual imaging and IFS system. In particular, the very expensive set of AO-quality filters are used by both the imager and spectrograph to allow simultaneous operation. The AO system can compensate, or sharpen, image quality all the way to the imager detector while simultaneously improving the IFS optical performance. This allows Liger to have low WFE (see Figure 11)and achieve excellent astrometric performance. The large pupil within the imager also allows for better masking of the thermal background than would occur within the re-imaging optics for the IFS. The imaging camera has a total FoV of 20.5" x 20.5" with a plate scale of 10 mas.

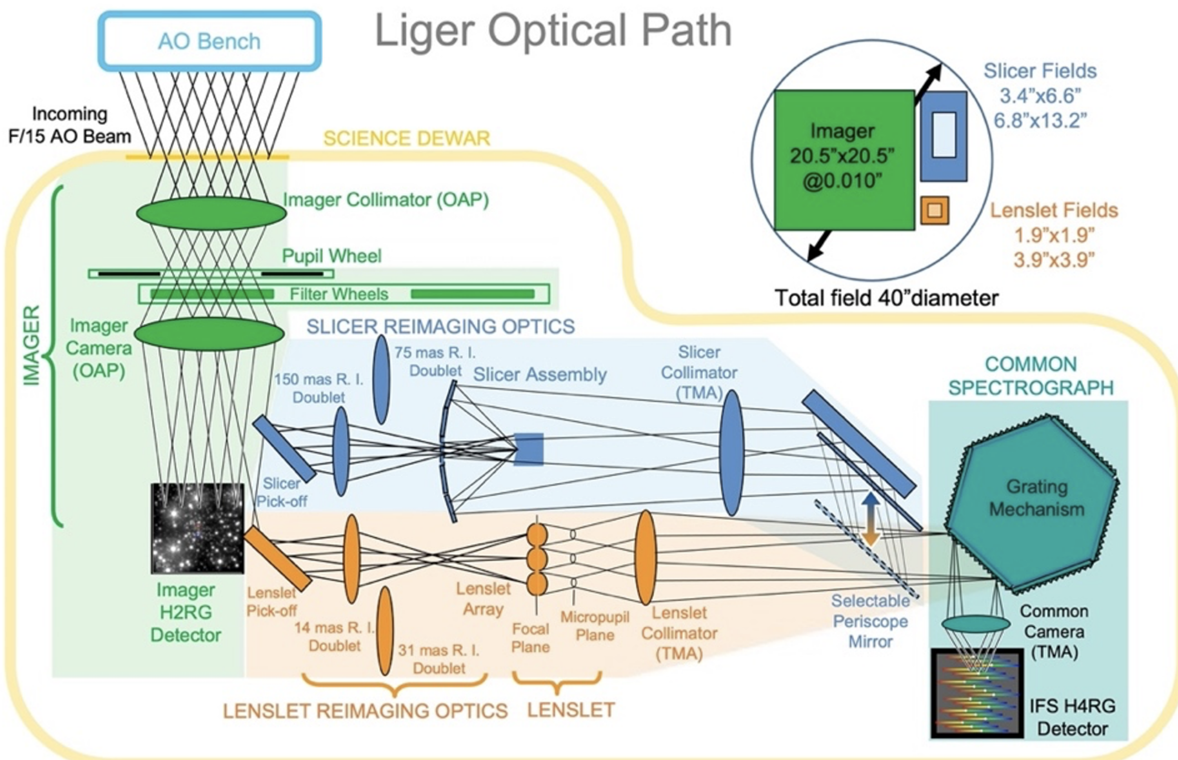

Figure 1: Liger's sequential optical design provides versatile capabilities with the lowest wavefront error of any AO spectrograph. This figure shows the light path of the Liger imager (green), the lenslet IFS (orange), the slicer IFS (blue), and common IFS components (teal). The Keck I AO f/15 beam is fed into Liger at the top left through the science dewar (yellow). The filter wheel and pupil stop feed both the imager and IFS. There are two pick-off mirrors that can select between slicer and lenslet IFS at the focal plane of the imager. The nominal Liger imager and IFS FOV is shown in the top right.

The hybrid IFS incorporates two channels, the slicer and the lenslet, with each offering two separate spaxel scale modes of sampling at the IFU. The choice of using lenslet and slicer spectrograph was heavily explored during the IRIS Conceptual Design Phase to optimize between plate scales and FoV between the finest and coarsest plate scales. It was determined that the lenslet array was capable of preserving excellent WFE, while the slicer design with maximized field coverage and surface brightness sensitivity with the coarsest plate scales.

This led to the hybrid IFS design that uses two sampling techniques while making use of the same gratings, detector, and complex three mirror anastigmat (TMA) optics.

The lenslet spectrograph is designed to offer the diffraction-limited performance with 14 and 31 mas plate scales, and the slicer spectrograph is made for coarser spatially sampling with 75 and 150 mas plate scales. Liger will offer three different spectral resolving powers with R=4000, R=8000, and R=10000 modes. As is true for all IFSs, the selection of the filter and grating (R) determines the FOV of the spectrographs. Liger has a flexible array of observing modes to meet the considerable breadth of science requirements (Table 1).

Table 1: Liger imager and IFS observational modes.

Capability Mode	**Spatial Sampling**	**Field of View arcsec×arcsec**	**IFS Resolution**	**Bandpass (%)**
Imager				
2048×2048	10 mas	20.5”×20.5”	Set by filter	1-20
Lenslet IFS				
128×128	14 mas	1.8”×1.8”	4000	5
128×128	31 mas	4.0”×4.0”	4000	5
16×128	14 mas	0.2”×1.8”	4000-10000	5, 20, 40
16×128	31 mas	0.5”×4.0”	4000-10000	5, 20, 40
Slicer IFS				
88×45	75 mas	6.6”×3.4”	4000	5, 20
88×45	150 mas	13.2”×6.8”	4000	5, 20
44×45	75 mas	3.3”×3.4”	4000-10000	5, 20, 40
44×45	150 mas	6.6”×6.8”	4000-10000	5, 20, 40

The performance of Liger, like any instrument, includes the capabilities and performance of the telescope and the AO system. Liger can be used with the Keck AO system in either natural guide star mode or laser guide star mode. The Keck AO system feeds an f/15 beam into Liger. Our team has developed an end-to-end data simulator and exposure time calculator for investigating performance design trade-offs to aid in developing the science cases and requirements. The data simulator generates both raw data products for developing the data reduction pipeline (Section 4.5) and final data products for investigating science cases, as presented in (Section 3). The simulator includes a full Zeemax model of the telescope, AO, and Liger. The optical path of the major subsystems are presented in Figure 2.

3. SCIENCE DRIVERS

Liger is designed to address fundamental questions in astrophysics. As a facility-class adaptive optics (AO)-fed instrument for the W.M. Keck Observatory, Liger takes advantage of the world's largest optical/infrared telescopes coupled with the best available AO system to maximize the scientific return and discovery potential. Liger represents a significant technological advancement in astronomical instrumentation, incorporating advanced cryogenic alignment techniques, utilizing cutting-edge near-infrared detector technology with various readout modes, and optimizing pristine optical performance across multiple spectral samplings.

In this paper we briefly highlight key scientific objectives for Liger: (1) measuring variation in the fine structure constant in a strong gravitational field and testing general relativity via three-dimensional orbits of hitherto inaccessible stars near the Galactic Center's supermassive black hole (SMBH); (2) determining the currently unknown prevalence of intermediate-mass black holes spanning five orders of magnitude in mass; (3) establishing the origin of the modern-day Hubble sequence of galaxies; (4) high-precision cosmological measurements of the dark matter halo mass function and the Hubble constant using lensed quasars; (5) and understanding the formation of extrasolar planets via their bulk chemical composition and atmospheric structure. We also provide a brief overview of the range of facility-class science that Liger enables.

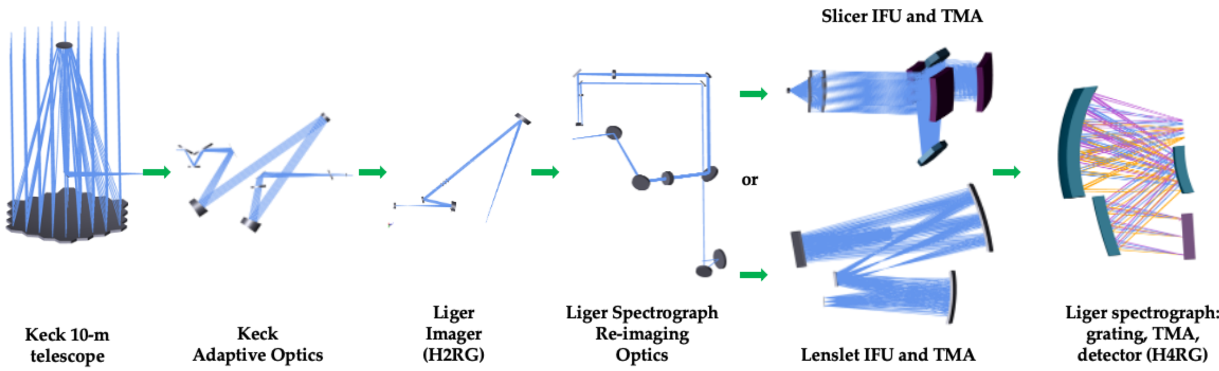

Figure 2: The end-to-end optical path of the Keck I telescope, AO system, and the Liger instrument is presented from left to right as follows: The Keck I telescope beam feeds the AO system, which is located on the Nasmyth deck enclosure. The Liger instrument resides in a cryostat at the fixed port in the AO enclosure. The AO-corrected beam enters the Liger instrument through the imager. Near the imager detector, light is picked off and directed into one of two selectable IFUs (slicer or lenslet). After the IFU divides the light into small apertures, the light path feeds into a common spectrograph.

3.1 Testing Fundamental Physics in the Galactic Center

Research focused on the Galactic Center is a key science case for Liger and Keck/AO. Liger's high spectral resolution, combined with increased sensitivity and parallel imaging and IFS observations (Figure 3), will enable new tests of general relativity (GR) and the underlying equivalence principle – tests that are out of reach for other facilities. A particularly important open question is whether the fine-structure constant varies in strong gravitational potentials; a recent claim for this effect was based on white dwarf measurements.[22] Liger will enable a clear test of this hypothesis by spectrally resolving the relative wavelengths of individual atomic lines, each of which has a unique dependence on the fine-structure constant. The offsets in wavelength between pairs of spectral lines, compared to their offsets on Earth, are a measurement of the variation in the fine-structure constant, as already demonstrated by a proof-of-concept analysis using existing Galactic Center observations.[23] These offsets cannot be resolved with R$\sim$4000 spectra provided by current AO-fed IFSs, as the relevant lines are blended and indistinguishable, with separations of only $2-3$ Angstroms for many important features. In contrast, Liger's R$\sim$10,000 resolution enables such measurements. Based on simulated Liger spectra (Figure 3), we expect to measure variation in the fine-structure constant with precision of for individual stars, comparable to or better than current white dwarf and quasar absorption probes, while reaching a uniquely strong gravitational potential.[24]

Liger's sensitivity will provide radial velocity measurements of faint, short-period (<12 years) stars that have only been observed with imaging, thus probing closer to the SMBH than is currently possible. For example, Liger will be able to measure the radial velocity for S0-102 with a precision of $\sim$10 km/s if it is a late-type star (or $\sim$50 km/s if early-type) within just a half night of observing time.[25] Liger monitoring of such short-period stars will reveal the precession of orbits due to GR effects, and will be able to determine if there is an extended "dark cusp" of compact objects (e.g., stellar mass black holes and neutron stars) predicted to reside in this region.[26,27] While dark cusps are assumed in almost all simulations with supermassive black holes, this theoretical prediction has never been observed, and Liger will provide the key measurements to verify or disprove this prediction. Such measurements require a precise astrometric reference frame and knowledge of the point spread function (PSF), for which Liger's parallel imaging is a critical new capability.

One of the most remarkable aspects of the Galactic Center is the presence of massive stars formed within the last few million years, despite intense tidal forces which should inhibit star formation near the central black hole (e.g., Paumard et al. 2006, Lu et al. 2013). The mystery of these stars' origin is deepened by the fact that the stellar initial mass function (IMF) appears to deviate strongly from the nearly universal IMF found elsewhere in the galaxy. Liger's higher spectral resolution R 10,000 will probe the formation and chemical evolution of

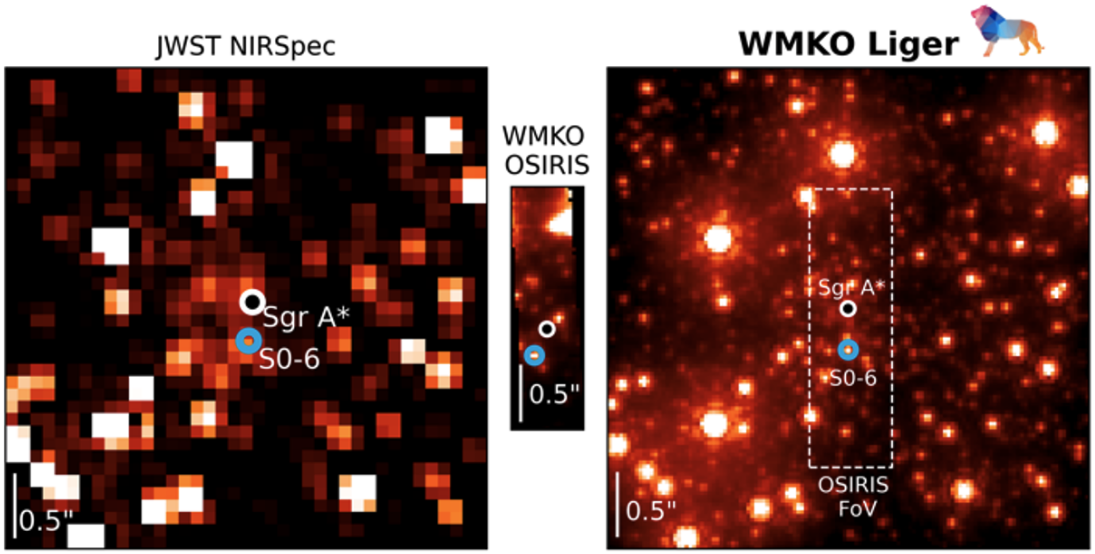

Figure 3: Liger's FOV and spatial resolution coupled with higher spectral resolution will enable high-precision measurements for studying fundamental physics in the Galactic Center. Liger's sampling and angular resolution allow clear separation of individual stars, which are blended even with JWST/NIRSpec (left). The larger IFS FOV compared to current WMKO/OSIRIS (center) covers a much greater number of stars, which improves both astrometric precision and radial-velocity-monitoring efficiency.

these stars by measuring bulk metallicity and, crucially, individual elemental abundances. Liger will enable new understanding of the chemical enrichment of these dense stellar environments and their star-formation history, which controls the rate of supernovae and the amount of gas fueling the growth of the SMBH – both in the Milky Way and, by extension, in other galaxies.

3.2 Quantifying Black Holes Across the Mass Spectrum

Liger will be capable of carrying out a unique search for black holes (BHs) from 10^{3-6} $M_\odot$in low-mass galaxy nuclei and globular clusters; no present-day observations are sensitive to BHs at the intermediate-mass scale $\sim 10^4$ $M_\odot$(Figure 4). With ten times the reach of current observations, Liger will be able measure the BH mass function in this range, providing clues on the seeding mechanism of supermassive BHs. The velocity dispersion around such BHs is only ∼15 km/s, requiring Liger's spectral resolution of R∼10,000 (cf. R<4000 for current AO-fed IFSs) coupled with AO to spatially resolve the sphere of influence. In addition to K-band features, Liger enables AO spectroscopy of the Ca triplet at 0.85 μm, envisioned as a key kinematic probe for next-generation AO systems.[28,29] Furthermore, IFS studies are more powerful when combined with high astrometric precision AO imaging to measure 3D velocity dispersion profiles of Milky Way globular clusters, pushing below the 10^3 $M_\odot$mass regime.

On the lower mass end (3–300 $M_\odot$), LIGO/Virgo has revealed the existence of numerous BHs with surprising masses, both between 3-5 $M_\odot$and with >50 $M_\odot$– all unexpected from stellar evolution theory.[31–33] However, gravitational waves can only probe BHs in merging binaries, and unknown binary characteristics leave the mass function uncertain. Liger will directly measure the BH mass function in the Milky Way from samples of BHs that are isolated or in non-accreting stellar binaries. For binaries, astrometric and radial velocity wobble can detect and determine the masses of BHs in the cores of globular clusters and the Galactic Center — crowded regions that require AO imaging and Liger's IFS with R∼10,000. We can also use gravitational microlensing to find and weigh isolated BHs, which requires <75 μas astrometric precision to detect 3 $M_\odot$black holes towards the Galactic bulge.[34–36] This precision is not possible today; the Gaia space observatory is ineffective in the crowded regions probed by microlensing surveys. Liger's imager with Keck AO at <1μm will uniquely achieve

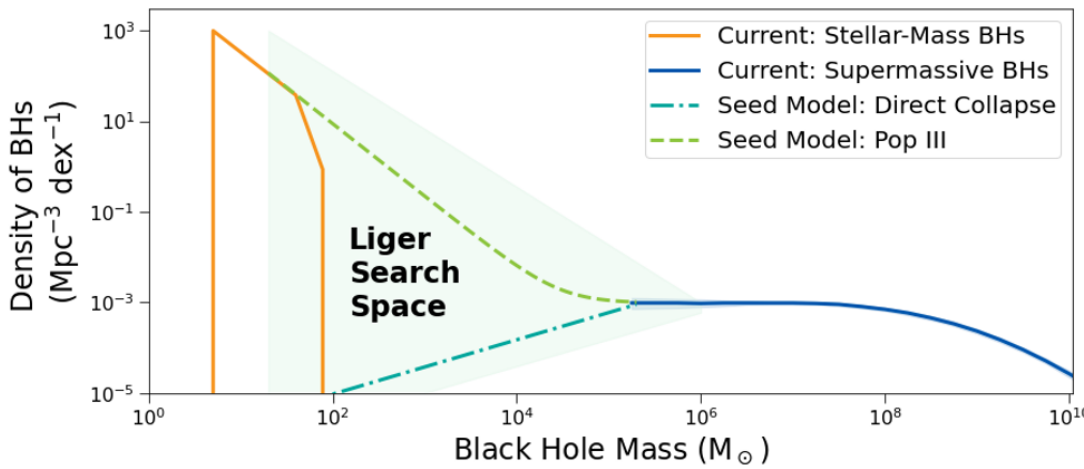

Figure 4: Liger will explore uncharted parameter space in search of elusive intermediate mass BHs. This will solve one of nature's great mysteries: how SMBHs came to exist. Liger enables novel searches across a wide range of mass, from stellar mass BHs via astrometric microlensing and binary companions, to intermediate mass BHs in the nuclei of low-mass galaxies. The results will distinguish between current widely differing theories of SMBH formation, such as accretion from Population III stars or direct collapse from supermassive gas clouds.[30]

this requirement. Additionally, accurate gravitational microlensing results require followup spectroscopy to rule out false positive signals from binary systems; Liger's IFS is ideally suited for this followup.

3.3 Resolving the Formation of the First Disk Galaxies

A key outcome of galaxy growth processes is the transition from clumpy and turbulent systems at early times (redshifts $z \gtrsim 1.5$)[37,38] to thin spiral disks seen today.[39] Determining when and why this thin-disk transition occurred are among the most pressing open questions in galaxy evolution. While the specific driver of this evolution remains unknown, it is widely thought to be a fundamental change in the accretion of gas onto galaxies, which can be tested via spatially resolved measurements of heavy element abundance.[40,41]

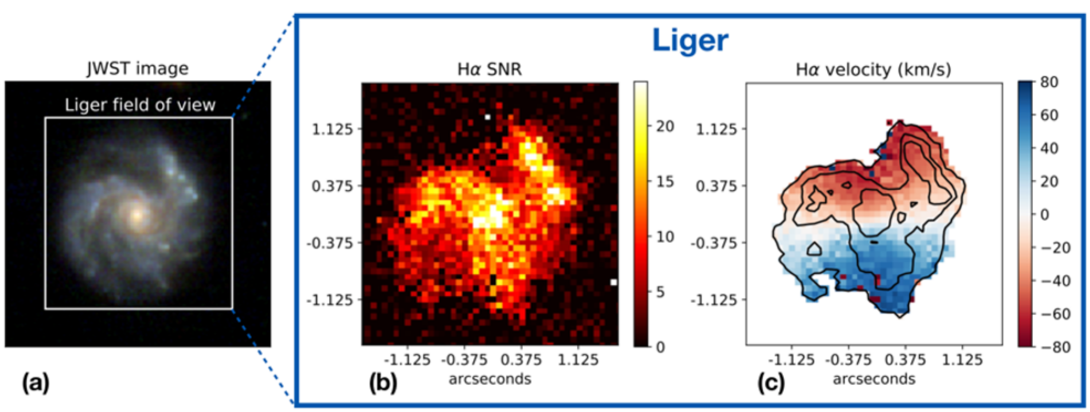

Figure 5: Liger will characterize the formation of high-redshift disk galaxies with its expanded field of view, exquisite sensitivity, and high spectral resolution. (a) The JWST image shows a spiral galaxy at z=1.0, for which the H-α flux is measured spectroscopically. The center and right panels show: (b) the expected H-α signal-to-noise ratio from Liger with 2 hours of integration time, and (c) the recovered velocity field for an inclined gaseous disk with σ=20 km/s, with contours showing H-α emission isophotes. This simulation demonstrates that Liger enables efficient mapping of z$\sim$1 galaxies, reaching the epoch when the first thin disks are thought to form.

Liger will be able to distinguish the emergence of thin disk galaxies using their degree of rotational support (i.e., circular velocity V relative to dispersion σ), and to map the distribution of heavy elements resulting from the baryon cycle. Analyses of galaxy morphologies from Hubble Space Telescope (HST) and JWST imaging reveals a dramatic structural transformation around roughly z$\sim$1: the majority of star-forming galaxies are clumpy and irregular at z$\gtrsim$1.5, while exponential disks dominate at z$\lesssim$1[42,43] (Figure 5). Basic dynamical theory suggests that this change reflects a transformation in the kinematics of rotating galaxies (i.e., V/σ). Yet no existing facility has the requisite spatial and spectral resolution to verify the kinematic properties of these early thin-disk candidates. Liger will aid in pinpointing the era when thin-disk galaxies emerge and the underlying cosmological cause, thanks to its new capabilities: (1) large slicer FOV and excellent sensitivity at wavelengths 1-1.5 μm, for mapping resolved kinematics (from Hα) and heavy element abundances (from emission line ratios) at z$\sim$1; and (2) sufficient spectral resolution to measure robust velocity dispersions down to the thermal broadening limit of $\sigma$$\sim$15 km/s, requiring R$\gtrsim$8,000 to reliably identify thin disks. This will lead to a comprehensive understanding of the physical mechanisms responsible for establishing the modern Hubble sequence of disk galaxies.

Figure 3 shows the ability of Liger's slicer IFS to efficiently map z 1 thin-disk galaxies on kiloparsec (kpc) spatial scales. Liger will enable finder angular resolution and >2$\times$ higher spectral resolution than existing ground-based AO IFSs and the JWST/NIRSpec IFU (for which the resolution limit is $\sigma$$\sim$50 km/s). Liger's higher spectral resolution is critical: with R=4000 resolution, a large correction factor is required to recover a thin-disk velocity dispersion of σ=15 km/s, resulting in large uncertainties. In contrast, for an emission line with the same total signal-to-noise (S/N), R=8000-10000 spectroscopy provides a factor $\sim$3$\times$ smaller uncertainty in the intrinsic velocity dispersion. With increased sensitivity and R$\sim$10,000, the result is that Liger can provide suitable precision in thin-disk kinematics (i.e., velocity dispersion) within a 2-hour integration, whereas the same precision would require >30 hours with Keck/OSIRIS at R$\sim$4000. Thus, Liger will be more than 10$\times$ faster than current instrumentation in studying early thin-disk galaxies.

3.4 Unveiling the Nature of Dark Matter and Dark Energy

The nature of dark matter and dark energy are among the most fundamental open questions in physics and astronomy. Strong gravitational lensing is a powerful tool for addressing both questions, when combined with high-resolution IFS. Liger will help be able to advance our understanding of dark matter and dark energy by enabling studies of strong gravitational lens systems at AO resolution.[44–46] A key requirement is the combination of sensitive high-resolution measurements with a sufficiently large FOV to encompass the full gravitational lens system (Figure 6) – a combination of capabilities unique to Liger.

Strong gravitational lensing constrains dark matter models through detection of low-mass dark matter halos. Low-mass probes are critical for understanding the nature of dark matter, as the widely adopted cold-dark-matter (CDM) paradigm faces several challenges on dwarf galaxy scales.[47] Competing models such as WIMPs (weakly interacting massive particles), ultra-light axions, and sterile neutrinos predict significantly different numbers of halos at masses $\sim$$10^8$ $M_\odot$and below. Such low-mass halos do not form stars and hence cannot be observed in visible light, but they have been demonstrated to affect the relative magnifications observed in strong gravitational lens systems. Thus they can be detected via their gravitational effect even if they contain no stars.[46,48,49]

Liger's FOV and increased sensitivity will revolutionize studies of dark matter using narrow-line emission in lensed quasars (Figure 6[46,50,51]). IFS+AO observations are essential to isolate the narrow-line flux in each lensed image (with typical separation <1 arcsecond). While continuum flux ratios are affected by microlensing from stars in the lens galaxy, the narrow-line region is free of microlensing effects thanks to its larger size, thus providing a clean probe of dark matter halos. Liger's larger FOV and faster throughput compared to OSIRIS will dramatically improve the ability to probe dark matter, including targeting fainter systems than can be currently resolved. With the combined improvement in sample size, and S/N for bright lenses, our performance simulations indicate that Liger will be able to detect a turnover in the dark matter halo mass function at 10^6 $M_\odot$ or larger. Liger will thus reach nearly two orders of magnitude lower in halo mass than the current upper limits ($10^{7.8}$ $M_\odot$),[48] probing into the critical range where dark matter models diverge.

Gravitational time delays between multiple images of lensed quasars have emerged as a powerful new probe of dark energy and the Hubble Constant, already competitive with other established methods.[52] Lensing provides

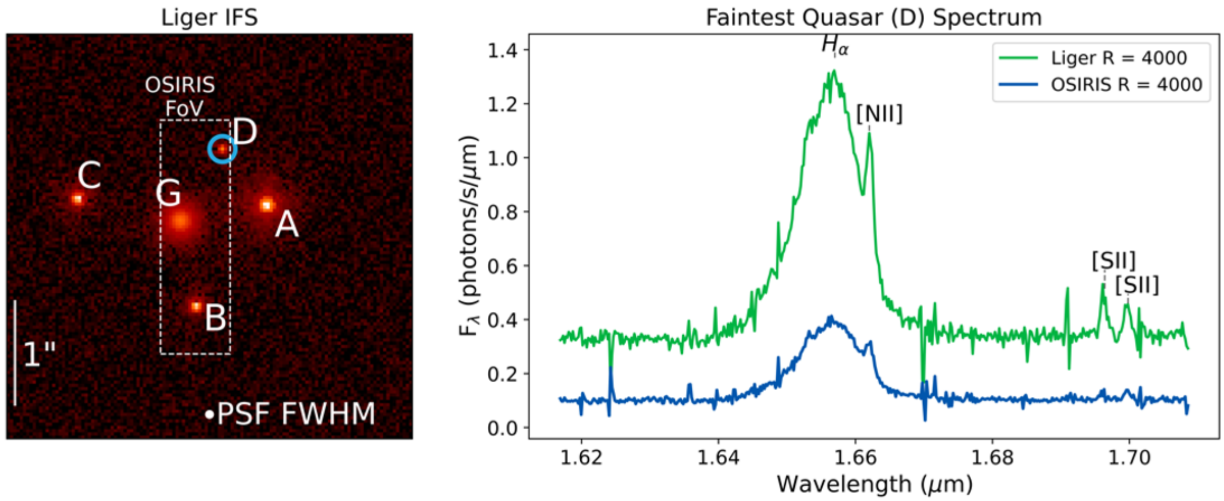

Figure 6: Liger will revolutionize strong gravitational lensing studies of dark matter. Narrow-line emission fluxes in lensed quasar spectra can reveal the presence of low-mass dark matter perturbations. Such a measurement is impossible without AO spectroscopy, given the typical quasar image separations of less than an arcsecond. The left panel shows simulated Liger data of SDSS J0924 with 5400-s exposure time, along with the smaller FOV for OSIRIS. Liger's FOV enables the entire lens to be imaged in a single pointing, reducing uncertainty in flux ratios, and increasing sensitivity to low-mass dark matter substructure via improved astrometry. The right panel shows the measured spectra (photons/s/μm) for the faintest source image, D. Liger's higher throughput and spectral resolution increase S/N in the narrow-line [NII] emission by a factor of 5, and enable the detection of [SII], providing sensitivity to lower-mass dark-matter halos.

an important independent contribution to the exploration of the "Hubble tension", in which the values of the Hubble Constant (H0) measured via traditional distance-ladder techniques[53] differ by more than 4σ from those predicted by combining cosmic microwave background measurements with the standard ΛCDM cosmological model.[54] If this tension is real, and not due to systematic effects, then any explanation requires new physics beyond the "standard model" of cosmology (i.e., ΛCDM), such as early dark energy.[55] The most prominent remaining systematic effect in the lensing technique is the so-called mass-sheet transform,[56] which is maximally degenerate with H0 from lenses. This degeneracy can be broken to a certain extent by measuring a luminosity-weighted central stellar velocity dispersion for the lensing galaxy, which provides an independent measurement of the lensing mass. However, to break the degeneracy and truly obtain robust time-delay H0 measurements requires resolved stellar kinematics of the lensing galaxy.[57] The high resolution provided by AO IFU measurements is critical, since the z 0.5 lensing galaxies have angular scales of an arcsecond or less. Attempts to use OSIRIS for this technique have suffered from low S/N ratios, resulting from the difficulty of detecting absorption lines in the spectra of the faint lensing galaxy.[58]

Liger will be transformational thanks to its enhanced sensitivity, especially given the relatively small number of lensed quasars needed to achieve percent-level measurements of H0 once resolved kinematics of the lensing galaxy are obtained.[57] As an added benefit, Liger observations will provide microlensing-free flux-ratio measurements, providing a key constraint for the mass models of the lens and a useful calibration for quasar microlensing studies.[59]

3.5 Probing the Formation of Exoplanets

Characterizing exoplanet atmospheres is critical to understand the complex processes that impact their structure and evolution, as well as to test leading formation theories. IFS studies of directly imaged planets have provided the best spectra of gas-giant exoplanets to-date,[60–64] with Liger's predecessor OSIRIS taking the first spectrum of a directly imaged exoplanet.[65] Liger, with its combination of short-wavelength sensitivity and high spatial and spectral resolution, offers a critical capability to study exoplanet atmospheres and formation.

Exoplanet formation scenarios in which the separation of solids and gases is important (e.g., core/pebble accretion) predict that gas-giant planets will display more heavy elements in their atmospheres.[66] In contrast, scenarios in which this separation is not critical (e.g., gravitational instability) instead predict fewer heavy elements.[67] Liger will distinguish these hypotheses by enabling the first robust measurements of total heavy element abundance (a.k.a. metallicity), which requires direct spectroscopy with sufficient spectral resolution and broad wavelength coverage (Figure 7).

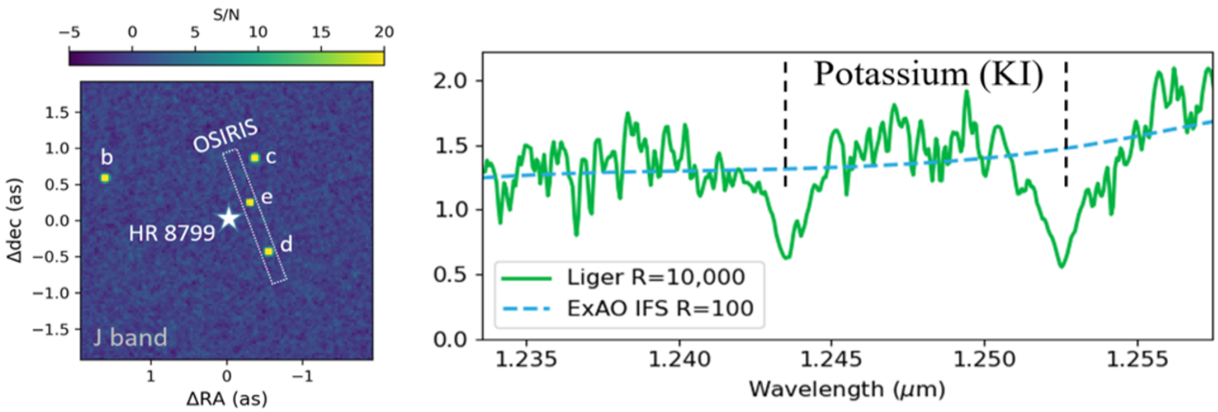

Figure 7: Liger will transform our understanding of exoplanet formation with excellent performance and resolution reaching shorter wavelengths than any other current or planned instruments. (Left) Liger S/N map of four simulated planets b,c,d,e based on the HR 8799 system. The simulation uses an atmospheric model with Teff=900 K, g=56 and solar metallicity (Sonora[68]). (Right) Atmospheric model spectrum of HR 8799 planet b of the prominent KI lines in J band, shown at two resolutions: the R∼100 typical of most direct imaging spectrographs, and Liger's proposed R∼10,000. Resolved lines from alkali features are required to robustly measure the metal enrichment of these exoplanet atmospheres, but no current IFS systems have sufficient short-wavelength sensitivity and spectral resolution. Liger's higher spectral resolution more than doubles the direct-imaging detection S/N, compared to current ExAO systems.

Current studies at high spectral resolution have focused primarily on K band (∼2.2 μm), where both AO and instrument performance have been optimized, detecting species such as CO, H2O, and CH4. These observations are powerful for constraining properties such as the carbon-to-oxygen ratio,[69] however, carbon and oxygen abundances are degenerate with atmospheric processes such as non-equilibrium chemistry.[70] Testing formation theories requires measurements of the overall heavy element enrichment including elements of higher atomic number, observable only at shorter wavelengths. Liger will provide excellent performance at shorter wavelengths, which no currently available or planned instrument offers at high enough spectral resolution (Figure 7). In particular, the J band at ∼1.2 μm includes strong potassium lines as well as metal hydride features, which are highly sensitive to metallicity.[71] Our simulations indicate that Liger addresses an unmet need that will enable the first robust bulk chemical abundance measurements for gas-giant exoplanets, thereby being able to aid in unlocking the fingerprints of their formation.

3.6 Revealing the Time-Variable Solar System

Time-variable phenomena are a major current focus of solar system science. This includes periodic phenomena such as rotational lightcurves and seasonal change,[72] as well as transient phenomena (e.g., cometary and interstellar object apparitions, storm and plume eruptions, occultations and other mutual events, and even impacts and collisions[73]). Liger will enable time-series observing with high spatial and spectral resolution as well as flexible cadence to reveal the rich temporal nature of our solar system, building on Keck Observatory's established legacy.[74–78] High spatial resolution from AO is essential for mapping inhomogenous surfaces and detecting discrete features such as atmospheric storms, volcanic calderas, rings, and satellites. Liger's spectral capabilities ensure that spatial variability will be not merely detected, but well characterized: for example by diagnosing molecular bands of surface ices and minerals, retrieving opacity and altitude distributions of clouds and hazes, and distinguishing outgassed volatile and organic components. In the time domain, observations are characterized by two main parameters: the sampling interval and the campaign duration. Both can be very short or long, spanning timescales from milliseconds (e.g., for occultation events) to decades (e.g., for seasonal variation in the giant planet systems).

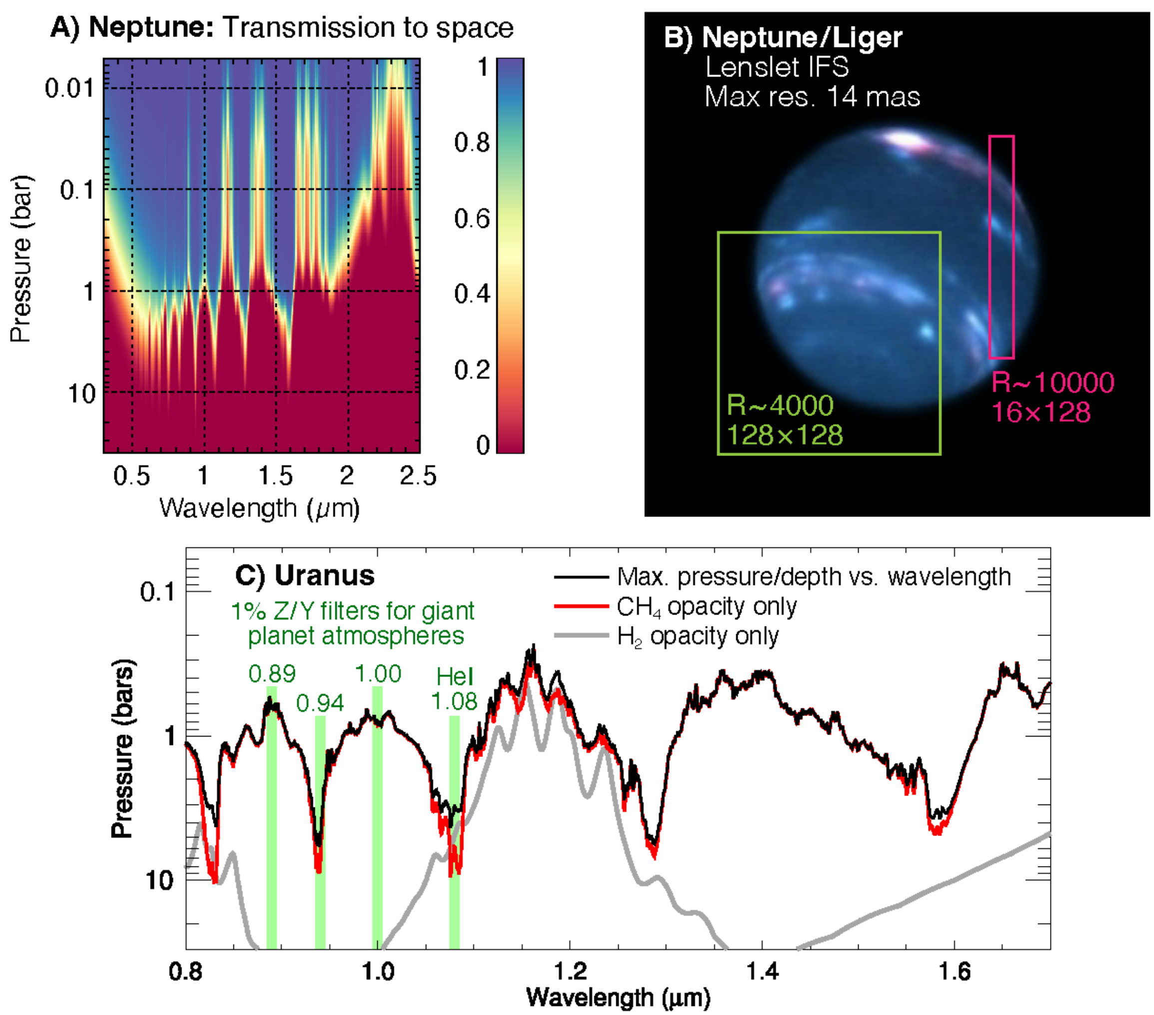

Figure 8: Liger will characterize a wide range of time-variable phenomena in our solar system, such as the atmospheric properties of Neptune and Uranus. Resolved spectral observations of the ice giants in the near infrared can probe aerosol distributions over more than 7 pressure scale heights (A). Liger's lenslet IFU field of view can efficiently map Neptune and can target discrete features on Uranus (B). The near infrared spectrum can be used to measure spatial variation in methane concentration as well as aerosols, and we highlight example features which can be efficiently mapped with narrowband imaging filters (C). Figures adapted from previous studies.[79–81]

We highlight atmospheric activity on the ice giants Uranus and Neptune as an example science case which requires Liger's spatial and spectral capabilities. Figure 8A shows the strong wavelength dependence of gas opacity, with sensitivity to aerosol distributions spanning from the troposphere (reaching pressures of 10 bar) to the stable stratosphere at ¡ 10 mbar. Liger spectroscopy will be able to characterize the highly variable aerosol structure in discrete cloud features (Fig. 8B; we note that Liger's lenslet field of view is well matched to the ice giants). Furthermore, narrowband imaging can efficiently probe similar atmospheric depths with different opacity sources, such as methane and hydrogen (Fig. 8C[81]). Narrowband filters in the Liger imager will thus enable global mapping of methane concentration as well as aerosol distributions in the ice giant atmospheres, combined with detailed spectral maps needed for accurate radiative transfer retrievals in specific atmospheric features. This will address issues such as the connection between convection and methane cloud activity in the hydrogen-rich ice giants,[82] and why they differ from the processes observed in the nitrogen-rich atmospheres of Earth and Titan. The methane cloud layer is expected to have a large molecular weight gradient such that it might inhibit convective activity,[83] providing an observable analog to convective processes in hydrogen-dominated atmospheres from the solar system to giant exoplanets.[84]

Time-series observations of the ice giants are particularly valuable for their ability to provide long-term temporal context for the eventual arrival of NASA's next flagship mission recommended by the planetary decadal survey:[85] the Uranus Orbiter and Probe (UOP) mission. Ground-based observations are essential for bridging the anticipated UOP observations with data from the previous spacecraft visit by Voyager 2 in 1986.[86] Keck observations have enhanced the science return from numerous other NASA planetary missions,[87–89] and Liger is now poised to continue this legacy of forefront planetary science.

4. TECHNICAL DESIGN

Liger is at an advanced state of fabrication readiness. The Liger Final Design Review was completed in March 2023. Liger's spectrograph design is identical to the first-light TMT instrument, Infrared Imaging Spectrograph (IRIS[19, 90, 91]), which has also completed its Final Design Review. Liger has benefitted from >10 years of design from TMT/IRIS partnership and private-foundation funding. This extensive work has produced a design that is capable of maximizing fields of view, spectral coverage, plate-scale flexibility, and image quality with high spectral resolution. Liger's imaging camera provides AO diffraction-limited images with excellent wavefront quality and serves as the feed optics to all simultaneous IFS spectra with the same image quality. Herein, we briefly review all major subsystem design of the instrument.

4.1 Liger Science Cryostat

Liger will be installed in the Keck I AO enclosure, which provides a clean working environment and access for servicing the instrument. The Liger cryostat, or dewar, is a large (1.38-meter diameter) octagonal aluminum cryostat container cooled to 30-77K that is mounted on three kinematic points to the AO enclosure floor. The optical structure including cold shields are mounted to the dewar bottom plate by a hexapod structure made of G-10 fiberglass tubes for thermal isolation (Figure 9). The sides and top of the dewar are a single welded structure that can be lifted off the base to give access to the cryogenic subsystems. To prevent excessive heat release into the AO enclosure, the majority of Liger's electronics will be installed in the AO electronics vault. A small housekeeping electronics rack will be installed next to Liger to monitor internal temperatures and pressures. WMKO has helium compressors and vacuum jacketed lines that provide multiple locations on the telescope ports for closed cycle refrigerators (CCRs). Liger's vibration isolation system for the CCRs is a third-generation system of low-frequency damping springs, where atmospheric pressure partially lifts the CCR bodies towards the dewar. This system is effective and was pioneered by the WMKO AO instruments NIRC2 and OSIRIS.

Internal to the dewar is a primary circular optical plate with secondary plate and mountings with optical housings and baffling around major and minor subsystem. The imager subsystem components are mounted to its own plate on top of the primary optical plate. The slicer assembly and components reside on the top of the optical place, while the lenslet assembly and common spectrograph components are underneath the primary optical plate. The optical plate is thermally isolated from the lower plate of the cryostat using G-10 frames. The optical plate supports two rigid cold shields; one over the top of the optical elements and one over the bottom. The cold shields are wrapped with "blankets" of aluminized mylar to reject radiative loading. Liger will make use of speed controllers with the CCRs to allow the CCRs to operate at high capacity during initial cooling of the cryostat, and then at reduced cooling capacity to provide temperature control and to extend CCR lifespan. Liger is designed to be pumped and cooled down within 10 days. We have designed small heaters for both the imager and spectrograph to maintain detector temperature stability.

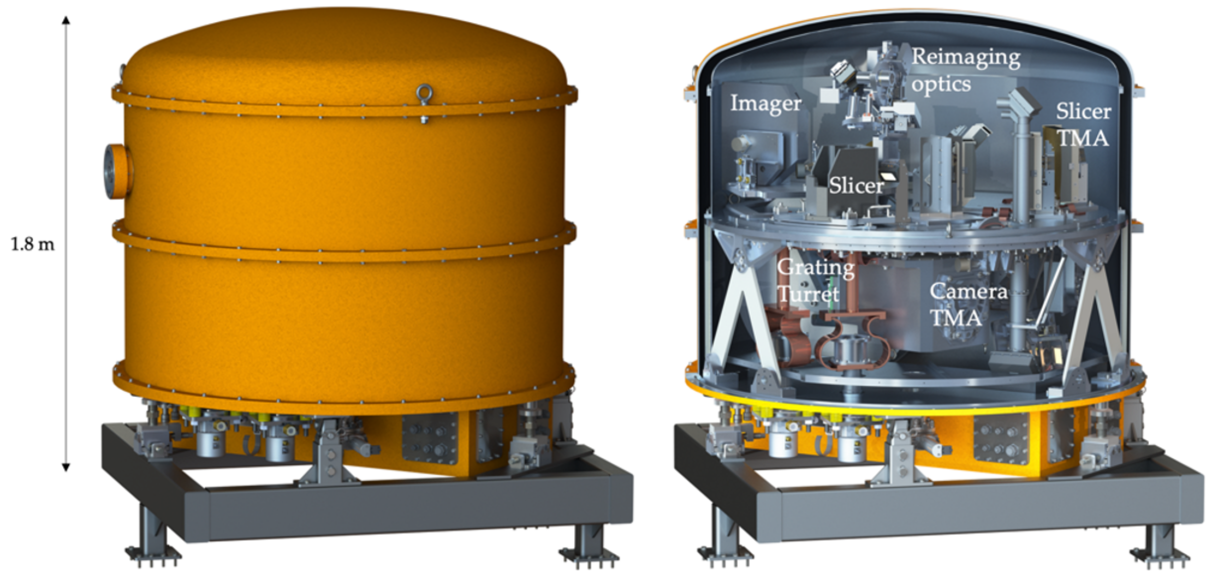

Figure 9: Renderings of the Liger cryostat (left), with the entrance window on the left wall. The cross-section of the dewar (right) shows the optical subsystems and support structure with baffles and cold shield removed. The imager and slicer IFS components are mounted on the top side of the bench, and the common IFS and lenslet IFS components are mounted below.

4.2 Liger imager

The design of the Liger imager is optimized for high throughput, low wavefront error, and low field distortion. The imager provides an optimal plate scale of 10 mas per pixel and a 20.5"x20.5" field of view with the Teledyne Hawaii-2RG (H2RG) detector.[92] A pair of off-axis parabolas (OAPs) provides an achromatic system with no intrinsic ghosts, few optical surfaces, and a high-quality pupil image for placement of a cold stop to mask thermal emission. The design of the filter wheel draws from the heritage of the OSIRIS imager upgrade,[93] and is expanded to provide a significant increase in the number of available filter slots for a total of 51 available bandpass filters. A separate pupil wheel located at the pupil plane houses a set of seven unique pupil masks which provide thermal baffling for both the imager and IFS systems. A trade study modelling the effects of using a mechanically fixed pupil versus rotating masks to match the field rotation on sky found the SNR gains of a rotating pupil mask were minor and would not justify the added complexity.[20] A full stray light analysis informed the mature design of a baffling system for the imager. The design of the H2RG detector mount includes a focusing stage for alignment and mounting for the two pick-off mirrors located at the focal plane to feed the light to the slicer and lenslet IFS, as shown in Figure 10. Performance of the imager is excellent, with <40 nm RMS wavefront error across the full field of view. Stable, low order field distortion of <1.6% will allow precise calibration for astrometry.

4.3 Liger integral field spectrograph

Liger features what we term a "sequential design" in which light passes first through the imager, where pick-off mirrors located next to the imager detector direct light into the slicer or lenslet IFS channels (see Figure 11). The advantages of this design include minimizing non-common path wavefront error between the imager and IFS channels. Without a sequential system, the IFS would require an additional optical relay to provide a pupil location for filters and cold stop. The AO system would not be able to correct for the aberrations in the imager without introducing aberrations into the IFS system, and vice-versa. By utilizing the imager as the feed to the IFS, we can optimize performance to the imager focal plane and simultaneously provide the best image quality to the IFS. Further, this solution significantly reduces the number of cryogenic mechanisms within the instrument and allows the imager detector to provide PSF measurements simultaneously in the same bandpass as the IFS.

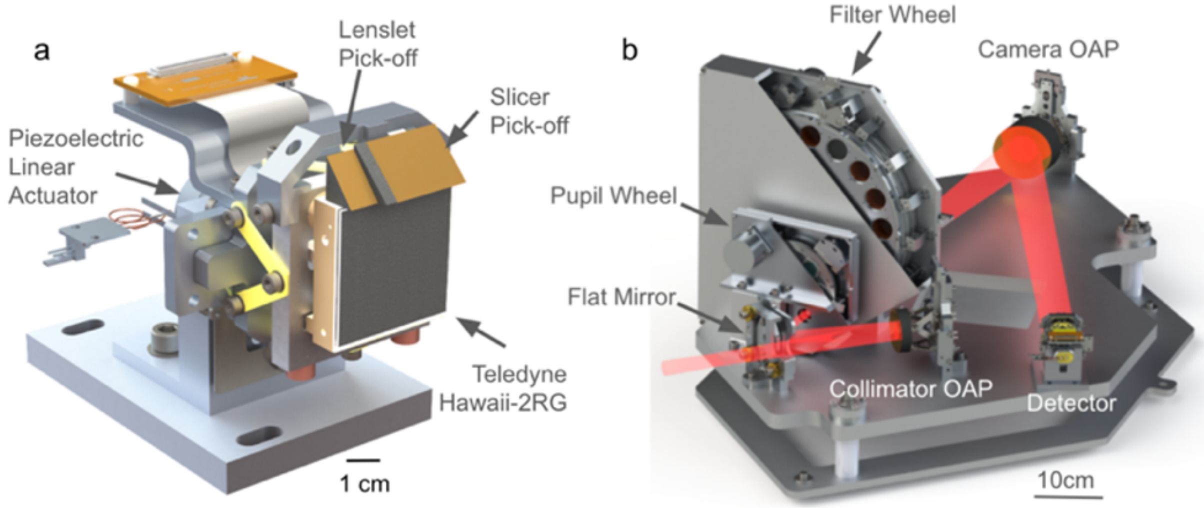

Figure 10: Renderings of the imager with housings and baffling removed or cut-away to show internal components. (a) The mounting mechanism for Teledyne Hawaii-2RG detector and IFS pick-off mirror. Lakeshore temperature sensors and a heater cartridge are attached to the Molybdenum block that the detector is mounted to. A single piezoelectric linear actuator sets the focus distance of both the detector and pick-offs which have a fixed offset between them. (b) All components of the Liger imager are rendered with the beam path highlighted in red. Portions of the filter and pupil wheel housings are removed to show the internal mechanisms. The imager optical plate mounts to the cryostat on three kinematic mounting points to ensure proper alignment with the telescope and IFS.

Liger's IFS design draws from years of experimentation with different IFS strategies for IRIS.[19,91] The resulting design combines a lenslet-based spectrograph for the two finest plate scales (14/31 mas) and a mirror slicer IFU for the two coarsest scales (75/150 mas). This arrangement not only optimizes the performance at each scale – critical for a diverse range of science drivers – but also greatly simplifies both types of spectrograph and allows for sharing of some of the most challenging and expensive components. Both the lenslet and slicer assemblies are built around a common three-mirror anastigmat (TMA) camera, a common grating turret which houses 14 gratings, and one Teledyne Hawaii-4RG-15 μm detector (H4RG), see Figure 12. The lenslet and slicer assemblies sharing the most critical and expensive optical components makes for an optimized and innovative IFS design.

4.3.1 Lenslet IFS

Among the greatest challenges for the spectrograph is the preservation of the excellent image quality provided by WMKO's KAPA system. In the finest plate scale (14 mas) we are required to have uncorrectable wavefront error (WFE) to the science focal plane of <50 nm RMS. In an IFS, this is particularly challenging since the AO system cannot correct aberrations due to different paths within the spectrograph. As demonstrated by WMKO/OSIRIS and Gemini/GPI, a spectrograph based on a lenslet array can preserve image quality at the level of 30 nm of RMS WFE by sampling the image plane prior to the spectrograph optics and by minimizing optics before the lenslet array.

To achieve a balance between spectrograph camera and collimator focal ratios, and to be compatible with the F/4 camera needed by the slicer spectrograph, we selected a lenslet pitch of 350 μm. The array is placed at the focal plane of an achromatic infrared doublet which provides the required spatial sampling on the 350 μm microlenses. The pupil produced by each lenslet is 32 times smaller than its own diameter, including the effects of pupil diffraction. With a clocking of the lenslet array, this compression is sufficient to allow 16 spectra to interleave together in the projected height of an individual lenslet. The full lenslet array provides 128x128

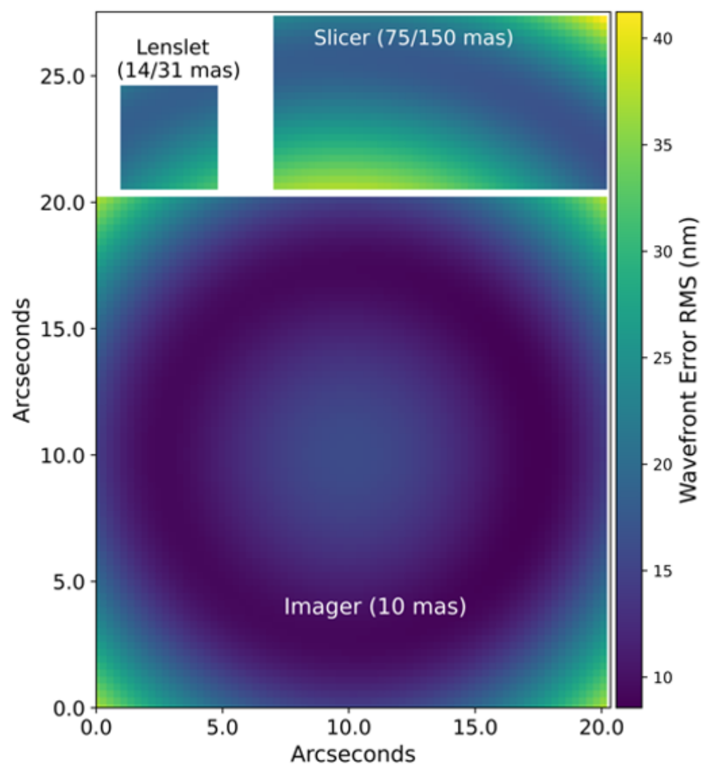

Figure 11: The imager and pick-off mirrors have been designed to optimize optical performance and preserves the fidelity of the WMKO AO performance. The root-mean-square (rms) wavefront error (nm) is shown for the imager field, lenslet pick-off, and slicer pick-off mirrors.

spatial samples, and each lenslet's spectrum can extend for the projected length of a 16x16 block or 512 pixels. In the modes where the spectral resolution is 4,000, this corresponds to a 5% bandpass in each exposure.

To enable high-resolution or long-bandpass spectroscopy and calibration, the IFS is equipped with a mechanized lenslet-masking capability. The lenslet array is mounted with a fixed mask which isolates a nominal serrated square pattern of 128x128 lenslets. For narrow field mode where very long spectra are desired, we mask off the central 16x128 lenslets by moving a mask located in the micro-pupil grid plane to isolate those lenslets. The same mask plate can also be used to isolate individual columns of lenslets for calibration purposes

4.3.2 Slicer IFS

The two coarsest spatial sampling modes of the Liger IFS are provided by an image slicer-based IFS. The slicer IFS provides the widest field-of-view coverage accompanied by a broad spectral bandpass. A small portion of the full Liger field-of-view (see Figure 10) is diverted into the Slicer IFS channel via a pick-off mirror located near the imager detector. The beam is reformatted by means of two sets of user-selectable re-imaging optics to produce the required optical f-ratios for the 75 mas and 150 mas sampling scales at the slicer integral field unit (IFU).

The slicer IFU is a low-expansion glass assembly designed by Winlight Systems, which includes mechanical packaging and baffling to eliminate stray light from the slicer stack mirror edges. The Slicer IFU uses 88 powered mirrors to dissect the rectangular field of view into slices. The 88 beams are then reorganized by pupil and slit mirror arrays into two linear feeds which form the entrance slits of the spectrograph. The two separated pseudo-slits formed by the slicer IFU then pass through the slicer collimator followed by the slicer periscope assembly. The slicer periscope directs the collimated light to the shared grating turret, with the second flat mirror of the periscope mounted as a deployable element to switch the working mode between slicer and lenslet IFS. The

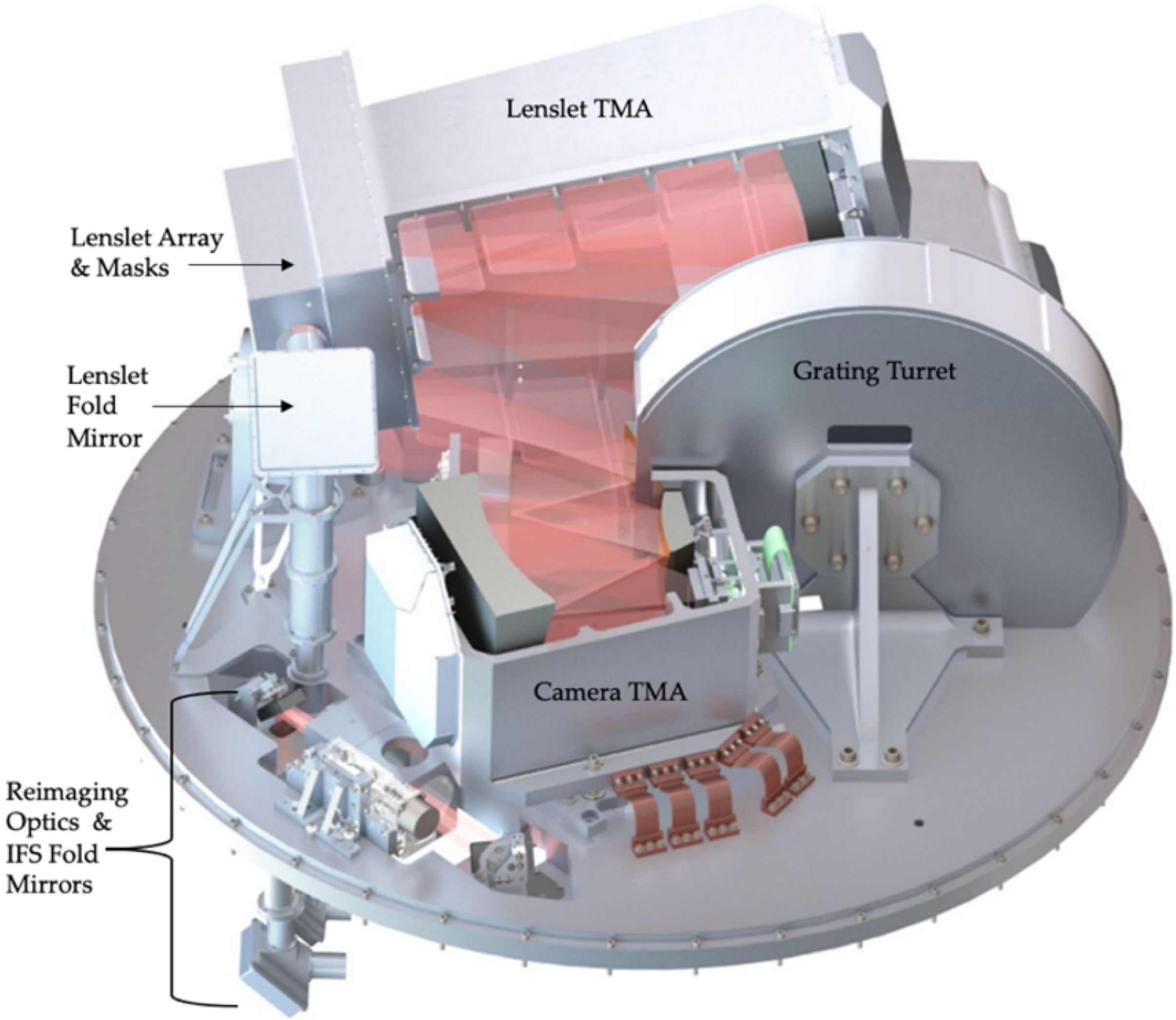

Figure 12: A rendering of the bottom view of the Liger optical plate showing the lenslet assemblies and common IFS assemblies with optical path highlighted (red). For ease of viewing, this image is presented upside down relative to its actual mounting within the instrument. The light from the reimaging optics for the lenslet IFS is on the bottom and then reaches a fold mirror where it enters the lenslet assembly that includes the lenslet array and mask mechanism. After the lenslet array generates individual micro-pupils, it feeds the lenslet TMA and then strikes the grating, which then becomes a common spectrograph with camera TMA and detector.

collimator forms a compound pupil on the grating for all slices and the dispersed light is imaged by the common camera TMA onto the H4RG detector.

4.3.3 IFS Common Components

One of the biggest benefits of Liger's design is the sharing of expensive components including all filters, Lyot stop, gratings, camera optics, and H4RG detector between the four spatial sampling modes of the IFS. The camera optics are fast, with a large field angle, and are perhaps the most complex optical system in the instrument. The large field angles led us early on to perform a trade study between ruled and holographic gratings.[94,95] We found that over our ranges of field angle and bandpass, ruled diffraction gratings had a higher overall efficiency compared to volume phase holographic gratings, given our spectrograph design. The beams from the lenslet and slicer collimators are designed to strike a common rotating turret of ruled diffraction gratings at the same incident angles and are dispersed in wavelength into the common camera optics to the detector, as shown in Figure 13.

For any spectrographic mode, one of fourteen gratings can be chosen for dispersion. The gratings are located on the outer diameter of a large turret, which consists of a 0.8-m diameter wheel with multiple grating positions. The turret has two stepper motors; one for driving its rotation, and a second to push the user selected grating into a kinematic capture system. The mechanism design incorporates cryogenically prepared stepper motors, which have been used in previous Keck observatory instruments; namely, MOSFIRE, OSIRIS, and GPI. All moving parts (bearings, springs, linear slides, etc.) will be similarly prepared and tested for cryogenic use. For the IRIS project, a two-thirds scaled prototype of the turret was fabricated and tested in a cryogenic chamber.[19,91] The prototype system has allowed extensive testing of several versions of the kinematic capture system to achieve the tight repeatability dictated by Liger's science and calibration requirements.

The camera subassembly is one of the most challenging optical systems in any large optical/infrared spectrograph. With a fast focal ratio of F/3.7 and a field angle over 13°, the optical solution requires a challenging three-mirror design with large optics and tight positional tolerances. The camera must accommodate input of collimated light from either the lenslet or slicer elements, after dispersion by the gratings. All Liger mirrors are made of Zerodur mounted to an invar adapter plate through invar flexures. The housings are milled from solid blocks of aluminum 6061-T6. A lightweight cover mounted on top provides no structural support but enables the optics to be aligned with the cover off in a special test chamber. The design of the mirror substrates and their polishing has been developed collaboratively with an outside vendor. Each Zerodur substrate is polished with respect to a coordinate system that is precision aligned to the square facets of the mirror sides and back. The edges of the mirrors can then be probed with a coordinate measuring machine to place all three mirrors within 100 μm of the required location for optical alignment. This is an important early step for the alignment process of the complicated optical subsystems.

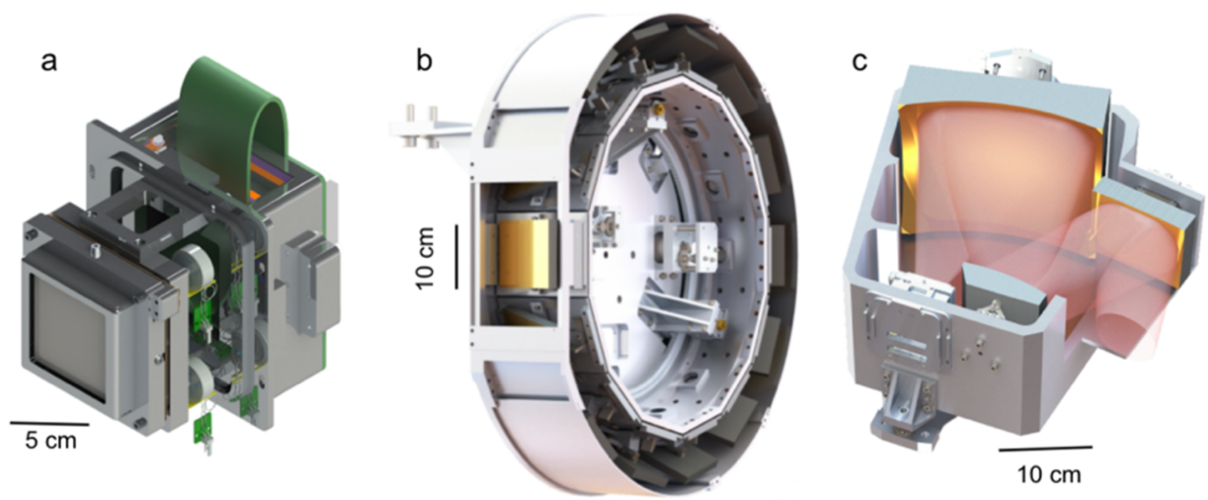

Figure 13: Common spectrograph components of Liger. (a) The Hawaii-4RG detector mount, electronics, and focus stage. Three piezo-electcric linear actuators set the focus of the detector as well as providing tip-tilt adjustments to the detector plane. (b) The grating turret houses 14 selectable gratings. (c) The common camera TMA with light path. The IFS detector records the light in the bottom left of the TMA housing assembly.

The IFS detector head design provides for focus, tip, and tilt at cryogenic temperatures for the H4RG detector. This is not used for science operations but will save months of time in the alignment and optimization process of the IFS. The focus and tip/tilt of the detector is achieved by three cryogenic linear actuators. The same actuators are placed on the lenslet mask slide mechanism to ensure that the lenslet array can be made parfocal with the slicer output pseudo-slits and optimized to the conjugate position of the detector. Figure 14 shows renderings of the common spectrograph components for the spectrograph detector, grating turret, and common camera TMA.

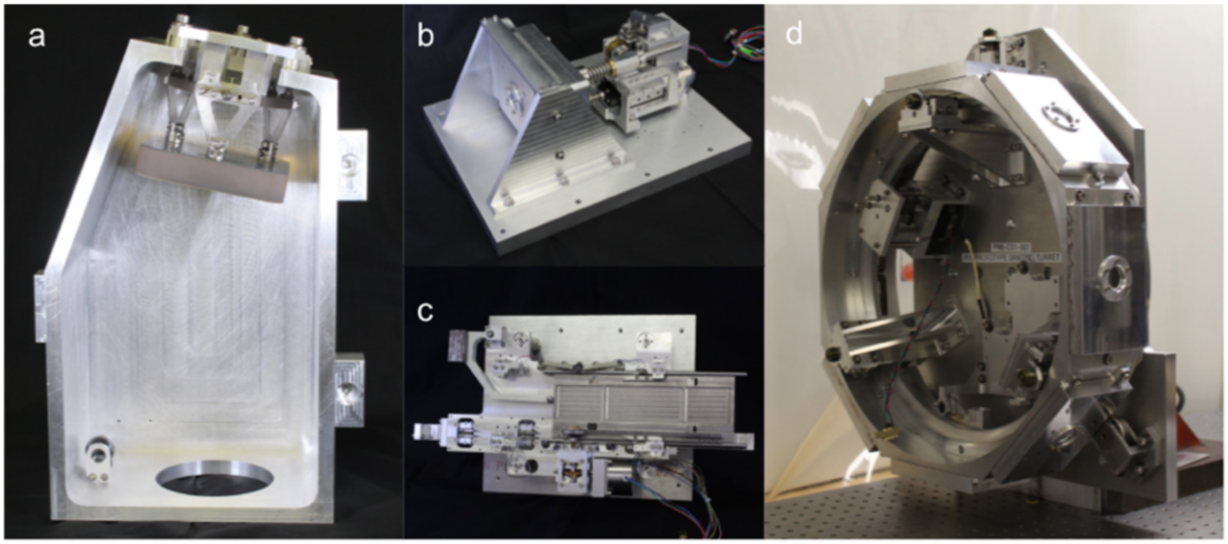

Figure 14: The Liger team has prototyped all cryogenic mechanisms in the Liger dewar. (a) The lenslet TMA assembly has been fabricated and the TMA mirror mounts have been tested and verified with the alignment method. (b) Grating plunger mechanism that drives train, plunger, and grating housing are identical to the full system, but here is separated from the turret. The capture mechanism is built into the bracket at the top of the image and is identical to the capture in the full turret housing. (c) The prototype mask slide mechanism for the selection of the IFS lenslet modes. (d) A 2/3rd size replica of the IFS grating turret was used for cryogenic testing to assess the repeatability of the grating mechanism. This testing aimed to ensure consistent positioning of the dispersed spectra for both the lenslet and slicer IFS.

4.4 Software & Electronics

All low-level control software is based on existing software from previous WMKO instruments. The interaction layer with WMKO is a standard remote-procedure-call (RPC) interface that we have used before. Although Liger requires additional interactions with the more advanced AO system and different Liger mechanisms like the pupil wheel and reimaging optics, these mechanisms are very similar to existing interactions developed for WMKO instruments.

Almost all cryogenic mechanisms use standard stepper motors that are specially prepared to operate at low temperature and under vacuum and use standard Galil motor controllers. These Galil controllers were used with the Gemini Planet Imager instrument and have become a standard for stepper motors. The only exceptions are the cryogenic linear actuators in the detector heads for tip/tilt and focus, but these actuators are used only during alignment and not at the observatory. These are commercial stages that use a standard software interface. A MACIE controller produced by the Markury company that is designed specifically for the Teledyne detectors will be used. In-house software for handling the wide variety of clocking patterns and readout modes are planned for both detectors. High-level software is still required to store data in the Keck data management system and to display to astronomers, but this is similar to several packages our laboratories have delivered before.

To operate at approximately 77K, the entire optical system including all benches, mechanisms and baffles must be cooled and monitored. The system must be maintained in a vacuum near 1 microTorr. To monitor the health and safety of the instrument, we will use two wide-range pressure gauges from Edwards, and Lakeshore temperature diodes and controllers. The pressure gauges provide a redundant system working from atmospheric pressure to well below the microTorr range. We use 16 sensors distributed throughout the dewar to monitor temperatures and gradients. The detectors require temperature control near the milliKelvin level. Each detector uses a Lakeshore temperature controller to monitor and control a heater cartridge and a pair of temperature sensors in an invar base. The heater cartridge uses milliamps of current to safely change the detector by a few degrees with great accuracy but cannot overheat the detector even with a severe electrical or software failure. For safety reasons, we do not use heaters to speed up the warmup of the cryostat. Warming will be done passively and rely on a small amount of residual gas released by the gettering system.

The Liger control electronics will be mounted in a small, insulated rack in a dedicated electronics vault within the AO enclosure. The temperature monitors, controllers and pressure controllers all reside next to the instrument to provide continuous monitoring of the system. The electronics are insulated and have a glycol cooling system to remove most of the waste heat. The control computers (which are by far the dominant source of electrical heating), the power supplies, and the motor controllers are installed in a dedicated electronics vault to the side of the AO enclosure.

4.5 Data Reduction Pipeline

The data reduction system (DRS) is an essential Liger software component that is crucial for meeting the top-level requirements. The Liger DRS includes detector-readout processing, real-time data-quality verification data sets, and post-processing routines for astronomical users to generate science-quality calibrated reduced frames for the imager and spectrograph. The Liger team is developing the DRS by building on existing code and enhancing it with new algorithms required for Liger science cases. The Liger pipeline is written in Python and will be made publicly available at the time of commissioning. The DRS is architected as two primary components: (1) The detector dispatchers will clock the detectors utilizing the MACIE detector controllers, and will assemble raw science frames utilizing CDS, MCDS, or UTR as sequenced from the detector-target computers with the DRS readout processing C library. These frames will then be passed to the pipeline computer. (2) The Liger pipeline is the Python package that implements all the higher-level algorithms that take as input raw science frames and calibrates them to reduced science-ready frames. It includes both the online calibration pipeline run routinely at the observatory and the offline calibration pipelines used for post-processing. The Liger DRS consists of Data

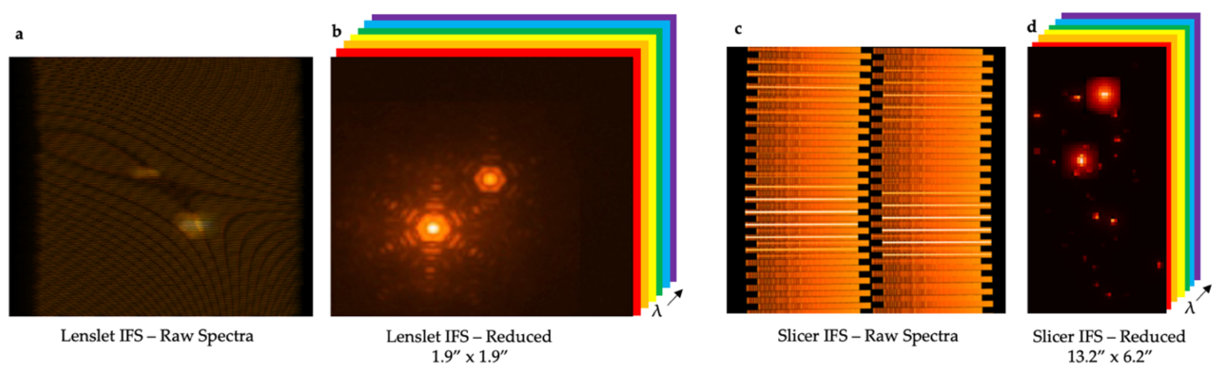

Figure 15: Simulation of the lenslet and slicer IFS data sets, with the Liger DRS reducing the raw products into science-ready data products. In the case of the lenslet IFS, the initial data consist of 16,000 interleaved spectra (a), and upon extraction, a data cube is generated, comprising the original image distributed across 500 independent spectral channels (b). For the slicer IFS, two extended slits created by the slicer Integral Field Unit (IFU) are each dispersed across half of the detector, with up to 2000 spectral pixels (c). The DRS then processes these raw data to yield a finalized science-ready data product (d).

Reduction Pipelines (DRPs) for both the imager and the spectrograph. The Liger pipeline is built upon the framework of the JWST "stpipe" package,[96] which allows for the implementation of data-reduction algorithms as distinct steps. These steps are organized into pipelines, configured, and then executed. In 2019, our team initiated a direct collaboration with the JWST team for pipeline development and calibration for Liger and TMT/IRIS. The choice to use a familiar pipeline from "stpipe" was deliberate, since it ensures that astronomers will be adept at easily reducing and analyzing Liger datasets and provides continuity to pipeline across the community.

The Liger team has developed an end-to-end data simulator to investigate performance and spectral layout on the detector, as well as to advance data-reduction algorithms like spectral extraction. Both the lenslet and slicer spectrographs produce a spectrum for each pixel that efficiently uses the detector pixels. Advanced DRP routines are used to extract the raw spectra from the detector (x, y) and to generate a wavelength-calibrated data cube. Using the Liger simulator we are able to verify spectral-extraction routines for both the lenslet and slicer IFS (see Figure 15)

All Liger data will be stored in the publicly accessible Keck Observatory Archive (KOA)[97] following standard data proprietary periods. The existing OSIRIS/WMKO pipeline, and the PI is the chief architect for the IRIS pipeline software development for TMT.[98–100] The Liger data simulator is based on the advanced IRIS simulator[101,102] that has been in development for many years.

5. SUMMARY

The Liger instrument for the W. M. Keck Observatory has transitioned into its fabrication phase following a decade of design and prototyping. Liger is now poised for construction and subsequent commissioning at Keck I. The instrument features a "sequential design" that integrates near-infrared integral field spectroscopy (IFS) slicer and lenslet-based techniques and imaging capabilities. Liger will be particularly unique and effective when combined with the upcoming KAPA system, which together will provide excellent AO sensitivities and performance.

The development of Liger reflects the broader evolution of ground-based near-infrared IFS instrumentation, which has become increasingly complex and sophisticated since the first generation of integral field spectrographs. The current era demands extensive design efforts, often spanning many years and requiring collaboration among large, multidisciplinary teams. This complexity also translates into substantial resource requirements, posing significant challenges for securing adequate funding. These challenges are evident not only within the national funding structures of the USA but also internationally, where coordination and resource allocation can be equally demanding.

The ground-based astronomical instrumentation community will need to proactively address these resource and development challenges and may need to engage more effectively with the space-based community on how to scale up new instrument programs in the coming decade. This complexity will only increase with the arrival of extremely large telescopes (ELTs). Instrument development programs like Liger are critical for the development of instruments for these ELT programs, supporting research and development efforts, while enabling cutting-edge synergistic science programs on 8-10m class telescopes.

Upon its commissioning, Liger will be a facility-class instrument for use on Keck I to the entire community, significantly expanding the observatory's AO scientific capabilities. The instrument's advanced design will support a wide array of new scientific investigations, providing exceptional data across a range of cosmic distances.

ACKNOWLEDGMENTS

The design and development of the Liger instrument have been made possible by the Heising-Simons Foundation (Grant 2018-1085), the Gordon and Betty Moore Foundation (Grant 11169), and the National Science Foundation (NSF) Advanced Technologies and Instrumentation (ATI Grant 2308190).

Instrumentation is a team effort spanning many years and involving numerous individuals. The Liger instrument design builds on the work from IRIS for the Thirty Meter Telescope International Observatory, including contributions from the authors herein, though it does not encompass all who have contributed to IRIS. Special thanks go to individuals like Eric Chisholm, Anna Moore, and Ryuji Suzuki for their support and early design efforts for IRIS. Additionally, we thank the UC San Diego administrative staff, particularly Sharon Franks, Wendy Groves, Sandy Rosas, I-Hsun Wu, and Muriel Croom, for their support of Liger.

The authors wish to recognize and acknowledge the significant cultural role and reverence that the summit of Maunakea holds within the Native Hawaiian community. We are deeply grateful for the land stewardship and the ongoing ability to conduct research on this mountain. Liger will be fabricated at University of California campuses, which reside on unceded land of the indigenous people of this area, including the Kumeyaay, Gabrielino, Tongva, and Awaswas nations.

REFERENCES

[1] Bacon, R., Adam, G., Baranne, A., Courtes, G., Dubet, D., Dubois, J. P., Emsellem, E., Ferruit, P., Georgelin, Y., Monnet, G., Pecontal, E., Rousset, A., and Say, F., "3D spectrography at high spatial resolution. I. Concept and realization of the integral field spectrograph TIGER.," A&AS **113**, 347 (Oct. 1995).

[2] Murphy, T. W., J., Matthews, K., and Soifer, B. T., "A Cryogenic Integral Field Spectrograph for the Palomar 200 Inch Telescope," PASP **111**, 1176–1184 (Sept. 1999).

[3] Hardy, J. W., [*Adaptive Optics for Astronomical Telescopes*] (1998).

[4] McGregor, P. J., Conroy, P., Bloxham, G., and van Harmelen, J., "Near-infrared Integral-Field Spectrograph (NIFS): An Instrument Proposed for Gemini," PASA **16**, 273–287 (Dec. 1999).

[5] Eisenhauer, F., Genzel, R., Alexander, T., Abuter, R., Paumard, T., Ott, T., Gilbert, A., Gillessen, S., Horrobin, M., Trippe, S., Bonnet, H., Dumas, C., Hubin, N., Kaufer, A., Kissler-Patig, M., Monnet, G., Ströbele, S., Szeifert, T., Eckart, A., Schödel, R., and Zucker, S., "SINFONI in the Galactic Center: Young Stars and Infrared Flares in the Central Light-Month," ApJ **628**, 246–259 (July 2005).

[6] Horrobin, M., Eisenhauer, F., Tecza, M., Thatte, N., Genzel, R., Abuter, R., Iserlohe, C., Schreiber, J., Schegerer, A., Lutz, D., Ott, T., and Schödel, R., "First results from SPIFFI. I: The Galactic Center," *Astronomische Nachrichten* **325**, 88–91 (Feb. 2004).

[7] Davies, R., Absil, O., Agapito, G., Agudo Berbel, A., Baruffolo, A., Biliotti, V., Black, M., Bonaglia, M., Bonse, M., Briguglio, R., Campana, P., Cao, Y., Carbonaro, L., Cortes, A., Cresci, G., Dallilar, Y., Dannert, F., De Rosa, R. J., Deysenroth, M., Di Antonio, I., Di Cianno, A., Di Rico, G., Doelman, D., Dolci, M., Dorn, R., Eisenhauer, F., Esposito, S., Fantinel, D., Ferruzzi, D., Feuchtgruber, H., Finger, G., Förster Schreiber, N. M., Gao, X., Gemperlein, H., Genzel, R., Gillessen, S., Ginski, C., Glauser, A. M., Glindemann, A., Grani, P., Hartl, M., Hayoz, J., Heida, M., Henry, D., Hofmann, R., Huber, H., Kasper, M., Keller, C., Kenworthy, M., Kravchenko, K., Kuntschner, H., Lacour, S., Lightfoot, J., Lunney, D., Lutz, D., Macintosh, M., Mannucci, F., Marsset, M., Modigliani, A., Neeser, M., Orban de Xivry, G., Ott, T., Pallanca, L., Patapis, P., Pearson, D., Peña, E., Percheron, I., Puglisi, A., Quanz, S. P., Rabien, S., Rau, C., Riccardi, A., Salasnich, B., Schmid, H. M., Schubert, J., Serra, B., Shimizu, T., Snik, F., Sturm, E., Tacconi, L., Taylor, W., Valentini, A., Waring, C., Wiezorrek, E., and Xompero, M., "The Enhanced Resolution Imager and Spectrograph for the VLT," A&A **674**, A207 (June 2023).

[8] Larkin, J., Barczys, M., Krabbe, A., Adkins, S., Aliado, T., Amico, P., Brims, G., Campbell, R., Canfield, J., Gasaway, T., Honey, A., Iserlohe, C., Johnson, C., Kress, E., LaFreniere, D., Lyke, J., Magnone, K., Magnone, N., McElwain, M., Moon, J., Quirrenbach, A., Skulason, G., Song, I., Spencer, M., Weiss, J., and Wright, S., "OSIRIS: a diffraction limited integral field spectrograph for Keck," in [*Society of Photo-Optical Instrumentation Engineers (SPIE) Conference Series*], McLean, I. S. and Iye, M., eds., *Society of Photo-Optical Instrumentation Engineers (SPIE) Conference Series* **6269**, 62691A (June 2006).

[9] Laurent, F., Henault, F., Renault, E., Bacon, R., and Dubois, J.-P., "Design of an Integral Field Unit for MUSE, and Results from Prototyping," PASP **118**, 1564–1573 (Nov. 2006).

[10] Stuik, R., Bacon, R., Conzelmann, R., Delabre, B., Fedrigo, E., Hubin, N., Le Louarn, M., and Ströbele, S., "GALACSI The ground layer adaptive optics system for MUSE," New A Rev. **49**, 618–624 (Jan. 2006).

[11] Macintosh, B., Graham, J., Palmer, D., Doyon, R., Gavel, D., Larkin, J., Oppenheimer, B., Saddlemyer, L., Wallace, J. K., Bauman, B., Erikson, D., Poyneer, L., Sivaramakrishnan, A., Soummer, R., and Veran, J.-P., "Adaptive optics for direct detection of extrasolar planets: the Gemini Planet Imager," *Comptes Rendus Physique* **8**, 365–373 (Apr. 2007).

[12] Carbillet, M., Bendjoya, P., Abe, L., Guerri, G., Boccaletti, A., Daban, J.-B., Dohlen, K., Ferrari, A., Robbe-Dubois, S., Douet, R., and Vakili, F., "Apodized Lyot coronagraph for SPHERE/VLT. I. Detailed numerical study," *Experimental Astronomy* **30**, 39–58 (May 2011).

[13] Laurent, F., Bonneville, C., Ferruit, P., Henault, F., Lemonnier, J.-P., Moreaux, G., Prieto, E., and Robert, D., "Optical design, fabrication, and testing a prototype of the NIRSpec IFU," in [*Optical Fabrication, Testing, and Metrology*], Geyl, R., Rimmer, D., and Wang, L., eds., *Society of Photo-Optical Instrumentation Engineers (SPIE) Conference Series* **5252**, 443–453 (Feb. 2004).

[14] Kruizinga, B., Visser, H., Pel, J. W., Moddemeijer, K., and Smorenburg, C., "MIRI spectrometer optical design," in [*5th International Conference on Space Optics*], Warmbein, B., ed., *ESA Special Publication* **554**, 263–271 (June 2004).

[15] Wright, S., Larkin, J. E., Jones, T., Kupke, R., Fitzgerald, M., Kassis, M., Cosens, M., Chisholm, E., Do, T., Fassnacht, C., Fisher, D., Ghez, A., Johnson, C., Keane, J., Kirby, E., Kress, E., Konopacky, Q., Lu, J. R., Maire, J., O'Meara, J., Reddy, N., Sanders, R., Sandstrom, K., Shapley, A., Sohn, J.-M., Surya, A., Treu, T., Weber, R., Wiley, J., Wizinowich, P., Wong, M., and Zonca, A., "Liger: Next Generation Imager and Spectrograph for Keck Observatory Adaptive Optics," in [*Bulletin of the American Astronomical Society*], **51**, 201 (Sept. 2019).

[16] Sivanandam, S., Chapman, S., Erickson, D., Hickson, P., Thibault, S., Sawicki, M., Muzzin, A., Dunn, J., Peck, A., Roberts, S., Venn, K., Sivo, G., Tschimmel, M., Henderson, D., Lamb, M., Chen, S., Dutt, S., Lardière, O., Anthony, A., Hill, A., Brousseau, D., and Chabot, T., "Gemini Infrared Multi-Object Spectrograph: preliminary design overview," in [*Ground-based and Airborne Instrumentation for Astronomy VIII*], Evans, C. J., Bryant, J. J., and Motohara, K., eds., *Society of Photo-Optical Instrumentation Engineers (SPIE) Conference Series* **11447**, 114471A (Dec. 2020).

[17] Skemer, A. J., Stelter, R. D., Sallum, S., MacDonald, N., Kupke, R., Ratliff, C., Banyal, R., Hasan, A., Varshney, H. M., Surya, A., Prakaesh, A., Thirupathi, S., Sethuram, R., K. V., G., Fitzgerald, M. P., Wang, E., Kassis, M., Absil, O., Alvarez, C., Batalha, N., Boucher, M.-A., Bourgenot, C., Brandt, T., Briesemeister, Z., de Kleer, K., de Pater, I., Deich, W., Divakar, D., Filion, G., Gauvin, É., Gonzales, M., Greene, T., Hinz, P., Jensen-Clem, R., Johnson, C., Kain, I., Kruglikov, G., Lach, M., Landry, J.-T., Li, J., Liu, M. C., Lyke, J., Magnone, K., Marin, E., Martin, E., Martinez, R., Mawet, D., Miles, B., Sandford, D., Sheehan, P., Sohn, J. M., and Stone, J., "Design of SCALES: a 2-5 micron coronagraphic integral field spectrograph for Keck Observatory," in [*Ground-based and Airborne Instrumentation for Astronomy IX*], Evans, C. J., Bryant, J. J., and Motohara, K., eds., *Society of Photo-Optical Instrumentation Engineers (SPIE) Conference Series* **12184**, 121840I (Aug. 2022).

[18] Wizinowich, P., Lu, J. R., Cetre, S., Chin, J., Correia, C., Delorme, J. R., Gers, L., Lilley, S., Lyke, J., Marin, E., Ragland, S., Richards, P., Surendran, A., Wetherell, E., Chen, C. F., Chu, D., Do, T., Fassnacht, C., Freeman, M., Gautam, A., Ghez, A., Hunter, L., Jones, T., Liu, M. C., Mawet, D., Max, C., Morris, M., Phillips, M., Ruffio, J. B., Rundquist, N. E., Sabhlok, S., Terry, S., Treu, T., and Wright, S., "Keck All sky Precision Adaptive optics program overview," in [*Adaptive Optics Systems VIII*], Schreiber, L., Schmidt, D., and Vernet, E., eds., *Society of Photo-Optical Instrumentation Engineers (SPIE) Conference Series* **12185**, 121850Q (Aug. 2022).

[19] Larkin, J. E., Wright, S. A., Chisholm, E. M., Andersen, D., Dekany, R. G., Dunn, J. S., Hayano, Y., Kupke, R., Smith, R., Suzuki, R., Weber, R. W., and Zhang, K., "The Infrared Imaging Spectrograph (IRIS) for TMT: instrument overview," in [*Ground-based and Airborne Instrumentation for Astronomy VIII*], Evans, C. J., Bryant, J. J., and Motohara, K., eds., *Society of Photo-Optical Instrumentation Engineers (SPIE) Conference Series* **11447**, 114471Y (Dec. 2020).

[20] Cosens, M., Wright, S. A., Arriaga, P., Brown, A., Fitzgerald, M., Jones, T., Kassis, M., Kress, E., Kupke, R., Larkin, J. E., Lyke, J., Wang, E., Wiley, J., and Yeh, S., "Liger for next-generation Keck AO: filter wheel and pupil design," in [*Ground-based and Airborne Instrumentation for Astronomy VIII*], Evans, C. J., Bryant, J. J., and Motohara, K., eds., *Society of Photo-Optical Instrumentation Engineers (SPIE) Conference Series* **11447**, 114474X (Dec. 2020).

[21] Wiley, J., Mathur, K., Brown, A., Wright, S., Cosens, M., Maire, J., Fitzgerald, Michael amd Jones, T., Kassis, M., Kress, E., Kupke, R., Larkin, J. E., Lyke, J., Wang, E., and Yey, S., "Liger for Next-Generation Keck Adaptive Optics: Cryogenic Chamber for the Imaging Camera," in [*Ground-based and Airborne Instrumentation for Astronomy VI*], Shields, J., ed., *Society of Photo-Optical Instrumentation Engineers (SPIE) Conference Series* **11447**, 11447–311 (Dec. 2020).

[22] Hu, J., Webb, J. K., Ayres, T. R., Bainbridge, M. B., Barrow, J. D., Barstow, M. A., Berengut, J. C., Carswell, R. F., Dumont, V., Dzuba, V., Flambaum, V. V., Lee, C. C., Reindl, N., Preval, S. P., and Tchang-Brillet, W. Ü. L., "Measuring the fine-structure constant on a white dwarf surface; a detailed analysis of Fe V absorption in G191-B2B," MNRAS **500**, 1466–1475 (Jan. 2021).

[23] Hees, A., Do, T., Roberts, B. M., Ghez, A. M., Nishiyama, S., Bentley, R. O., Gautam, A. K., Jia, S., Kara, T., Lu, J. R., Saida, H., Sakai, S., Takahashi, M., and Takamori, Y., "Search for a Variation of the Fine Structure Constant around the Supermassive Black Hole in Our Galactic Center," Phys. Rev. Lett. **124**, 081101 (Feb. 2020).

[24] Murphy, M. T., Malec, A. L., and Prochaska, J. X., "Precise limits on cosmological variability of the fine-structure constant with zinc and chromium quasar absorption lines," MNRAS **461**, 2461–2479 (Sept. 2016).

[25] Meyer, L., Ghez, A. M., Schödel, R., Yelda, S., Boehle, A., Lu, J. R., Do, T., Morris, M. R., Becklin, E. E., and Matthews, K., "The Shortest-Known-Period Star Orbiting Our Galaxy's Supermassive Black Hole," *Science* **338**, 84 (Oct. 2012).

[26] Alexander, T., "Stellar Dynamics and Stellar Phenomena Near a Massive Black Hole," ARA&A **55**, 17–57 (Aug. 2017).

[27] Baumgardt, H., Amaro-Seoane, P., and Schödel, R., "The distribution of stars around the Milky Way's central black hole. III. Comparison with simulations," A&A **609**, A28 (Jan. 2018).

[28] Do, T., Wright, S. A., Barth, A. J., Barton, E. J., Simard, L., Larkin, J. E., Moore, A. M., Wang, L., and Ellerbroek, B., "Prospects for Measuring Supermassive Black Hole Masses with Future Extremely Large Telescopes," AJ **147**, 93 (Apr. 2014).

[29] Greene, J., Barth, A., Bellini, A., Bellovary, J., Holley-Bockelmann, K., Do, T., Gallo, E., Gebhardt, K., Gultekin, K., Haiman, Z., Hosek, Matthew, J., Kim, D., Libralato, M., Lu, J., Nyland, K., Malkan, M., Reines, A., Seth, A., Treu, T., Walsh, J., and Wrobel, J., "The Local Relics of of Supermassive Black Hole Seeds," BAAS **51**, 83 (May 2019).

[30] Greene, J. E., Strader, J., and Ho, L. C., "Intermediate-Mass Black Holes," ARA&A **58**, 257–312 (Aug. 2020).

[31] Abbott, B. P., Abbott, R., Abbott, T. D., Abraham, S., Acernese, F., Ackley, K., Adams, C., Adhikari, R. X., Adya, V. B., Affeldt, C., Agathos, M., Agatsuma, K., Aggarwal, N., Aguiar, O. D., Aiello, L., Ain, A., Ajith, P., Allen, G., Allocca, A., Aloy, M. A., Altin, P. A., Amato, A., Ananyeva, A., Anderson, S. B., Anderson, W. G., Angelova, S. V., Antier, S., Appert, S., Arai, K., Araya, M. C., Areeda, J. S., Arène, M., Arnaud, N., Arun, K. G., Ascenzi, S., Ashton, G., Aston, S. M., Astone, P., Aubin, F., Aufmuth, P., AultONeal, K., Austin, C., Avendano, V., Avila-Alvarez, A., Babak, S., Bacon, P., Badaracco, F., Bader, M. K. M., Bae, S., Baker, P. T., Baldaccini, F., Ballardin, G., Ballmer, S. W., Banagiri, S., Barayoga, J. C., Barclay, S. E., Barish, B. C., Barker, D., Barkett, K., Barnum, S., Barone, F., Barr, B., Barsotti, L., Barsuglia, M., Barta, D., Bartlett, J., Bartos, I., Bassiri, R., Basti, A., Bawaj, M., Bayley, J. C., Bazzan, M., Bécsy, B., Bejger, M., Belahcene, I., Bell, A. S., Beniwal, D., Berger, B. K., Bergmann, G., Bernuzzi, S., Bero, J. J., Berry, C. P. L., Bersanetti, D., Bertolini, A., Betzwieser, J., Bhandare, R., Bidler, J., Bilenko, I. A., Bilgili, S. A., Billingsley, G., Birch, J., Birney, R., Birnholtz, O., Biscans, S., Biscoveanu, S., Bisht, A., Bitossi, M., Bizouard, M. A., Blackburn, J. K., Blair, C. D., Blair, D. G., Blair, R. M., Bloemen, S., Bode, N., Boer, M., Boetzel, Y., Bogaert, G., Bondu, F., Bonilla, E., Bonnand, R., Booker, P., Boom, B. A., Booth, C. D., Bork, R., Boschi, V., Bose, S., Bossie, K., Bossilkov, V., Bosveld, J., Bouffanais, Y., Bozzi, A., Bradaschia, C., Brady, P. R., Bramley, A., Branchesi, M., Brau, J. E., Briant, T., Briggs, J. H., Brighenti, F., Brillet, A., Brinkmann, M., Brisson, V., Brockill, P., Brooks, A. F., Brown, D. D., Brunett, S., Buikema, A., Bulik, T., Bulten, H. J., Buonanno, A., Buscicchio, R., Buskulic, D., Buy, C., Byer, R. L., Cabero, M., Cadonati, L., Cagnoli, G., Cahillane, C., Calderón Bustillo, J., Callister, T. A., Calloni, E., Camp, J. B., Campbell, W. A., Canepa, M., Cannon, K. C., Cao, H., Cao, J., Capocasa, E., Carbognani, F., Caride, S., Carney, M. F., Carullo, G., Casanueva Diaz, J., Casentini, C., Caudill, S., Cavaglià, M., Cavalier, F., Cavalieri, R., Cella, G., Cerdá-Durán, P., Cerretani, G., Cesarini, E., Chaibi, O., Chakravarti, K., Chamberlin, S. J., Chan, M., Chao, S., Charlton, P., Chase, E. A., Chassande-Mottin, E., Chatterjee, D., Chaturvedi, M., Chatziioannou, K., Cheeseboro, B. D., Chen, H. Y., Chen, X., Chen, Y., Cheng, H. P., Cheong, C. K., Chia, H. Y., Chincarini, A., Chiummo, A., Cho, G., Cho, H. S., Cho, M., Christensen, N., Chu, Q., Chua, S., Chung, K. W., Chung, S., Ciani, G., Ciobanu, A. A., Ciolfi, R., Cipriano, F., Cirone, A., Clara, F., Clark, J. A., Clearwater, P., Cleva, F., Cocchieri, C., Coccia, E., Cohadon, P. F., Cohen, D., Colgan, R., Colleoni, M., Collette, C. G., Collins, C., Cominsky, L. R., Constancio, M., J., Conti, L., Cooper, S. J., Corban, P., Corbitt, T. R., Cordero-Carrión, I., Corley,

K. R., Cornish, N., Corsi, A., Cortese, S., Costa, C. A., Cotesta, R., Coughlin, M. W., Coughlin, S. B., Coulon, J. P., Countryman, S. T., Couvares, P., Covas, P. B., Cowan, E. E., Coward, D. M., Cowart, M. J., Coyne, D. C., Coyne, R., Creighton, J. D. E., Creighton, T. D., Cripe, J., Croquette, M., Crowder, S. G., Cullen, T. J., Cumming, A., Cunningham, L., Cuoco, E., Dal Canton, T., Dálya, G., Danilishin, S. L., D'Antonio, S., Danzmann, K., Dasgupta, A., Da Silva Costa, C. F., Datrier, L. E. H., Dattilo, V., Dave, I., Davier, M., Davis, D., Daw, E. J., DeBra, D., Deenadayalan, M., Degallaix, J., De Laurentis, M., Deléglise, S., Del Pozzo, W., DeMarchi, L. M., Demos, N., Dent, T., De Pietri, R., Derby, J., De Rosa, R., De Rossi, C., DeSalvo, R., de Varona, O., Dhurandhar, S., Díaz, M. C., Dietrich, T., Di Fiore, L., Di Giovanni, M., Di Girolamo, T., Di Lieto, A., Ding, B., Di Pace, S., Di Palma, I., Di Renzo, F., Dmitriev, A., Doctor, Z., Donovan, F., Dooley, K. L., Doravari, S., Dorrington, I., Downes, T. P., Drago, M., Driggers, J. C., Du, Z., Ducoin, J. G., Dupej, P., Dwyer, S. E., Easter, P. J., Edo, T. B., Edwards, M. C., Effler, A., Ehrens, P., Eichholz, J., Eikenberry, S. S., Eisenmann, M., Eisenstein, R. A., Essick, R. C., Estelles, H., Estevez, D., Etienne, Z. B., Etzel, T., Evans, M., Evans, T. M., Fafone, V., Fair, H., Fairhurst, S., Fan, X., Farinon, S., Farr, B., Farr, W. M., Fauchon-Jones, E. J., Favata, M., Fays, M., Fazio, M., Fee, C., Feicht, J., Fejer, M. M., Feng, F., Fernandez-Galiana, A., Ferrante, I., Ferreira, E. C., Ferreira, T. A., Ferrini, F., Fidecaro, F., Fiori, I., Fiorucci, D., Fishbach, M., Fisher, R. P., Fishner, J. M., Fitz-Axen, M., Flaminio, R., Fletcher, M., Flynn, E., Fong, H., Font, J. A., Forsyth, P. W. F., Fournier, J. D., Frasca, S., Frasconi, F., Frei, Z., Freise, A., Frey, R., Frey, V., Fritschel, P., Frolov, V. V., Fulda, P., Fyffe, M., Gabbard, H. A., Gadre, B. U., Gaebel, S. M., Gair, J. R., Gammaitoni, L., Ganija, M. R., Gaonkar, S. G., Garcia, A., García-Quirós, C., Garufi, F., Gateley, B., Gaudio, S., Gaur, G., Gayathri, V., Gemme, G., Genin, E., Gennai, A., George, D., George, J., Gergely, L., Germain, V., Ghonge, S., Ghosh, A., Ghosh, A., Ghosh, S., Giacomazzo, B., Giaime, J. A., Giardina, K. D., Giazotto, A., Gill, K., Giordano, G., Glover, L., Godwin, P., Goetz, E., Goetz, R., Goncharov, B., González, G., Gonzalez Castro, J. M., Gopakumar, A., Gorodetsky, M. L., Gossan, S. E., Gosselin, M., Gouaty, R., Grado, A., Graef, C., Granata, M., Grant, A., Gras, S., Grassia, P., Gray, C., Gray, R., Greco, G., Green, A. C., Green, R., Gretarsson, E. M., Groot, P., Grote, H., Grunewald, S., Gruning, P., Guidi, G. M., Gulati, H. K., Guo, Y., Gupta, A., Gupta, M. K., Gustafson, E. K., Gustafson, R., Haegel, L., Halim, O., Hall, B. R., Hall, E. D., Hamilton, E. Z., Hammond, G., Haney, M., Hanke, M. M., Hanks, J., Hanna, C., Hannam, M. D., Hannuksela, O. A., Hanson, J., Hardwick, T., Haris, K., Harms, J., Harry, G. M., Harry, I. W., Haster, C. J., Haughian, K., Hayes, F. J., Healy, J., Heidmann, A., Heintze, M. C., Heitmann, H., Hello, P., Hemming, G., Hendry, M., Heng, I. S., Hennig, J., Heptonstall, A. W., Hernandez Vivanco, F., Heurs, M., Hild, S., Hinderer, T., Hoak, D., Hochheim, S., Hofman, D., Holgado, A. M., Holland, N. A., Holt, K., Holz, D. E., Hopkins, P., Horst, C., Hough, J., Howell, E. J., Hoy, C. G., Hreibi, A., Huerta, E. A., Huet, D., Hughey, B., Hulko, M., Husa, S., Huttner, S. H., Huynh-Dinh, T., Idzkowski, B., Iess, A., Ingram, C., Inta, R., Intini, G., Irwin, B., Isa, H. N., Isac, J. M., Isi, M., Iyer, B. R., Izumi, K., Jacqmin, T., Jadhav, S. J., Jani, K., Janthalur, N. N., Jaranowski, P., Jenkins, A. C., Jiang, J., Johnson, D. S., Jones, A. W., Jones, D. I., Jones, R., Jonker, R. J. G., Ju, L., Junker, J., Kalaghatgi, C. V., Kalogera, V., Kamai, B., Kandhasamy, S., Kang, G., Kanner, J. B., Kapadia, S. J., Karki, S., Karvinen, K. S., Kashyap, R., Kasprzack, M., Katsanevas, S., Katsavounidis, E., Katzman, W., Kaufer, S., Kawabe, K., Keerthana, N. V., Kéfélian, F., Keitel, D., Kennedy, R., Key, J. S., Khalili, F. Y., Khan, H., Khan, I., Khan, S., Khan, Z., Khazanov, E. A., Khursheed, M., Kijbunchoo, N., Kim, C., Kim, J. C., Kim, K., Kim, W., Kim, W. S., Kim, Y. M., Kimball, C., King, E. J., King, P. J., Kinley-Hanlon, M., Kirchhoff, R., Kissel, J. S., Kleybolte, L., Klika, J. H., Klimenko, S., Knowles, T. D., Koch, P., Koehlenbeck, S. M., Koekoek, G., Koley, S., Kondrashov, V., Kontos, A., Koper, N., Korobko, M., Korth, W. Z., Kowalska, I., Kozak, D. B., Kringel, V., Krishnendu, N., Królak, A., Kuehn, G., Kumar, A., Kumar, P., Kumar, R., Kumar, S., Kuo, L., Kutynia, A., Kwang, S., Lackey, B. D., Lai, K. H., Lam, T. L., Landry, M., Lane, B. B., Lang, R. N., Lange, J., Lantz, B., Lanza, R. K., Lartaux-Vollard, A., Lasky, P. D., Laxen, M., Lazzarini, A., Lazzaro, C., Leaci, P., Leavey, S., Lecoeuche, Y. K., Lee, C. H., Lee, H. K., Lee, H. M., Lee, H. W., Lee, J., Lee, K., Lehmann, J., Lenon, A., Leroy, N., Letendre, N., Levin, Y., Li, J., Li, K. J. L., Li, T. G. F., Li, X., Lin, F., Linde, F., Linker, S. D., Littenberg, T. B., Liu, J., Liu, X., Lo, R. K. L., Lockerbie, N. A., London, L. T., Longo, A., Lorenzini, M., Loriette, V., Lormand, M., Losurdo, G., Lough, J. D., Lousto, C. O., Lovelace, G., Lower, M. E., Lück, H., Lumaca, D., Lundgren, A. P., Lynch, R., Ma, Y., Macas, R., Macfoy, S., MacInnis, M., Macleod, D. M., Macquet, A., Magaña-Sandoval, F., Magaña Zertuche, L., Magee, R. M., Majorana, E., Maksimovic, I., Malik, A., Man, N., Mandic, V., Mangano, V., Mansell, G. L., Manske, M., Mantovani, M., Mapelli, M., Marchesoni, F., Marion, F., Márka, S., Márka, Z., Markakis, C., Markosyan, A. S., Markowitz, A., Maros, E., Marquina, A., Marsat, S., Martelli, F., Martin, I. W., Martin, R. M., Martynov, D. V., Mason, K., Massera, E., Masserot, A., Massinger, T. J., Masso-Reid, M., Mastrogiovanni, S., Matas, A., Matichard, F., Matone, L., Mavalvala, N., Mazumder, N., McCann, J. J., McCarthy, R., McClelland, D. E., McCormick, S., McCuller, L., McGuire, S. C., McIver, J., McManus, D. J., McRae, T., McWilliams, S. T., Meacher, D., Meadors, G. D., Mehmet, M., Mehta, A. K., Meidam, J., Melatos, A., Mendell, G., Mercer, R. A., Mereni, L., Merilh, E. L., Merzougui, M., Meshkov, S., Messenger, C., Messick, C., Metzdorff, R., Meyers, P. M., Miao, H., Michel, C., Middleton, H., Mikhailov, E. E., Milano, L., Miller, A. L., Miller, A., Millhouse, M., Mills, J. C., Milovich-Goff, M. C., Minazzoli, O., Minenkov, Y., Mishkin, A., Mishra, C., Mistry, T., Mitra, S., Mitrofanov, V. P., Mitselmakher, G., Mittleman, R., Mo, G., Moffa, D., Mogushi, K., Mohapatra, S. R. P., Montani, M., Moore, C. J., Moraru, D., Moreno, G., Morisaki, S., Mours, B., Mow-Lowry, C. M., Mukherjee, A., Mukherjee, D., Mukherjee, S., Mukund, N., Mullavey, A., Munch, J., Muñiz, E. A., Muratore, M., Murray, P. G., Nagar, A., Nardecchia, I., Naticchioni, L., Nayak, R. K., Neilson, J., Nelemans, G., Nelson, T. J. N., Nery, M., Neunzert, A., Ng, K. Y., Ng, S., Nguyen, P., Nichols, D., Nissanke, S., Nocera, F., North, C., Nuttall, L. K., Obergaulinger, M., Oberling, J., O'Brien, B. D., O'Dea, G. D., Ogin, G. H., Oh, J. J., Oh, S. H., Ohme, F., Ohta, H., Okada, M. A., Oliver, M., Oppermann, P., Oram, R. J., O'Reilly, B., Ormiston, R. G., Ortega, L. F., O'Shaughnessy, R., Ossokine, S., Ottaway, D. J., Overmier, H., Owen, B. J., Pace, A. E., Pagano, G., Page, M. A., Pai, A., Pai, S. A., Palamos, J. R., Palashov, O., Palomba, C., Pal-Singh, A., Pan, H.-W., Pang, B., Pang, P. T. H., Pankow, C., Pannarale, F., Pant, B. C., Paoletti, F., Paoli, A., Parida, A., Parker, W., Pascucci, D., Pasqualetti, A., Passaquieti, R., Passuello, D., Patil, M., Patricelli, B., Pearlstone, B. L., Pedersen, C., Pedraza, M., Pedurand, R., Pele, A., Penn, S., Perez, C. J., Perreca, A., Pfeiffer, H. P., Phelps, M., Phukon, K. S., Piccinni, O. J., Pichot, M., Piergiovanni, F., Pillant, G., Pinard, L., Pirello, M., Pitkin, M., Poggiani, R., Pong, D. Y. T., Ponrathnam, S., Popolizio, P., Porter, E. K., Powell, J., Prajapati, A. K., Prasad, J., Prasai, K., Prasanna, R., Pratten, G., Prestegard, T., Privitera, S., Prodi, G. A., Prokhorov, L. G., Puncken, O., Punturo, M., Puppo, P., Pürrer, M., Qi, H., Quetschke, V., Quinonez, P. J., Quintero, E. A., Quitzow-James, R., Raab, F. J., Radkins, H., Radulescu, N., Raffai, P., Raja, S., Rajan, C., Rajbhandari, B., Rakhmanov, M., Ramirez, K. E., Ramos-Buades, A., Rana, J., Rao, K., Rapagnani, P., Raymond, V., Razzano, M., Read, J., Regimbau, T., Rei, L., Reid, S., Reitze, D. H., Ren, W., Ricci, F., Richardson, C. J., Richardson, J. W., Ricker, P. M., Riles, K., Rizzo, M., Robertson, N. A., Robie, R., Robinet, F., Rocchi, A., Rolland, L., Rollins, J. G., Roma, V. J., Romanelli, M., Romano, R., Romel, C. L., Romie, J. H., Rose, K., Rosińska, D., Rosofsky, S. G., Ross, M. P., Rowan, S., Rüdiger, A., Ruggi, P., Rutins, G., Ryan, K., Sachdev, S., Sadecki, T., Sakellariadou, M., Salconi, L., Saleem, M., Samajdar, A., Sammut, L., Sanchez, E. J., Sanchez, L. E., Sanchis-Gual, N., Sandberg, V., Sanders, J. R., Santiago, K. A., Sarin, N., Sassolas, B., Sathyaprakash, B. S., Saulson, P. R., Sauter, O., Savage, R. L., Schale, P., Scheel, M., Scheuer, J., Schmidt, P., Schnabel, R., Schofield, R. M. S., Schönbeck, A., Schreiber, E., Schulte, B. W., Schutz, B. F., Schwalbe, S. G., Scott, J., Scott, S. M., Seidel, E., Sellers, D., Sengupta, A. S., Sennett, N., Sentenac, D., Sequino, V., Sergeev, A., Setyawati, Y., Shaddock, D. A., Shaffer, T., Shahriar, M. S., Shaner, M. B., Shao, L., Sharma, P., Shawhan, P., Shen, H., Shink, R., Shoemaker, D. H., Shoemaker, D. M., ShyamSundar, S., Siellez, K., Sieniawska, M., Sigg, D., Silva, A. D., Singer, L. P., Singh, N., Singhal, A., Sintes, A. M., Sitmukhambetov, S., Skliris, V., Slagmolen, B. J. J., Slaven-Blair, T. J., Smith, J. R., Smith, R. J. E., Somala, S., Son, E. J., Sorazu, B., Sorrentino, F., Souradeep, T., Sowell, E., Spencer, A. P., Spera, M., Srivastava, A. K., Srivastava, V., Staats, K., Stachie, C., Standke, M., Steer, D. A., Steinke, M., Steinlechner, J., Steinlechner, S., Steinmeyer, D., Stevenson, S. P., Stocks, D., Stone, R., Stops, D. J., Strain, K. A., Stratta, G., Strigin, S. E., Strunk, A., Sturani, R., Stuver, A. L., Sudhir, V., Summerscales, T. Z., Sun, L., Sunil, S., Suresh, J., Sutton, P. J., Swinkels, B. L., Szczepańczyk, M. J., Tacca, M., Tait, S. C., Talbot, C., Talukder, D., Tanner, D. B., Tápai, M., Taracchini, A., Tasson, J. D., Taylor, R., Thies, F., Thomas, M., Thomas, P., Thondapu, S. R., Thorne, K. A., Thrane, E., Tiwari, S., Tiwari, S., Tiwari, V., Toland, K., Tonelli, M., Tornasi, Z., Torres-Forné, A., Torrie, C. I., Töyrä, D., Travasso, F., Traylor, G., Tringali, M. C., Trovato, A., Trozzo, L., Trudeau, R., Tsang, K. W., Tse, M., Tso, R., Tsukada, L., Tsuna, D., Tuyenbayev, D., Ueno, K., Ugolini, D., Unnikrishnan, C. S., Urban, A. L., Usman, S. A., Vahlbruch, H., Vajente, G., Valdes, G., van Bakel, N., van Beuzekom, M., van den Brand, J. F. J., Van Den Broeck, C., Vander-Hyde, D. C., van der Schaaf, L., van Heijningen, J. V., van Veggel, A. A., Vardaro, M., Varma, V., Vass, S., Vasúth, M., Vecchio, A., Vedovato, G., Veitch, J., Veitch, P. J., Venkateswara, K., Venugopalan, G., Verkindt, D., Vetrano, F., Viceré, A., Viets, A. D., Vine, D. J., Vinet, J. Y., Vitale, S., Vo, T., Vocca, H., Vorvick, C., Vyatchanin, S. P., Wade, A. R., Wade, L. E., Wade, M., Walet, R., Walker, M., Wallace, L., Walsh, S., Wang, G., Wang, H., Wang, J. Z., Wang, W. H., Wang, Y. F., Ward, R. L., Warden, Z. A., Warner, J., Was, M., Watchi, J., Weaver, B., Wei, L. W., Weinert, M., Weinstein, A. J., Weiss, R., Wellmann, F., Wen, L., Wessel, E. K., Weßels, P., Westhouse, J. W., Wette, K., Whelan, J. T., Whiting, B. F., Whittle, C., Wilken, D. M., Williams, D., Williamson, A. R., Willis, J. L., Willke, B., Wimmer, M. H., Winkler, W., Wipf, C. C., Wittel, H., Woan, G., Woehler, J., Wofford, J. K., Worden, J., Wright, J. L., Wu, D. S., Wysocki, D. M., Xiao, L., Yamamoto, H., Yancey, C. C., Yang, L., Yap, M. J., Yazback, M., Yeeles, D. W., Yu, H., Yu, H., Yuen, S. H. R., Yvert, M., Zadrożny, A. K., Zanolin, M., Zelenova, T., Zendri, J. P., Zevin, M., Zhang, J., Zhang, L., Zhang, T., Zhao, C., Zhou, M., Zhou, Z., Zhu, X. J., Zimmerman, A. B., Zlochower, Y., Zucker, M. E., Zweizig, J., LIGO Scientific Collaboration, and Virgo Collaboration, "Binary Black Hole Population Properties Inferred from the First and Second Observing Runs of Advanced LIGO and Advanced Virgo," ApJ **882**, L24 (Sept. 2019).

[32] Abbott, R., Abbott, T. D., Abraham, S., Acernese, F., Ackley, K., Adams, A., Adams, C., Adhikari, R. X., Adya, V. B., Affeldt, C., Agathos, M., Agatsuma, K., Aggarwal, N., Aguiar, O. D., Aiello, L., Ain, A., Ajith, P., Akcay, S., Allen, G., Allocca, A., Altin, P. A., Amato, A., Anand, S., Ananyeva, A., Anderson, S. B., Anderson, W. G., Angelova, S. V., Ansoldi, S., Antelis, J. M., Antier, S., Appert, S., Arai, K., Araya, M. C., Areeda, J. S., Arène, M., Arnaud, N., Aronson, S. M., Arun, K. G., Asali, Y., Ascenzi, S., Ashton, G., Aston, S. M., Astone, P., Aubin, F., Aufmuth, P., AultONeal, K., Austin, C., Avendano, V., Babak, S., Badaracco, F., Bader, M. K. M., Bae, S., Baer, A. M., Bagnasco, S., Baird, J., Ball, M., Ballardin, G., Ballmer, S. W., Bals, A., Balsamo, A., Baltus, G., Banagiri, S., Bankar, D., Bankar, R. S., Barayoga, J. C., Barbieri, C., Barish, B. C., Barker, D., Barneo, P., Barnum, S., Barone, F., Barr, B., Barsotti, L., Barsuglia, M., Barta, D., Bartlett, J., Bartos, I., Bassiri, R., Basti, A., Bawaj, M., Bayley, J. C., Bazzan, M., Becher, B. R., Bécsy, B., Bedakihale, V. M., Bejger, M., Belahcene, I., Beniwal, D., Benjamin, M. G., Bennett, T. F., Bentley, J. D., Bergamin, F., Berger, B. K., Bergmann, G., Bernuzzi, S., Berry, C. P. L., Bersanetti, D., Bertolini, A., Betzwieser, J., Bhandare, R., Bhandari, A. V., Bhattacharjee, D., Bidler, J., Bilenko, I. A., Billingsley, G., Birney, R., Birnholtz, O., Biscans, S., Bischi, M., Biscoveanu, S., Bisht, A., Bitossi, M., Bizouard, M. A., Blackburn, J. K., Blackman, J., Blair, C. D., Blair, D. G., Blair, R. M., Blanch, O., Bobba, F., Bode, N., Boer, M., Boetzel, Y., Bogaert, G., Boldrini, M., Bondu, F., Bonilla, E., Bonnand, R., Booker, P., Boom, B. A., Bork, R., Boschi, V., Bose, S., Bossilkov, V., Boudart, V., Bouffanais, Y., Bozzi, A., Bradaschia, C., Brady, P. R., Bramley, A., Branchesi, M., Brau, J. E., Breschi, M., Briant, T., Briggs, J. H., Brighenti, F., Brillet, A., Brinkmann, M., Brockill, P., Brooks, A. F., Brooks, J., Brown, D. D., Brunett, S., Bruno, G., Bruntz, R., Buikema, A., Bulik, T., Bulten, H. J., Buonanno, A., Buscicchio, R., Buskulic, D., Byer, R. L., Cabero, M., Cadonati, L., Caesar, M., Cagnoli, G., Cahillane, C., Calderón Bustillo, J., Callaghan, J. D., Callister, T. A., Calloni, E., Camp, J. B., Canepa, M., Cannon, K. C., Cao, H., Cao, J., Carapella, G., Carbognani, F., Carney, M. F., Carpinelli, M., Carullo, G., Carver, T. L., Casanueva Diaz, J., Casentini, C., Caudill, S., Cavaglià, M., Cavalier, F., Cavalieri, R., Cella, G., Cerdá-Durán, P., Cesarini, E., Chaibi, W., Chakravarti, K., Chan, C. L., Chan, C., Chandra, K., Chanial, P., Chao, S., Charlton, P., Chase, E. A., Chassande-Mottin, E., Chatterjee, D., Chattopadhyay, D., Chaturvedi, M., Chatziioannou, K., Chen, A., Chen, H. Y., Chen, X., Chen, Y., Cheng, H. P., Cheong, C. K., Chia, H. Y., Chiadini, F., Chierici, R., Chincarini, A., Chiummo, A., Cho, G., Cho, H. S., Cho, M., Choate, S., Christensen, N., Chu, Q., Chua, S., Chung, K. W., Chung, S., Ciani, G., Ciecielag, P., Cieślar, M., Cifaldi, M., Ciobanu, A. A., Ciolfi, R., Cipriano, F., Cirone, A., Clara, F., Clark, E. N., Clark, J. A., Clarke, L., Clearwater, P., Clesse, S., Cleva, F., Coccia, E., Cohadon, P. F., Cohen, D. E., Colleoni, M., Collette, C. G., Collins, C., Colpi, M., Constancio, M., Conti, L., Cooper, S. J., Corban, P., Corbitt, T. R., Cordero-Carrión, I., Corezzi, S., Corley, K. R., Cornish, N., Corre, D., Corsi, A., Cortese, S., Costa, C. A., Cotesta, R., Coughlin, M. W., Coughlin, S. B., Coulon, J. P., Countryman, S. T., Cousins, B., Couvares, P., Covas, P. B., Coward, D. M., Cowart, M. J., Coyne,

D. C., Coyne, R., Creighton, J. D. E., Creighton, T. D., Croquette, M., Crowder, S. G., Cudell, J. R., Cullen, T. J., Cumming, A., Cummings, R., Cunningham, L., Cuoco, E., Curyło, M., Canton, T. D., Dálya, G., Dana, A., DaneshgaranBajastani, L. M., D'Angelo, B., Danila, B., Danilishin, S. L., D'Antonio, S., Danzmann, K., Darsow-Fromm, C., Dasgupta, A., Datrier, L. E. H., Dattilo, V., Dave, I., Davier, M., Davies, G. S., Davis, D., Daw, E. J., Dean, R., DeBra, D., Deenadayalan, M., Degallaix, J., De Laurentis, M., Deléglise, S., Del Favero, V., De Lillo, F., De Lillo, N., Del Pozzo, W., DeMarchi, L. M., De Matteis, F., D'Emilio, V., Demos, N., Denker, T., Dent, T., Depasse, A., De Pietri, R., De Rosa, R., De Rossi, C., DeSalvo, R., de Varona, O., Dhurandhar, S., Díaz, M. C., Diaz-Ortiz, M., Didio, N. A., Dietrich, T., Di Fiore, L., DiFronzo, C., Di Giorgio, C., Di Giovanni, F., Di Giovanni, M., Di Girolamo, T., Di Lieto, A., Ding, B., Di Pace, S., Di Palma, I., Di Renzo, F., Divakarla, A. K., Dmitriev, A., Doctor, Z., D'Onofrio, L., Donovan, F., Dooley, K. L., Doravari, S., Dorrington, I., Downes, T. P., Drago, M., Driggers, J. C., Du, Z., Ducoin, J. G., Dupej, P., Durante, O., D'Urso, D., Duverne, P. A., Dwyer, S. E., Easter, P. J., Eddolls, G., Edelman, B., Edo, T. B., Edy, O., Effler, A., Eichholz, J., Eikenberry, S. S., Eisenmann, M., Eisenstein, R. A., Ejlli, A., Errico, L., Essick, R. C., Estellés, H., Estevez, D., Etienne, Z. B., Etzel, T., Evans, M., Evans, T. M., Ewing, B. E., Fafone, V., Fair, H., Fairhurst, S., Fan, X., Farah, A. M., Farinon, S., Farr, B., Farr, W. M., Fauchon-Jones, E. J., Favata, M., Fays, M., Fazio, M., Feicht, J., Fejer, M. M., Feng, F., Fenyvesi, E., Ferguson, D. L., Fernandez-Galiana, A., Ferrante, I., Ferreira, T. A., Fidecaro, F., Figura, P., Fiori, I., Fiorucci, D., Fishbach, M., Fisher, R. P., Fishner, J. M., Fittipaldi, R., Fitz-Axen, M., Fiumara, V., Flaminio, R., Floden, E., Flynn, E., Fong, H., Font, J. A., Forsyth, P. W. F., Fournier, J. D., Frasca, S., Frasconi, F., Frei, Z., Freise, A., Frey, R., Frey, V., Fritschel, P., Frolov, V. V., Fronzé, G. G., Fulda, P., Fyffe, M., Gabbard, H. A., Gadre, B. U., Gaebel, S. M., Gair, J. R., Gais, J., Galaudage, S., Gamba, R., Ganapathy, D., Ganguly, A., Gaonkar, S. G., Garaventa, B., García-Quirós, C., Garufi, F., Gateley, B., Gaudio, S., Gayathri, V., Gemme, G., Gennai, A., George, D., George, J., George, R. N., Gergely, L., Ghonge, S., Ghosh, A., Ghosh, A., Ghosh, S., Giacomazzo, B., Giacoppo, L., Giaime, J. A., Giardina, K. D., Gibson, D. R., Gier, C., Gill, K., Giri, P., Glanzer, J., Gleckl, A. E., Godwin, P., Goetz, E., Goetz, R., Gohlke, N., Goncharov, B., González, G., Gopakumar, A., Gossan, S. E., Gosselin, M., Gouaty, R., Grace, B., Grado, A., Granata, M., Granata, V., Grant, A., Gras, S., Grassia, P., Gray, C., Gray, R., Greco, G., Green, A. C., Green, R., Gretarsson, E. M., Griggs, H. L., Grignani, G., Grimaldi, A., Grimes, E., Grimm, S. J., Grote, H., Grunewald, S., Gruning, P., Guerrero, J. G., Guidi, G. M., Guimaraes, A. R., Guixé, G., Gulati, H. K., Guo, Y., Gupta, A., Gupta, A., Gupta, P., Gustafson, E. K., Gustafson, R., Guzman, F., Haegel, L., Halim, O., Hall, E. D., Hamilton, E. Z., Hammond, G., Haney, M., Hanke, M. M., Hanks, J., Hanna, C., Hannam, M. D., Hannuksela, O. A., Hannuksela, O., Hansen, H., Hansen, T. J., Hanson, J., Harder, T., Hardwick, T., Haris, K., Harms, J., Harry, G. M., Harry, I. W., Hartwig, D., Hasskew, R. K., Haster, C. J., Haughian, K., Hayes, F. J., Healy, J., Heidmann, A., Heintze, M. C., Heinze, J., Heinzel, J., Heitmann, H., Hellman, F., Hello, P., Helmling-Cornell, A. F., Hemming, G., Hendry, M., Heng, I. S., Hennes, E., Hennig, J., Hennig, M. H., Hernandez Vivanco, F., Heurs, M., Hild, S., Hill, P., Hines, A. S., Hochheim, S., Hofgard, E., Hofman, D., Hohmann, J. N., Holgado, A. M., Holland, N. A., Hollows, I. J., Holmes, Z. J., Holt, K., Holz, D. E., Hopkins, P., Horst, C., Hough, J., Howell, E. J., Hoy, C. G., Hoyland, D., Huang, Y., Hübner, M. T., Huddart, A. D., Huerta, E. A., Hughey, B., Hui, V., Husa, S., Huttner, S. H., Hutzler, B. M., Huxford, R., Huynh-Dinh, T., Idzkowski, B., Iess, A., Imperato, S., Inchauspe, H., Ingram, C., Intini, G., Isi, M., Iyer, B. R., JaberianHamedan, V., Jacqmin, T., Jadhav, S. J., Jadhav, S. P., James, A. L., Jani, K., Janssens, K., Janthalur, N. N., Jaranowski, P., Jariwala, D., Jaume, R., Jenkins, A. C., Jeunon, M., Jiang, J., Johns, G. R., Johnson-McDaniel, N. K., Jones, A. W., Jones, D. I., Jones, J. D., Jones, P., Jones, R., Jonker, R. J. G., Ju, L., Junker, J., Kalaghatgi, C. V., Kalogera, V., Kamai, B., Kandhasamy, S., Kang, G., Kanner, J. B., Kapadia, S. J., Kapasi, D. P., Karathanasis, C., Karki, S., Kashyap, R., Kasprzack, M., Kastaun, W., Katsanevas, S., Katsavounidis, E., Katzman, W., Kawabe, K., Kéfélian, F., Keitel, D., Key, J. S., Khadka, S., Khalili, F. Y., Khan, I., Khan, S., Khazanov, E. A., Khetan, N., Khursheed, M., Kijbunchoo, N., Kim, C., Kim, G. J., Kim, J. C., Kim, K., Kim, W. S., Kim, Y. M., Kimball, C., King, P. J., Kinley-Hanlon, M., Kirchhoff, R., Kissel, J. S., Kleybolte, L., Klimenko, S., Knowles, T. D., Knyazev, E., Koch, P., Koehlenbeck, S. M., Koekoek, G., Koley, S., Kolstein, M., Komori, K., Kondrashov, V., Kontos, A., Koper, N., Korobko, M., Korth, W. Z., Kovalam, M., Kozak, D. B., Krämer, C., Kringel, V., Krishnendu, N. V., Królak, A., Kuehn, G., Kumar, A., Kumar, P., Kumar, R., Kumar, R., Kuns, K., Kwang, S., Lackey, B. D., Laghi, D., Lalande, E., Lam, T. L., Lamberts, A., Landry, M., Lane, B. B., Lang, R. N., Lange, J., Lantz, B., Lanza, R. K., La Rosa, I., Lartaux-Vollard, A., Lasky, P. D., Laxen, M., Lazzarini, A., Lazzaro, C., Leaci, P., Leavey, S., Lecoeuche, Y. K., Lee, H. M., Lee, H. W., Lee, J., Lee, K., Lehmann, J., Leon, E., Leroy, N., Letendre, N., Levin, Y., Li, A., Li, J., Li, K. J. L., Li, T. G. F., Li, X., Linde, F., Linker, S. D., Linley, J. N., Littenberg, T. B., Liu, J., Liu, X., Llorens-Monteagudo, M., Lo, R. K. L., Lockwood, A., London, L. T., Longo, A., Lorenzini, M., Loriette, V., Lormand, M., Losurdo, G., Lough, J. D., Lousto, C. O., Lovelace, G., Lück, H., Lumaca, D., Lundgren, A. P., Ma, Y., Macas, R., MacInnis, M., Macleod, D. M., MacMillan, I. A. O., Macquet, A., Magaña Hernandez, I., Magaña-Sandoval, F., Magazzù, C., Magee, R. M., Majorana, E., Maksimovic, I., Maliakal, S., Malik, A., Man, N., Mandic, V., Mangano, V., Mansell, G. L., Manske, M., Mantovani, M., Mapelli, M., Marchesoni, F., Marion, F., Márka, S., Márka, Z., Markakis, C., Markosyan, A. S., Markowitz, A., Maros, E., Marquina, A., Marsat, S., Martelli, F., Martin, I. W., Martin, R. M., Martinez, M., Martinez, V., Martynov, D. V., Masalehdan, H., Mason, K., Massera, E., Masserot, A., Massinger, T. J., Masso-Reid, M., Mastrogiovanni, S., Matas, A., Mateu-Lucena, M., Matichard, F., Matiushechkina, M., Mavalvala, N., Maynard, E., McCann, J. J., McCarthy, R., McClelland, D. E., McCormick, S., McCuller, L., McGuire, S. C., McIsaac, C., McIver, J., McManus, D. J., McRae, T., McWilliams, S. T., Meacher, D., Meadors, G. D., Mehmet, M., Mehta, A. K., Melatos, A., Melchor, D. A., Mendell, G., Menendez-Vazquez, A., Mercer, R. A., Mereni, L., Merfeld, K., Merilh, E. L., Merritt, J. D., Merzougui, M., Meshkov, S., Messenger, C., Messick, C., Metzdorff, R., Meyers, P. M., Meylahn, F., Mhaske, A., Miani, A., Miao, H., Michaloliakos, I., Michel, C., Middleton, H., Milano, L., Miller, A. L., Millhouse, M., Mills, J. C., Milotti, E., Milovich-Goff, M. C., Minazzoli, O., Minenkov, Y., Mir, L. M., Mishkin, A., Mishra, C., Mistry, T., Mitra, S., Mitrofanov, V. P., Mitselmakher, G., Mittleman, R., Mo, G., Mogushi, K., Mohapatra, S. R. P., Mohite, S. R., Molina, I., Molina-Ruiz, M., Mondin, M., Montani, M., Moore, C. J., Moraru, D., Morawski, F., Moreno, G., Morisaki, S., Mours, B., Mow-Lowry, C. M., Mozzon, S., Muciaccia, F., Mukherjee, A., Mukherjee, D., Mukherjee, S., Mukherjee, S., Mukund, N., Mullavey, A., Munch, J., Muñiz, E. A., Murray, P. G., Nadji, S. L., Nagar, A., Nardecchia, I., Naticchioni, L., Nayak, R. K., Neil, B. F., Neilson, J., Nelemans, G., Nelson, T. J. N., Nery, M., Neunzert, A., Nitz, A. H., Ng, K. Y., Ng, S., Nguyen, C., Nguyen, P., Nguyen, T., Nichols, S. A., Nissanke, S., Nocera, F., Noh, M., North, C., Nothard, D., Nuttall, L. K., Oberling, J., O'Brien, B. D., O'Dell, J., Oganesyan, G., Ogin, G. H., Oh, J. J., Oh, S. H., Ohme, F., Ohta, H., Okada, M. A., Olivetto, C., Oppermann, P., Oram, R. J., O'Reilly, B., Ormiston, R. G., Ortega, L. F., O'Shaughnessy, R., Ossokine, S., Osthelder, C., Ottaway, D. J., Overmier, H., Owen, B. J., Pace, A. E., Pagano, G., Page, M. A., Pagliaroli, G., Pai, A., Pai, S. A., Palamos, J. R., Palashov, O., Palomba, C., Pan, H., Panda, P. K., Pang, T. H., Pankow, C., Pannarale, F., Pant, B. C., Paoletti, F., Paoli, A., Paolone, A., Parker, W., Pascucci, D., Pasqualetti, A., Passaquieti, R., Passuello, D., Patel, M., Patricelli, B., Payne, E., Pechsiri, T. C., Pedraza, M., Pegoraro, M., Pele, A., Penn, S., Perego, A., Perez, C. J., Périgois, C., Perreca, A., Perriès, S., Petermann, J., Petterson, D., Pfeiffer, H. P., Pham, K. A., Phukon, K. S., Piccinni, O. J., Pichot, M., Piendibene, M., Piergiovanni, F., Pierini, L., Pierro, V., Pillant, G., Pilo, F., Pinard, L., Pinto, I. M., Piotrzkowski, K., Pirello, M., Pitkin, M., Placidi, E., Plastino, W., Pluchar, C., Poggiani, R., Polini, E., Pong, D. Y. T., Ponrathnam, S., Popolizio, P., Porter, E. K., Poverman, A., Powell, J., Pracchia, M., Prajapati, A. K., Prasai, K., Prasanna, R., Pratten, G., Prestegard, T., Principe, M., Prodi, G. A., Prokhorov, L., Prosposito, P., Prudenzi, L., Puecher, A., Punturo, M., Puosi, F., Puppo, P., Pürrer, M., Qi, H., Quetschke, V., Quinonez, P. J., Quitzow-James, R., Raab, F. J., Raaijmakers, G., Radkins, H., Radulesco, N., Raffai, P., Rafferty, H., Rail, S. X., Raja, S., Rajan, C., Rajbhandari, B., Rakhmanov, M., Ramirez, K. E., Ramirez, T. D., Ramos-Buades, A., Rana, J., Rao, K., Rapagnani, P., Rapol, U. D., Ratto, B., Raymond, V., Razzano, M., Read, J., Regimbau, T., Rei, L., Reid, S., Reitze, D. H., Rettegno, P., Ricci, F., Richardson, C. J., Richardson, J. W., Richardson, L., Ricker, P. M., Riemenschneider, G., Riles, K., Rizzo, M., Robertson, N. A., Robinet, F., Rocchi, A., Rocha, J. A., Rodriguez, S., Rodriguez-Soto, R. D., Rolland, L., Rollins, J. G., Roma, V. J., Romanelli, M., Romano, R., Romel, C. L., Romero, A., Romero-Shaw, I. M., Romie, J. H., Ronchini, S., Rose, C. A., Rose, D., Rose, K., Rosell, M. J. B., Rosińska, D., Rosofsky, S. G., Ross, M. P., Rowan, S., Rowlinson, S. J., Roy, S., Roy, S., Ruggi, P., Ryan, K., Sachdev, S., Sadecki, T., Sadiq, J., Sakellariadou, M., Salafia, O. S., Salconi, L., Saleem, M., Samajdar, A., Sanchez, E. J., Sanchez, J. H., Sanchez, L. E., Sanchis-Gual, N., Sanders, J. R., Sandles, L., Santiago, K. A., Santos, E., Saravanan, T. R., Sarin, N., Sassolas, B., Sathyaprakash, B. S., Sauter, O., Savage, R. L., Savant, V., Sawant, D., Sayah, S., Schaetzl, D., Schale, P., Scheel, M., Scheuer, J., Schindler-Tyka, A., Schmidt, P., Schnabel, R., Schofield, R. M. S., Schönbeck, A., Schreiber, E., Schulte, B. W., Schutz, B. F., Schwarm, O., Schwartz, E., Scott, J., Scott, S. M., Seglar-Arroyo, M., Seidel, E., Sellers, D., Sengupta, A. S., Sennett, N., Sentenac, D., Sequino, V., Sergeev, A., Setyawati, Y., Shaffer, T., Shahriar, M. S., Sharifi, S., Sharma, A., Sharma, P., Shawhan, P., Shen, H., Shikauchi, M., Shink, R., Shoemaker, D. H., Shoemaker, D. M., Shukla, K., ShyamSundar, S., Sieniawska, M., Sigg, D., Singer, L. P., Singh, D., Singh, N., Singha, A., Singhal, A., Sintes, A. M., Sipala, V., Skliris, V., Slagmolen, B. J. J., Slaven-Blair, T. J., Smetana, J., Smith, J. R., Smith, R. J. E., Somala, S. N., Son, E. J., Soni, K., Soni, S., Sorazu, B., Sordini, V., Sorrentino, F., Sorrentino, N., Soulard, R., Souradeep, T., Sowell, E., Spencer, A. P., Spera, M., Srivastava, A. K., Srivastava, V., Staats, K., Stachie, C., Steer, D. A., Steinhoff, J., Steinke, M., Steinlechner, J., Steinlechner, S., Steinmeyer, D., Stevenson, S. P., Stolle-McAllister, G., Stops, D. J., Stover, M., Strain, K. A., Stratta, G., Strunk, A., Sturani, R., Stuver, A. L., Südbeck, J., Sudhagar, S., Sudhir, V., Suh, H. G., Summerscales, T. Z., Sun, H., Sun, L., Sunil, S., Sur, A., Suresh, J., Sutton, P. J., Swinkels, B. L., Szczepańczyk, M. J., Tacca, M., Tait, S. C., Talbot, C., Tanasijczuk, A. J., Tanner, D. B., Tao, D., Tapia, A., Tapia San Martin, E. N., Tasson, J. D., Taylor, R., Tenorio, R., Terkowski, L., Thirugnanasambandam, M. P., Thomas, L. M., Thomas, M., Thomas, P., Thompson, J. E., Thondapu, S. R., Thorne, K. A., Thrane, E., Tiwari, S., Tiwari, S., Tiwari, V., Toland, K., Tolley, A. E., Tonelli, M., Tornasi, Z., Torres-Forné, A., Torrie, C. I., e Melo, I. T., Töyrä, D., Tran, A. T., Trapananti, A., Travasso, F., Traylor, G., Tringali, M. C., Tripathee, A., Trovato, A., Trudeau, R. J., Tsai, D. S., Tsang, K. W., Tse, M., Tso, R., Tsukada, L., Tsuna, D., Tsutsui, T., Turconi, M., Ubhi, A. S., Udall, R. P., Ueno, K., Ugolini, D., Unnikrishnan, C. S., Urban, A. L., Usman, S. A., Utina, A. C., Vahlbruch, H., Vajente, G., Vajpeyi, A., Valdes, G., Valentini, M., Valsan, V., van Bakel, N., van Beuzekom, M., van den Brand, J. F. J., Van Den Broeck, C., Vander-Hyde, D. C., van der Schaaf, L., van Heijningen, J. V., Vardaro, M., Vargas, A. F., Varma, V., Vass, S., Vasúth, M., Vecchio, A., Vedovato, G., Veitch, J., Veitch, P. J., Venkateswara, K., Venneberg, J., Venugopalan, G., Verkindt, D., Verma, Y., Veske, D., Vetrano, F., Viceré, A., Viets, A. D., Vijaykumar, A., Villa-Ortega, V., Vinet, J. Y., Vitale, S., Vo, T., Vocca, H., Vorvick, C., Vyatchanin, S. P., Wade, A. R., Wade, L. E., Wade, M., Walet, R. C., Walker, M., Wallace, G. S., Wallace, L., Walsh, S., Wang, J. Z., Wang, S., Wang, W. H., Wang, Y. F., Ward, R. L., Warner, J., Was, M., Washington, N. Y., Watchi, J., Weaver, B., Wei, L., Weinert, M., Weinstein, A. J., Weiss, R., Wellmann, F., Wen, L., Weßels, P., Westhouse, J. W., Wette, K., Whelan, J. T., White, D. D., White, L. V., Whiting, B. F., Whittle, C., Wilken, D. M., Williams, D., Williams, M. J., Williamson, A. R., Willis, J. L., Willke, B., Wilson, D. J., Wimmer, M. H., Winkler, W., Wipf, C. C., Woan, G., Woehler, J., Wofford, J. K., Wong, I. C. F., Wrangel, J., Wright, J. L., Wu, D. S., Wysocki, D. M., Xiao, L., Yamamoto, H., Yang, L., Yang, Y., Yang, Z., Yap, M. J., Yeeles, D. W., Yoon, A., Yu, H., Yu, H., Yuen, S. H. R., ZadroŻny, A., Zanolin, M., Zelenova, T., Zendri, J. P., Zevin, M., Zhang, J., Zhang, L., Zhang, R., Zhang, T., Zhao, C., Zhao, G., Zheng, Y., Zhou, M., Zhou, Z., Zhu, X. J., Zimmerman, A. B., Zlochower, Y., Zucker, M. E., Zweizig, J., LIGO Scientific Collaboration, and Virgo Collaboration, "GWTC-2: Compact Binary Coalescences Observed by LIGO and Virgo during the First Half of the Third Observing Run," *Physical Review X* **11**, 021053 (Apr. 2021).

[33] Abbott, R., Abbott, T. D., Abraham, S., Acernese, F., Ackley, K., Adams, A., Adams, C., Adhikari, R. X., Adya, V. B., Affeldt, C., Agathos, M., Agatsuma, K., Aggarwal, N., Aguiar, O. D., Aiello, L., Ain, A., Ajith, P., Allen, G., Allocca, A., Altin, P. A., Amato, A., Anand, S., Ananyeva, A., Anderson, S. B., Anderson, W. G., Angelova, S. V., Ansoldi, S., Antelis, J. M., Antier, S., Appert, S., Arai, K., Araya, M. C., Areeda, J. S., Arène, M., Arnaud, N., Aronson, S. M., Arun, K. G., Asali, Y., Ascenzi, S., Ashton, G., Aston, S. M., Astone, P., Aubin, F., Aufmuth, P., AultONeal, K., Austin, C., Avendano, V., Babak, S., Badaracco, F., Bader, M. K. M., Bae, S., Baer, A. M., Bagnasco, S., Baird, J., Ball, M., Ballardin, G., Ballmer, S. W., Bals, A., Balsamo, A., Baltus, G., Banagiri, S., Bankar, D., Bankar, R. S., Barayoga, J. C., Barbieri, C., Barish, B. C., Barker, D., Barneo, P., Barnum, S., Barone, F., Barr, B., Barsotti, L., Barsuglia, M., Barta, D., Bartlett, J., Bartos, I., Bassiri, R., Basti, A., Bawaj, M., Bayley, J. C., Bazzan, M., Becher, B. R., Bécsy, B., Bedakihale, V. M., Bejger, M., Belahcene, I., Beniwal, D., Benjamin, M. G., Bennett, T. F., Bentley, J. D., Bergamin, F., Berger, B. K., Bergmann, G., Bernuzzi, S.,

Berry, C. P. L., Bersanetti, D., Bertolini, A., Betzwieser, J., Bhandare, R., Bhandari, A. V., Bhattacharjee, D., Bidler, J., Bilenko, I. A., Billingsley, G., Birney, R., Birnholtz, O., Biscans, S., Bischi, M., Biscoveanu, S., Bisht, A., Bitossi, M., Bizouard, M. A., Blackburn, J. K., Blackman, J., Blair, C. D., Blair, D. G., Blair, R. M., Blanch, O., Bobba, F., Bode, N., Boer, M., Boetzel, Y., Bogaert, G., Boldrini, M., Bondu, F., Bonilla, E., Bonnand, R., Booker, P., Boom, B. A., Bork, R., Boschi, V., Bose, S., Bossilkov, V., Boudart, V., Bouffanais, Y., Bozzi, A., Bradaschia, C., Brady, P. R., Bramley, A., Branchesi, M., Brau, J. E., Breschi, M., Briant, T., Briggs, J. H., Brighenti, F., Brillet, A., Brinkmann, M., Brockill, P., Brooks, A. F., Brooks, J., Brown, D. D., Brunett, S., Bruno, G., Bruntz, R., Buikema, A., Bulik, T., Bulten, H. J., Buonanno, A., Buscicchio, R., Buskulic, D., Byer, R. L., Cabero, M., Cadonati, L., Caesar, M., Cagnoli, G., Cahillane, C., Calderón Bustillo, J., Callaghan, J. D., Callister, T. A., Calloni, E., Camp, J. B., Canepa, M., Cannon, K. C., Cao, H., Cao, J., Carapella, G., Carbognani, F., Carney, M. F., Carpinelli, M., Carullo, G., Carver, T. L., Casanueva Diaz, J., Casentini, C., Caudill, S., Cavaglià, M., Cavalier, F., Cavalieri, R., Cella, G., Cerdá-Durán, P., Cesarini, E., Chaibi, W., Chakravarti, K., Chan, C. L., Chan, C., Chandra, K., Chanial, P., Chao, S., Charlton, P., Chase, E. A., Chassande-Mottin, E., Chatterjee, D., Chattopadhyay, D., Chaturvedi, M., Chatziioannou, K., Chen, A., Chen, H. Y., Chen, X., Chen, Y., Cheng, H. P., Cheong, C. K., Chia, H. Y., Chiadini, F., Chierici, R., Chincarini, A., Chiummo, A., Cho, G., Cho, H. S., Cho, M., Choate, S., Christensen, N., Chu, Q., Chua, S., Chung, K. W., Chung, S., Ciani, G., Ciecielag, P., Cieślar, M., Cifaldi, M., Ciobanu, A. A., Ciolfi, R., Cipriano, F., Cirone, A., Clara, F., Clark, E. N., Clark, J. A., Clarke, L., Clearwater, P., Clesse, S., Cleva, F., Coccia, E., Cohadon, P. F., Cohen, D. E., Colleoni, M., Collette, C. G., Collins, C., Colpi, M., Constancio, M., J., Conti, L., Cooper, S. J., Corban, P., Corbitt, T. R., Cordero-Carrión, I., Corezzi, S., Corley, K. R., Cornish, N., Corre, D., Corsi, A., Cortese, S., Costa, C. A., Cotesta, R., Coughlin, M. W., Coughlin, S. B., Coulon, J. P., Countryman, S. T., Couvares, P., Covas, P. B., Coward, D. M., Cowart, M. J., Coyne, D. C., Coyne, R., Creighton, J. D. E., Creighton, T. D., Croquette, M., Crowder, S. G., Cudell, J. R., Cullen, T. J., Cumming, A., Cummings, R., Cunningham, L., Cuoco, E., Curylo, M., Dal Canton, T., Dálya, G., Dana, A., DaneshgaranBajastani, L. M., D'Angelo, B., Danilishin, S. L., D'Antonio, S., Danzmann, K., Darsow-Fromm, C., Dasgupta, A., Datrier, L. E. H., Dattilo, V., Dave, I., Davier, M., Davies, G. S., Davis, D., Daw, E. J., Dean, R., DeBra, D., Deenadayalan, M., Degallaix, J., De Laurentis, M., Deléglise, S., Del Favero, V., De Lillo, F., De Lillo, N., Del Pozzo, W., DeMarchi, L. M., De Matteis, F., D'Emilio, V., Demos, N., Denker, T., Dent, T., Depasse, A., De Pietri, R., De Rosa, R., De Rossi, C., DeSalvo, R., de Varona, O., Dhurandhar, S., Díaz, M. C., Diaz-Ortiz, M., J., Didio, N. A., Dietrich, T., Di Fiore, L., DiFronzo, C., Di Giorgio, C., Di Giovanni, F., Di Giovanni, M., Di Girolamo, T., Di Lieto, A., Ding, B., Di Pace, S., Di Palma, I., Di Renzo, F., Divakarla, A. K., Dmitriev, A., Doctor, Z., D'Onofrio, L., Donovan, F., Dooley, K. L., Doravari, S., Dorrington, I., Downes, T. P., Drago, M., Driggers, J. C., Du, Z., Ducoin, J. G., Dupej, P., Durante, O., D'Urso, D., Duverne, P. A., Dwyer, S. E., Easter, P. J., Eddolls, G., Edelman, B., Edo, T. B., Edy, O., Effler, A., Eichholz, J., Eikenberry, S. S., Eisenmann, M., Eisenstein, R. A., Ejlli, A., Errico, L., Essick, R. C., Estellés, H., Estevez, D., Etienne, Z. B., Etzel, T., Evans, M., Evans, T. M., Ewing, B. E., Fafone, V., Fair, H., Fairhurst, S., Fan, X., Farah, A. M., Farinon, S., Farr, B., Farr, W. M., Fauchon-Jones, E. J., Favata, M., Fays, M., Fazio, M., Feicht, J., Fejer, M. M., Feng, F., Fenyvesi, E., Ferguson, D. L., Fernandez-Galiana, A., Ferrante, I., Ferreira, T. A., Fidecaro, F., Figura, P., Fiori, I., Fiorucci, D., Fishbach, M., Fisher, R. P., Fishner, J. M., Fittipaldi, R., Fitz-Axen, M., Fiumara, V., Flaminio, R., Floden, E., Flynn, E., Fong, H., Font, J. A., Forsyth, P. W. F., Fournier, J. D., Frasca, S., Frasconi, F., Frei, Z., Freise, A., Frey, R., Frey, V., Fritschel, P., Frolov, V. V., Fronzé, G. G., Fulda, P., Fyffe, M., Gabbard, H. A., Gadre, B. U., Gaebel, S. M., Gair, J. R., Gais, J., Galaudage, S., Gamba, R., Ganapathy, D., Ganguly, A., Gaonkar, S. G., Garaventa, B., García-Quirós, C., Garufi, F., Gateley, B., Gaudio, S., Gayathri, V., Gemme, G., Gennai, A., George, D., George, J., Gergely, L., Ghonge, S., Ghosh, A., Ghosh, A., Ghosh, S., Giacomazzo, B., Giacoppo, L., Giaime, J. A., Giardina, K. D., Gibson, D. R., Gier, C., Gill, K., Giri, P., Glanzer, J., Gleckl, A. E., Godwin, P., Goetz, E., Goetz, R., Gohlke, N., Goncharov, B., González, G., Gopakumar, A., Gossan, S. E., Gosselin, M., Gouaty, R., Grace, B., Grado, A., Granata, M., Granata, V., Grant, A., Gras, S., Grassia, P., Gray, C., Gray, R., Greco, G., Green, A. C., Green, R., Gretarsson, E. M., Griggs, H. L., Grignani, G., Grimaldi, A., Grimes, E., Grimm, S. J., Grote, H., Grunewald, S., Gruning, P., Guerrero, J. G., Guidi, G. M., Guimaraes, A. R., Guixé, G., Gulati,

H. K., Guo, Y., Gupta, A., Gupta, A., Gupta, P., Gustafson, E. K., Gustafson, R., Guzman, F., Haegel, L., Halim, O., Hall, E. D., Hamilton, E. Z., Hammond, G., Haney, M., Hanke, M. M., Hanks, J., Hanna, C., Hannuksela, O. A., Hannuksela, O., Hansen, H., Hansen, T. J., Hanson, J., Harder, T., Hardwick, T., Haris, K., Harms, J., Harry, G. M., Harry, I. W., Hartwig, D., Hasskew, R. K., Haster, C. J., Haughian, K., Hayes, F. J., Healy, J., Heidmann, A., Heintze, M. C., Heinze, J., Heinzel, J., Heitmann, H., Hellman, F., Hello, P., Helmling-Cornell, A. F., Hemming, G., Hendry, M., Heng, I. S., Hennes, E., Hennig, J., Hennig, M. H., Hernandez Vivanco, F., Heurs, M., Hild, S., Hill, P., Hines, A. S., Hochheim, S., Hofgard, E., Hofman, D., Hohmann, J. N., Holgado, A. M., Holland, N. A., Hollows, I. J., Holmes, Z. J., Holt, K., Holz, D. E., Hopkins, P., Horst, C., Hough, J., Howell, E. J., Hoy, C. G., Hoyland, D., Huang, Y., Hübner, M. T., Huddart, A. D., Huerta, E. A., Hughey, B., Hui, V., Husa, S., Huttner, S. H., Hutzler, B. M., Huxford, R., Huynh-Dinh, T., Idzkowski, B., Iess, A., Imperato, S., Inchauspe, H., Ingram, C., Intini, G., Isi, M., Iyer, B. R., JaberianHamedan, V., Jacqmin, T., Jadhav, S. J., Jadhav, S. P., James, A. L., Jani, K., Janssens, K., Janthalur, N. N., Jaranowski, P., Jariwala, D., Jaume, R., Jenkins, A. C., Jeunon, M., Jiang, J., Johns, G. R., Jones, A. W., Jones, D. I., Jones, J. D., Jones, P., Jones, R., Jonker, R. J. G., Ju, L., Junker, J., Kalaghatgi, C. V., Kalogera, V., Kamai, B., Kandhasamy, S., Kang, G., Kanner, J. B., Kapadia, S. J., Kapasi, D. P., Karathanasis, C., Karki, S., Kashyap, R., Kasprzack, M., Kastaun, W., Katsanevas, S., Katsavounidis, E., Katzman, W., Kawabe, K., Kéfélian, F., Keitel, D., Key, J. S., Khadka, S., Khalili, F. Y., Khan, I., Khan, S., Khazanov, E. A., Khetan, N., Khursheed, M., Kijbunchoo, N., Kim, C., Kim, G. J., Kim, J. C., Kim, K., Kim, W. S., Kim, Y. M., Kimball, C., King, P. J., Kinley-Hanlon, M., Kirchhoff, R., Kissel, J. S., Kleybolte, L., Klimenko, S., Knowles, T. D., Knyazev, E., Koch, P., Koehlenbeck, S. M., Koekoek, G., Koley, S., Kolstein, M., Komori, K., Kondrashov, V., Kontos, A., Koper, N., Korobko, M., Korth, W. Z., Kovalam, M., Kozak, D. B., Krämer, C., Kringel, V., Krishnendu, N. V., Królak, A., Kuehn, G., Kumar, A., Kumar, P., Kumar, R., Kumar, R., Kuns, K., Kwang, S., Lackey, B. D., Laghi, D., Lalande, E., Lam, T. L., Lamberts, A., Landry, M., Lane, B. B., Lang, R. N., Lange, J., Lantz, B., Lanza, R. K., La Rosa, I., Lartaux-Vollard, A., Lasky, P. D., Laxen, M., Lazzarini, A., Lazzaro, C., Leaci, P., Leavey, S., Lecoeuche, Y. K., Lee, H. M., Lee, H. W., Lee, J., Lee, K., Lehmann, J., Leon, E., Leroy, N., Letendre, N., Levin, Y., Li, A., Li, J., Li, K. J. L., Li, T. G. F., Li, X., Linde, F., Linker, S. D., Linley, J. N., Littenberg, T. B., Liu, J., Liu, X., Llorens-Monteagudo, M., Lo, R. K. L., Lockwood, A., London, L. T., Longo, A., Lorenzini, M., Loriette, V., Lormand, M., Losurdo, G., Lough, J. D., Lousto, C. O., Lovelace, G., Lück, H., Lumaca, D., Lundgren, A. P., Ma, Y., Macas, R., MacInnis, M., Macleod, D. M., MacMillan, I. A. O., Macquet, A., Magaña Hernandez, I., Magaña-Sandoval, F., Magazzù, C., Magee, R. M., Majorana, E., Maksimovic, I., Maliakal, S., Malik, A., Man, N., Mandic, V., Mangano, V., Mansell, G. L., Manske, M., Mantovani, M., Mapelli, M., Marchesoni, F., Marion, F., Márka, S., Márka, Z., Markakis, C., Markosyan, A. S., Markowitz, A., Maros, E., Marquina, A., Marsat, S., Martelli, F., Martin, I. W., Martin, R. M., Martinez, M., Martinez, V., Martynov, D. V., Masalehdan, H., Mason, K., Massera, E., Masserot, A., Massinger, T. J., Masso-Reid, M., Mastrogiovanni, S., Matas, A., Mateu-Lucena, M., Matichard, F., Matiushechkina, M., Mavalvala, N., Maynard, E., McCann, J. J., McCarthy, R., McClelland, D. E., McCormick, S., McCuller, L., McGuire, S. C., McIsaac, C., McIver, J., McManus, D. J., McRae, T., McWilliams, S. T., Meacher, D., Meadors, G. D., Mehmet, M., Mehta, A. K., Melatos, A., Melchor, D. A., Mendell, G., Menendez-Vazquez, A., Mercer, R. A., Mereni, L., Merfeld, K., Merilh, E. L., Merritt, J. D., Merzougui, M., Meshkov, S., Messenger, C., Messick, C., Metzdorff, R., Meyers, P. M., Meylahn, F., Mhaske, A., Miani, A., Miao, H., Michaloliakos, I., Michel, C., Middleton, H., Milano, L., Miller, A. L., Miller, S., Millhouse, M., Mills, J. C., Milotti, E., Milovich-Goff, M. C., Minazzoli, O., Minenkov, Y., Mir, L. M., Mishkin, A., Mishra, C., Mistry, T., Mitra, S., Mitrofanov, V. P., Mitselmakher, G., Mittleman, R., Mo, G., Mogushi, K., Mohapatra, S. R. P., Mohite, S. R., Molina, I., Molina-Ruiz, M., Mondin, M., Montani, M., Moore, C. J., Moraru, D., Morawski, F., Moreno, G., Morisaki, S., Mours, B., Mow-Lowry, C. M., Mozzon, S., Muciaccia, F., Mukherjee, A., Mukherjee, D., Mukherjee, S., Mukherjee, S., Mukund, N., Mullavey, A., Munch, J., Muñiz, E. A., Murray, P. G., Nadji, S. L., Nagar, A., Nardecchia, I., Naticchioni, L., Nayak, R. K., Neil, B. F., Neilson, J., Nelemans, G., Nelson, T. J. N., Nery, M., Neunzert, A., Ng, K. Y., Ng, S., Nguyen, C., Nguyen, P., Nguyen, T., Nichols, S. A., Nissanke, S., Nocera, F., Noh, M., North, C., Nothard, D., Nuttall, L. K., Oberling, J., O'Brien, B. D., O'Dell, J., Oganesyan, G., Ogin, G. H., Oh, J. J., Oh, S. H., Ohme, F., Ohta, H., Okada, M. A.,

Olivetto, C., Oppermann, P., Oram, R. J., O'Reilly, B., Ormiston, R. G., Ormsby, N., Ortega, L. F., O'Shaughnessy, R., Ossokine, S., Osthelder, C., Ottaway, D. J., Overmier, H., Owen, B. J., Pace, A. E., Pagano, G., Page, M. A., Pagliaroli, G., Pai, A., Pai, S. A., Palamos, J. R., Palashov, O., Palomba, C., Pan, H., Panda, P. K., Pang, T. H., Pankow, C., Pannarale, F., Pant, B. C., Paoletti, F., Paoli, A., Paolone, A., Parker, W., Pascucci, D., Pasqualetti, A., Passaquieti, R., Passuello, D., Patel, M., Patricelli, B., Payne, E., Pechsiri, T. C., Pedraza, M., Pegoraro, M., Pele, A., Penn, S., Perego, A., Perez, C. J., Périgois, C., Perreca, A., Perriès, S., Petermann, J., Petterson, D., Pfeiffer, H. P., Pham, K. A., Phukon, K. S., Piccinni, O. J., Pichot, M., Piendibene, M., Piergiovanni, F., Pierini, L., Pierro, V., Pillant, G., Pilo, F., Pinard, L., Pinto, I. M., Piotrzkowski, K., Pirello, M., Pitkin, M., Placidi, E., Plastino, W., Pluchar, C., Poggiani, R., Polini, E., Pong, D. Y. T., Ponrathnam, S., Popolizio, P., Porter, E. K., Poverman, A., Powell, J., Pracchia, M., Prajapati, A. K., Prasai, K., Prasanna, R., Pratten, G., Prestegard, T., Principe, M., Prodi, G. A., Prokhorov, L., Prosposito, P., Puecher, A., Punturo, M., Puosi, F., Puppo, P., Pürrer, M., Qi, H., Quetschke, V., Quinonez, P. J., Quitzow-James, R., Raab, F. J., Raaijmakers, G., Radkins, H., Radulesco, N., Raffai, P., Rafferty, H., Rail, S. X., Raja, S., Rajan, C., Rajbhandari, B., Rakhmanov, M., Ramirez, K. E., Ramirez, T. D., Ramos-Buades, A., Rana, J., Rao, K., Rapagnani, P., Rapol, U. D., Ratto, B., Raymond, V., Razzano, M., Read, J., Regimbau, T., Rei, L., Reid, S., Reitze, D. H., Rettegno, P., Ricci, F., Richardson, C. J., Richardson, J. W., Richardson, L., Ricker, P. M., Riemenschneider, G., Riles, K., Rizzo, M., Robertson, N. A., Robinet, F., Rocchi, A., Rocha, J. A., Rodriguez, S., Rodriguez-Soto, R. D., Rolland, L., Rollins, J. G., Roma, V. J., Romanelli, M., Romano, R., Romel, C. L., Romero, A., Romero-Shaw, I. M., Romie, J. H., Ronchini, S., Rose, C. A., Rose, D., Rose, K., Rosell, M. J. B., Rosińska, D., Rosofsky, S. G., Ross, M. P., Rowan, S., Rowlinson, S. J., Roy, S., Roy, S., Ruggi, P., Ryan, K., Sachdev, S., Sadecki, T., Sakellariadou, M., Salafia, O. S., Salconi, L., Saleem, M., Samajdar, A., Sanchez, E. J., Sanchez, J. H., Sanchez, L. E., Sanchis-Gual, N., Sanders, J. R., Santiago, K. A., Santos, E., Saravanan, T. R., Sarin, N., Sassolas, B., Sathyaprakash, B. S., Sauter, O., Savage, R. L., Savant, V., Sawant, D., Sayah, S., Schaetzl, D., Schale, P., Scheel, M., Scheuer, J., Schindler-Tyka, A., Schmidt, P., Schnabel, R., Schofield, R. M. S., Schönbeck, A., Schreiber, E., Schulte, B. W., Schutz, B. F., Schwarm, O., Schwartz, E., Scott, J., Scott, S. M., Seglar-Arroyo, M., Seidel, E., Sellers, D., Sengupta, A. S., Sennett, N., Sentenac, D., Sequino, V., Sergeev, A., Setyawati, Y., Shaffer, T., Shahriar, M. S., Sharifi, S., Sharma, A., Sharma, P., Shawhan, P., Shen, H., Shikauchi, M., Shink, R., Shoemaker, D. H., Shoemaker, D. M., Shukla, K., ShyamSundar, S., Sieniawska, M., Sigg, D., Singer, L. P., Singh, D., Singh, N., Singha, A., Singhal, A., Sintes, A. M., Sipala, V., Skliris, V., Slagmolen, B. J. J., Slaven-Blair, T. J., Smetana, J., Smith, J. R., Smith, R. J. E., Somala, S. N., Son, E. J., Soni, S., Sorazu, B., Sordini, V., Sorrentino, F., Sorrentino, N., Soulard, R., Souradeep, T., Sowell, E., Spencer, A. P., Spera, M., Srivastava, A. K., Srivastava, V., Staats, K., Stachie, C., Steer, D. A., Steinke, M., Steinlechner, J., Steinlechner, S., Steinmeyer, D., Stevenson, S. P., Stolle-McAllister, G., Stops, D. J., Stover, M., Strain, K. A., Stratta, G., Strunk, A., Sturani, R., Stuver, A. L., Südbeck, J., Sudhagar, S., Sudhir, V., Suh, H. G., Summerscales, T. Z., Sun, H., Sun, L., Sunil, S., Sur, A., Suresh, J., Sutton, P. J., Swinkels, B. L., Szczepańczyk, M. J., Tacca, M., Tait, S. C., Talbot, C., Tanasijczuk, A. J., Tanner, D. B., Tao, D., Tapia, A., Tapia San Martin, E. N., Tasson, J. D., Taylor, R., Tenorio, R., Terkowski, L., Thirugnanasambandam, M. P., Thomas, L., Thomas, M., Thomas, P., Thompson, J. E., Thondapu, S. R., Thorne, K. A., Thrane, E., Tiwari, S., Tiwari, S., Tiwari, V., Toland, K., Tolley, A. E., Tonelli, M., Tornasi, Z., Torres-Forné, A., Torrie, C. I., Tosta e Melo, I., Töyrä, D., Tran, A. T., Trapananti, A., Travasso, F., Traylor, G., Tringali, M. C., Tripathee, A., Trovato, A., Trudeau, R. J., Tsai, D. S., Tsang, K. W., Tse, M., Tso, R., Tsukada, L., Tsuna, D., Tsutsui, T., Turconi, M., Ubhi, A. S., Udall, R. P., Ueno, K., Ugolini, D., Unnikrishnan, C. S., Urban, A. L., Usman, S. A., Utina, A. C., Vahlbruch, H., Vajente, G., Vajpeyi, A., Valdes, G., Valentini, M., Valsan, V., van Bakel, N., Beuzekom, M. v., van den Brand, J. F. J., Van Den Broeck, C., Vander-Hyde, D. C., van der Schaaf, L., van Heijningen, J. V., Vardaro, M., Vargas, A. F., Varma, V., Vass, S., Vasúth, M., Vecchio, A., Vedovato, G., Veitch, J., Veitch, P. J., Venkateswara, K., Venneberg, J., Venugopalan, G., Verkindt, D., Verma, Y., Veske, D., Vetrano, F., Viceré, A., Viets, A. D., Villa-Ortega, V., Vinet, J. Y., Vitale, S., Vo, T., Vocca, H., Vorvick, C., Vyatchanin, S. P., Wade, A. R., Wade, L. E., Wade, M., Walet, R. C., Walker, M., Wallace, G. S., Wallace, L., Walsh, S., Wang, J. Z., Wang, S., Wang, W. H., Wang, Y. F., Ward, R. L., Warner, J., Was, M., Washington, N. Y., Watchi, J., Weaver, B., Wei, L., Weinert, M., Weinstein, A. J., Weiss, R., Wellmann, F., Wen, L., Weßels, P., Westhouse, J. W., Wette, K., Whelan, J. T., White, D. D., White, L. V., Whiting, B. F., Whittle, C., Wilken, D. M., Williams, D., Williams, M. J., Williamson, A. R., Willis, J. L., Willke, B., Wilson, D. J., Wimmer, M. H., Winkler, W., Wipf, C. C., Woan, G., Woehler, J., Wofford, J. K., Wong, I. C. F., Wrangel, J., Wright, J. L., Wu, D. S., Wysocki, D. M., Xiao, L., Yamamoto, H., Yang, L., Yang, Y., Yang, Z., Yap, M. J., Yeeles, D. W., Yoon, A., Yu, H., Yu, H., Yuen, S. H. R., Zadrożny, A., Zanolin, M., Zelenova, T., Zendri, J. P., Zevin, M., Zhang, J., Zhang, L., Zhang, R., Zhang, T., Zhao, C., Zhao, G., Zhou, M., Zhou, Z., Zhu, X. J., Zimmerman, A. B., Zucker, M. E., Zweizig, J., LIGO Scientific Collaboration, and Virgo Collaboration, "Population Properties of Compact Objects from the Second LIGO-Virgo Gravitational-Wave Transient Catalog," ApJ **913**, L7 (May 2021).

[34] Lu, J. R., Sinukoff, E., Ofek, E. O., Udalski, A., and Kozlowski, S., "A Search For Stellar-mass Black Holes Via Astrometric Microlensing," ApJ **830**, 41 (Oct. 2016).

[35] Lu, J. R., Lam, C. Y., Medford, M., Dawson, W., and Golovich, N., "Primordial Black Hole Microlensing: The Einstein Crossing Time Distribution," *Research Notes of the American Astronomical Society* **3**, 58 (Apr. 2019).

[36] Lam, C. Y., Lu, J. R., Hosek, Matthew W., J., Dawson, W. A., and Golovich, N. R., "PopSyCLE: A New Population Synthesis Code for Compact Object Microlensing Events," ApJ **889**, 31 (Jan. 2020).

[37] Elmegreen, B. G. and Elmegreen, D. M., "Observations of Thick Disks in the Hubble Space Telescope Ultra Deep Field," ApJ **650**, 644–660 (Oct. 2006).

[38] Genzel, R., Förster Schreiber, N. M., Lang, P., Tacchella, S., Tacconi, L. J., Wuyts, S., Bandara, K., Burkert, A., Buschkamp, P., Carollo, C. M., Cresci, G., Davies, R., Eisenhauer, F., Hicks, E. K. S., Kurk, J., Lilly, S. J., Lutz, D., Mancini, C., Naab, T., Newman, S., Peng, Y., Renzini, A., Shapiro Griffin, K., Sternberg, A., Vergani, D., Wisnioski, E., Wuyts, E., and Zamorani, G., "The SINS/zC-SINF Survey of z ˜2 Galaxy Kinematics: Evidence for Gravitational Quenching," ApJ **785**, 75 (Apr. 2014).

[39] van der Kruit, P. C. and Freeman, K. C., "Galaxy Disks," ARA&A **49**, 301–371 (Sept. 2011).

[40] Jones, T., Ellis, R. S., Richard, J., and Jullo, E., "The Origin and Evolution of Metallicity Gradients: Probing the Mode of Mass Assembly at z ˜= 2," ApJ **765**, 48 (Mar. 2013).

[41] Wang, X., Jones, T. A., Treu, T., Daddi, E., Brammer, G. B., Sharon, K., Morishita, T., Abramson, L. E., Colbert, J. W., Henry, A. L., Hopkins, P. F., Malkan, M. A., Schmidt, K. B., Teplitz, H. I., and Vulcani, B., "A Census of Sub-kiloparsec Resolution Metallicity Gradients in Star-forming Galaxies at Cosmic Noon from HST Slitless Spectroscopy," ApJ **900**, 183 (Sept. 2020).

[42] Jacobs, C., Glazebrook, K., Calabrò, A., Treu, T., Nannayakkara, T., Jones, T., Merlin, E., Abraham, R., Stevens, A. R. H., Vulcani, B., Yang, L., Bonchi, A., Boyett, K., Bradač, M., Castellano, M., Fontana, A., Marchesini, D., Malkan, M., Mason, C., Morishita, T., Paris, D., Santini, P., Trenti, M., and Wang, X., "Early Results from GLASS-JWST. XVIII. A First Morphological Atlas of the 1 ¡ z ¡ 5 Universe in the Rest-frame Optical," ApJ **948**, L13 (May 2023).

[43] Zhang, H., Primack, J. R., Faber, S. M., Koo, D. C., Dekel, A., Chen, Z., Ceverino, D., Chang, Y.-Y., Fang, J. J., Guo, Y., Lin, L., and Wel, A. v. d., "The evolution of galaxy shapes in CANDELS: from prolate to discy," MNRAS **484**, 5170–5191 (Apr. 2019).

[44] Vegetti, S., Koopmans, L. V. E., Bolton, A., Treu, T., and Gavazzi, R., "Detection of a dark substructure through gravitational imaging," MNRAS **408**, 1969–1981 (Nov. 2010).

[45] Vegetti, S., Koopmans, L. V. E., Auger, M. W., Treu, T., and Bolton, A. S., "Inference of the cold dark matter substructure mass function at z = 0.2 using strong gravitational lenses," MNRAS **442**, 2017–2035 (Aug. 2014).

[46] Nierenberg, A. M., Treu, T., Wright, S. A., Fassnacht, C. D., and Auger, M. W., "Detection of substructure with adaptive optics integral field spectroscopy of the gravitational lens B1422+231," MNRAS **442**, 2434–2445 (Aug. 2014).

[47] Bullock, J. S. and Boylan-Kolchin, M., "Small-Scale Challenges to the ΛCDM Paradigm," ARA&A **55**, 343–387 (Aug. 2017).

[48] Gilman, D., Du, X., Benson, A., Birrer, S., Nierenberg, A., and Treu, T., "Constraints on the mass-concentration relation of cold dark matter halos with 11 strong gravitational lenses," MNRAS **492**, L12–L16 (Feb. 2020).

[49] Zelko, I. A., Nierenberg, A. M., and Treu, T., "Probing dark matter with adaptive-optics based flux ratio anomalies: photometric and astrometric precision," MNRAS **531**, 885–897 (June 2024).

[50] Nierenberg, A. M., Treu, T., Brammer, G., Peter, A. H. G., Fassnacht, C. D., Keeton, C. R., Kochanek, C. S., Schmidt, K. B., Sluse, D., and Wright, S. A., "Probing dark matter substructure in the gravitational lens HE 0435-1223 with the WFC3 grism," MNRAS **471**, 2224–2236 (Oct. 2017).

[51] Nierenberg, A. M., Gilman, D., Treu, T., Brammer, G., Birrer, S., Moustakas, L., Agnello, A., Anguita, T., Fassnacht, C. D., Motta, V., Peter, A. H. G., and Sluse, D., "Double dark matter vision: twice the number of compact-source lenses with narrow-line lensing and the WFC3 grism," MNRAS **492**, 5314–5335 (Mar. 2020).

[52] Wong, K. C., Suyu, S. H., Chen, G. C. F., Rusu, C. E., Millon, M., Sluse, D., Bonvin, V., Fassnacht, C. D., Taubenberger, S., Auger, M. W., Birrer, S., Chan, J. H. H., Courbin, F., Hilbert, S., Tihhonova, O., Treu, T., Agnello, A., Ding, X., Jee, I., Komatsu, E., Shajib, A. J., Sonnenfeld, A., Blandford, R. D., Koopmans, L. V. E., Marshall, P. J., and Meylan, G., "H0LiCOW - XIII. A 2.4 per cent measurement of H_0 from lensed quasars: 5.3σ tension between early- and late-Universe probes," MNRAS **498**, 1420–1439 (Oct. 2020).

[53] Riess, A. G., Macri, L. M., Hoffmann, S. L., Scolnic, D., Casertano, S., Filippenko, A. V., Tucker, B. E., Reid, M. J., Jones, D. O., Silverman, J. M., Chornock, R., Challis, P., Yuan, W., Brown, P. J., and Foley, R. J., "A 2.4% Determination of the Local Value of the Hubble Constant," ApJ **826**, 56 (July 2016).

[54] Verde, L., Treu, T., and Riess, A. G., "Tensions between the early and late Universe," *Nature Astronomy* **3**, 891–895 (Sept. 2019).

[55] Knox, L. and Millea, M., "Hubble constant hunter's guide," Phys. Rev. D **101**, 043533 (Feb. 2020).

[56] Birrer, S., Shajib, A. J., Galan, A., Millon, M., Treu, T., Agnello, A., Auger, M., Chen, G. C. F., Christensen, L., Collett, T., Courbin, F., Fassnacht, C. D., Koopmans, L. V. E., Marshall, P. J., Park, J. W., Rusu, C. E., Sluse, D., Spiniello, C., Suyu, S. H., Wagner-Carena, S., Wong, K. C., Barnabè, M., Bolton, A. S., Czoske, O., Ding, X., Frieman, J. A., and Van de Vyvere, L., "TDCOSMO. IV. Hierarchical time-delay cosmography - joint inference of the Hubble constant and galaxy density profiles," A&A **643**, A165 (Nov. 2020).

[57] Birrer, S. and Treu, T., "TDCOSMO. V. Strategies for precise and accurate measurements of the Hubble constant with strong lensing," A&A **649**, A61 (May 2021).

[58] Shajib, A. J., Treu, T., and Agnello, A., "Improving time-delay cosmography with spatially resolved kinematics," MNRAS **473**, 210–226 (Jan. 2018).

[59] Vernardos, G., "A joint microlensing analysis of lensing mass and accretion disc models," MNRAS **480**, 4675–4683 (Nov. 2018).

[60] Konopacky, Q. M., Barman, T. S., Macintosh, B. A., and Marois, C., "Detection of Carbon Monoxide and Water Absorption Lines in an Exoplanet Atmosphere," *Science* **339**, 1398–1401 (Mar. 2013).

[61] Hoeijmakers, H. J., Schwarz, H., Snellen, I. A. G., de Kok, R. J., Bonnefoy, M., Chauvin, G., Lagrange, A. M., and Girard, J. H., "Medium-resolution integral-field spectroscopy for high-contrast exoplanet imaging. Molecule maps of the β Pictoris system with SINFONI," A&A **617**, A144 (Oct. 2018).

[62] Wilcomb, K. K., Konopacky, Q. M., Barman, T. S., Theissen, C. A., Ruffio, J.-B., Brock, L., Macintosh, B., and Marois, C., "Moderate-resolution K-band Spectroscopy of Substellar Companion κ Andromedae b," AJ **160**, 207 (Nov. 2020).

[63] Petrus, S., Bonnefoy, M., Chauvin, G., Charnay, B., Marleau, G. D., Gratton, R., Lagrange, A. M., Rameau, J., Mordasini, C., Nowak, M., Delorme, P., Boccaletti, A., Carlotti, A., Houllé, M., Vigan, A., Allard, F., Desidera, S., D'Orazi, V., Hoeijmakers, H. J., Wyttenbach, A., and Lavie, B., "Medium-resolution spectrum of the exoplanet HIP 65426 b," A&A **648**, A59 (Apr. 2021).

[64] Miles, B. E., Biller, B. A., Patapis, P., Worthen, K., Rickman, E., Hoch, K. K. W., Skemer, A., Perrin, M. D., Whiteford, N., Chen, C. H., Sargent, B., Mukherjee, S., Morley, C. V., Moran, S. E., Bonnefoy, M., Petrus, S., Carter, A. L., Choquet, E., Hinkley, S., Ward-Duong, K., Leisenring, J. M., Millar-Blanchaer, M. A., Pueyo, L., Ray, S., Sallum, S., Stapelfeldt, K. R., Stone, J. M., Wang, J. J., Absil, O., Balmer, W. O., Boccaletti, A., Bonavita, M., Booth, M., Bowler, B. P., Chauvin, G., Christiaens, V., Currie, T., Danielski, C., Fortney, J. J., Girard, J. H., Grady, C. A., Greenbaum, A. Z., Henning, T., Hines, D. C.,

Janson, M., Kalas, P., Kammerer, J., Kennedy, G. M., Kenworthy, M. A., Kervella, P., Lagage, P.-O., Lew, B. W. P., Liu, M. C., Macintosh, B., Marino, S., Marley, M. S., Marois, C., Matthews, E. C., Matthews, B. C., Mawet, D., McElwain, M. W., Metchev, S., Meyer, M. R., Molliere, P., Pantin, E., Quirrenbach, A., Rebollido, I., Ren, B. B., Schneider, G., Vasist, M., Wyatt, M. C., Zhou, Y., Briesemeister, Z. W., Bryan, M. L., Calissendorff, P., Cantalloube, F., Cugno, G., De Furio, M., Dupuy, T. J., Factor, S. M., Faherty, J. K., Fitzgerald, M. P., Franson, K., Gonzales, E. C., Hood, C. E., Howe, A. R., Kraus, A. L., Kuzuhara, M., Lagrange, A.-M., Lawson, K., Lazzoni, C., Liu, P., Llop-Sayson, J., Lloyd, J. P., Martinez, R. A., Mazoyer, J., Quanz, S. P., Redai, J. A., Samland, M., Schlieder, J. E., Tamura, M., Tan, X., Uyama, T., Vigan, A., Vos, J. M., Wagner, K., Wolff, S. G., Ygouf, M., Zhang, X., Zhang, K., and Zhang, Z., "The JWST Early-release Science Program for Direct Observations of Exoplanetary Systems II: A 1 to 20 μm Spectrum of the Planetary-mass Companion VHS 1256-1257 b," ApJ **946**, L6 (Mar. 2023).

[65] Barman, T. S., Macintosh, B., Konopacky, Q. M., and Marois, C., "Clouds and Chemistry in the Atmosphere of Extrasolar Planet HR8799b," ApJ **733**, 65 (May 2011).

[66] Mordasini, C., Alibert, Y., Benz, W., Klahr, H., and Henning, T., "Extrasolar planet population synthesis . IV. Correlations with disk metallicity, mass, and lifetime," A&A **541**, A97 (May 2012).

[67] Boley, A. C., Hayfield, T., Mayer, L., and Durisen, R. H., "Clumps in the outer disk by disk instability: Why they are initially gas giants and the legacy of disruption," Icarus **207**, 509–516 (June 2010).

[68] Marley, M. S., Saumon, D., Fortney, J. J., Morley, C., Lupu, R. E., Freedman, R., and Visscher, C., "Sonora: A New Generation Model Atmosphere Grid for Brown Dwarfs and Young Extrasolar Giant Planets," in [*American Astronomical Society Meeting Abstracts #230*], *American Astronomical Society Meeting Abstracts* **230**, 315.07 (June 2017).

[69] Öberg, K. I., Murray-Clay, R., and Bergin, E. A., "The Effects of Snowlines on C/O in Planetary Atmospheres," ApJ **743**, L16 (Dec. 2011).

[70] Zahnle, K. J. and Marley, M. S., "Methane, Carbon Monoxide, and Ammonia in Brown Dwarfs and Self-Luminous Giant Planets," ApJ **797**, 41 (Dec. 2014).

[71] Reiners, A., Homeier, D., Hauschildt, P. H., and Allard, F., "A high resolution spectral atlas of brown dwarfs," A&A **473**, 245–255 (Oct. 2007).

[72] Wong, M. H., Otarola, A., de Kleer, K. R., Cook, S. H., Hendrix, A., Sayanagi, K., Simon, A., Greathouse, T., Holler, B., de Pater, I., Lucas, M., Trilling, D., Cartwright, R., Chanover, N., Tiscareno, M., Orton, G., Nixon, C., Milam, S. N., Fry, P. M., Giles, R., Sinclair, J., and Adamkovics, M., "Solar system Deep Time-Surveys of atmospheres, surfaces, and rings," *Bulletin of the American Astronomical Society* **51**, 541 (May 2019).

[73] Chanover, N., Wong, M. H., Greathouse, T., Trilling, D., Conrad, A., de Pater, I., Gaidos, E., Cartwright, R., Lucas, M., Meech, K., Orton, G., Pinilla-Alonso, N., Sayanagi, K., Schwamb, M. E., Tiscareno, M., Veillet, C., Holler, B., de Kleer, K., Hammel, H., Hendrix, A., Otarola, A., Nixon, C., Benecchi, S., Simon, A., Mandt, K., Verbiscer, A., Giles, R., Retherford, K., Fry, P., Bell, J. F., Milam, S., Rivkin, A., and Luszcz-Cook, S., "Triggered High-Priority Observations of Dynamic Solar System Phenomena," *Bulletin of the American Astronomical Society* **51**, 340 (May 2019).

[74] Hanuš, J., Marchis, F., and Ďurech, J., "Sizes of main-belt asteroids by combining shape models and Keck adaptive optics observations," Icarus **226**, 1045–1057 (Sept. 2013).

[75] Simon, A. A., Wong, M. H., Sromovsky, L. A., Fletcher, L. N., and Fry, P. M., "Giant Planet Atmospheres: Dynamics and Variability from UV to Near-IR Hubble and Adaptive Optics Imaging," *Remote Sensing* **14**, 1518 (Mar. 2022).

[76] Sánchez-Lavega, A., Irwin, P., and García Muñoz, A., "Dynamics and clouds in planetary atmospheres from telescopic observations," *Astronomy and Astrophysics Review* **31**, 5 (Dec. 2023).

[77] Helfenbein, M., Molter, E. M., de Pater, I., and Souami, D., "Near-Infrared photometry of Neptune's small regular satellites with Keck," Icarus **413**, 116004 (May 2024).

[78] Sromovsky, L. A., Fry, P. M., de Pater, I., and Hammel, H. B., "The puzzling north polar region of Uranus: Continued zero-shear winds and increasing brightness from 2015 through 2022 according to 7 years of Keck AO imaging," *Icarus* **420**, 116186 (Sept. 2024).

[79] Irwin, P. G. J., Teanby, N. A., Fletcher, L. N., Toledo, D., Orton, G. S., Wong, M. H., Roman, M. T., Pérez-Hoyos, S., James, A., and Dobinson, J., "Hazy Blue Worlds: A Holistic Aerosol Model for Uranus and Neptune, Including Dark Spots," *Journal of Geophysical Research (Planets)* **127**, e07189 (June 2022).

[80] Wizinowich, P., Acton, D. S., Shelton, C., Stomski, P., Gathright, J., Ho, K., Lupton, W., Tsubota, K., Lai, O., Max, C., Brase, J., An, J., Avicola, K., Olivier, S., Gavel, D., Macintosh, B., Ghez, A., and Larkin, J., "First Light Adaptive Optics Images from the Keck II Telescope: A New Era of High Angular Resolution Imagery," PASP **112**, 315–319 (Mar. 2000).

[81] Sromovsky, L. A., Karkoschka, E., Fry, P. M., de Pater, I., and Hammel, H. B., "The methane distribution and polar brightening on Uranus based on HST/STIS, Keck/NIRC2, and IRTF/SpeX observations through 2015," Icarus **317**, 266–306 (Jan. 2019).

[82] Hueso, R., Guillot, T., and Sánchez-Lavega, A., "Convective storms and atmospheric vertical structure in Uranus and Neptune," *Philosophical Transactions of the Royal Society of London Series A* **378**, 20190476 (Dec. 2020).

[83] Guillot, T., "Condensation of Methane, Ammonia, and Water and the Inhibition of Convection in Giant Planets," *Science* **269**, 1697–1699 (Sept. 1995).

[84] Leconte, J., Spiga, A., Clément, N., Guerlet, S., Selsis, F., Milcareck, G., Cavalié, T., Moreno, R., Lellouch, E., Carrión-González, Ó., Charnay, B., and Lefèvre, M., "A 3D picture of moist-convection inhibition in hydrogen-rich atmospheres: Implications for K2-18 b," A&A **686**, A131 (June 2024).

[85] National Academies of Sciences, Engineering, and Medicine, [*Origins, Worlds, and Life: A Decadal Strategy for Planetary Science and Astrobiology 2023-2032*], The National Academies Press, Washington, DC (2023).

[86] Smith, B. A., Soderblom, L. A., Beebe, R., Bliss, D., Boyce, J. M., Brahic, A., Briggs, G. A., Brown, R. H., Collins, S. A., Cook, A. F., Croft, S. K., Cuzzi, J. N., Danielson, G. E., Davies, M. E., Dowling, T. E., Godfrey, D., Hansen, C. J., Harris, C., Hunt, G. E., Ingersoll, A. P., Johnson, T. V., Krauss, R. J., Masursky, H., Morrison, D., Owen, T., Plescia, J. B., Pollack, J. B., Porco, C. C., Rages, K., Sagan, C., Shoemaker, E. M., Sromovsky, L. A., Stoker, C., Strom, R. G., Suomi, V. E., Synnott, S. P., Terrile, R. J., Thomas, P., Thompson, W. R., and Veverka, J., "Voyager 2 in the Uranian System: Imaging Science Results," *Science* **233**, 43–64 (July 1986).

[87] Bjoraker, G. L., "Jupiter's elusive water," *Nature Astronomy* **4**, 558–559 (Apr. 2020).

[88] Wang, R., Stallard, T. S., Melin, H., Baines, K. H., Achilleos, N., Rymer, A. M., Ray, L. C., Nichols, J. D., Moore, L., O'Donoghue, J., Chowdhury, M. N., Thomas, E. M., Knowles, K. L., Tiranti, P. I., and Miller, S., "Asymmetric Ionospheric Jets in Jupiter's Aurora," *Journal of Geophysical Research (Space Physics)* **128**, e2023JA031861 (Dec. 2023).

[89] Wong, M. H., Bjoraker, G. L., Goullaud, C., Stephens, A. W., Luszcz-Cook, S. H., Atreya, S. K., de Pater, I. d., and Brown, S. T., "Deep Clouds on Jupiter," *Remote Sensing* **15**, 702 (Jan. 2023).

[90] Wright, S. A., Walth, G., Do, T., Marshall, D., Larkin, J. E., Moore, A. M., Adamkovics, M., Andersen, D., Armus, L., Barth, A., Cote, P., Cooke, J., Chisholm, E. M., Davidge, T., Dunn, J. S., Dumas, C., Ellerbroek, B. L., Ghez, A. M., Hao, L., Hayano, Y., Liu, M., Lopez-Rodriguez, E., Lu, J. R., Mao, S., Marois, C., Pandey, S. B., Phillips, A. C., Schoeck, M., Subramaniam, A., Subramanian, S., Suzuki, R., Tan, J. C., Terai, T., Treu, T., Simard, L., Weiss, J. L., Wincentsen, J., Wong, M., and Zhang, K., "The infrared imaging spectrograph (IRIS) for TMT: latest science cases and simulations," in [*Adaptive Optics Systems V*], Marchetti, E., Close, L. M., and Véran, J.-P., eds., *Society of Photo-Optical Instrumentation Engineers (SPIE) Conference Series* **9909**, 990905 (July 2016).

[91] Warad, K., "The infrared imaging spectrograph (iris): project status report," Presented at SPIE Astronomical Telescopes + Instrumentation 2024. Forthcoming publication (July 2024).

[92] Wiley, J., Brown, A., Kupke, R., Wright, S. A., Magnone, K., Maire, J., Cosens, M., Kress, E., Wang, E., Johnson, C., Larkin, J. E., Fitzgerald, M. P., Kassis, M. F., and Jones, T., "Liger at W.M. Keck Observatory: imager structural analysis, fabrication, and characterization plan," Presented at SPIE Astronomical Telescopes + Instrumentation 2024. Forthcoming publication (July 2024).

[93] Arriaga, P., Fitzgerald, M., Johnson, C., Weiss, J., and Lyke, J. E., "Upgrade and characterization of the OSIRIS imager detector," in [*Ground-based and Airborne Instrumentation for Astronomy VII*], Evans, C. J., Simard, L., and Takami, H., eds., *Society of Photo-Optical Instrumentation Engineers (SPIE) Conference Series* **10702**, 107022U (July 2018).

[94] Chen, S., Meyer, E., Wright, S. A., Moore, A. M., Larkin, J. E., Maire, J., Mieda, E., and Simard, L., "The infrared imaging spectrograph (IRIS) for TMT: volume phase holographic grating performance testing and discussion," in [*Ground-based and Airborne Instrumentation for Astronomy V*], Ramsay, S. K., McLean, I. S., and Takami, H., eds., *Society of Photo-Optical Instrumentation Engineers (SPIE) Conference Series* **9147**, 91478X (July 2014).

[95] Meyer, E., Chen, S., Wright, S. A., Moore, A. M., Larkin, J. E., Simard, L., Marie, J., Mieda, E., and Gordon, J., "The infrared imaging spectrograph (IRIS) for TMT: reflective ruled diffraction grating performance testing and discussion," in [*Ground-based and Airborne Instrumentation for Astronomy V*], Ramsay, S. K., McLean, I. S., and Takami, H., eds., *Society of Photo-Optical Instrumentation Engineers (SPIE) Conference Series* **9147**, 91479C (July 2014).

[96] Bushouse, H., Eisenhamer, J., Dencheva, N., Davies, J., Greenfield, P., Morrison, J., Hodge, P., Simon, B., Grumm, D., Droettboom, M., Slavich, E., Sosey, M., Pauly, T., Miller, T., Jedrzejewski, R., Hack, W., Davis, D., Crawford, S., Law, D., Gordon, K., Regan, M., Cara, M., MacDonald, K., Bradley, L., Shanahan, C., Jamieson, W., Teodoro, M., Williams, T., and Pena-Guerrero, M., "JWST Calibration Pipeline," (Mar. 2024).

[97] Oluyide, T., Lynn, M. S., Coda, T., Berriman, G. B., Brown, M., Fuhrman, L., Gelino, C., Good, J., Hayashi, J., Lee, C. H., Mader, J., and Swain, M. A., "The Observers' Data Access Portal at the Keck Observatory Archive," *arXiv e-prints* , arXiv:2402.04528 (Feb. 2024).

[98] Walth, G., Wright, S. A., Weiss, J., Larkin, J. E., Moore, A. M., Chapin, E. L., Do, T., Dunn, J., Ellerbroek, B., Gillies, K., Hayano, Y., Johnson, C., Marshall, D., Riddle, R. L., Simard, L., Sohn, J. M., Suzuki, R., and Wincentsen, J., "The Infrared Imaging Spectrograph (IRIS) for TMT: data reduction system," in [*Software and Cyberinfrastructure for Astronomy IV*], Chiozzi, G. and Guzman, J. C., eds., *Society of Photo-Optical Instrumentation Engineers (SPIE) Conference Series* **9913**, 99134A (Aug. 2016).

[99] Walth, G. L., Wright, S. A., Rundquist, N.-E., Andersen, D., Chapin, E., Chisholm, E., Do, T., Dunn, J., Ellerbroek, B., Gillies, K., Hayano, Y., Johnson, C., Larkin, J., Nakamoto, T., Riddle, R., Simard, L., Smith, R., Suzuki, R., Sohn, J. M., Weber, R., Weiss, J., and Zhang, K., "The Infrared Imaging Spectrograph (IRIS) for TMT: advancing the data reduction system," in [*Software and Cyberinfrastructure for Astronomy V*], Guzman, J. C. and Ibsen, J., eds., *Society of Photo-Optical Instrumentation Engineers (SPIE) Conference Series* **10707**, 1070731 (July 2018).

[100] Surya, A., Zonca, A., Rundquist, N.-E., Wright, S. A., Walth, G. L., Anderson, D. R., Chapin, E. L., Chisholm, E. M., Do, T., Dunn, J. S., Gillies, K., Hayano, Y., Johnson, C. A., Kupke, R., Larkin, J. E., Nakamoto, T., Riddle, R., Smith, R., Suzuki, R., Sohn, J. M., Weber, R., Weiss, J. L., and Zhang, K., "The Infrared Imaging Spectrograph (IRIS) for TMT: final design development of the data reduction system," in [*Software and Cyberinfrastructure for Astronomy VI*], Guzman, J. C. and Ibsen, J., eds., *Society of Photo-Optical Instrumentation Engineers (SPIE) Conference Series* **11452**, 114521K (Dec. 2020).

[101] Rundquist, N.-E., Wright, S. A., Schöck, M., Surya, A., Lu, J., Turri, P., Chapin, E. L., Chisholm, E., Do, T., Dunn, J., Ghez, A., Hayano, Y., Johnson, C., Larkin, J. E., Riddle, R. L., Sohn, J. M., Suzuki, R., Walth, G., and Zonca, A., "The InfraRed Imaging Spectrograph (IRIS) for TMT: photometric characterization of anisoplanatic PSFs and testing of PSF-Reconstruction via AIROPA," in [*Ground-based and Airborne Instrumentation for Astronomy VIII*], Evans, C. J., Bryant, J. J., and Motohara, K., eds., *Society of Photo-Optical Instrumentation Engineers (SPIE) Conference Series* **11447**, 114472Z (Dec. 2020).

[102] Walth, G., Surya, A., Rundquist, N.-E., Wright, S. A., Cosens, M., Vayner, A., Oh, E., Llamas, J. A., Skidmore, W., Chisholm, E. M., and Larkin, J. E., "The Infrared Imaging Spectrograph (IRIS) for TMT: exposure time calculator for IRIS," in [*Society of Photo-Optical Instrumentation Engineers (SPIE) Conference Series*], Guzman, J. C. and Ibsen, J., eds., *Society of Photo-Optical Instrumentation Engineers (SPIE) Conference Series* **11452**, 1145236 (Jan. 2021).